STUDYING THE ROLE OF PTEN IN THE GUT AND INVESTIGATING THE GUT-BRAIN INFLAMMATORY INTERACTION

by

CODY SCOTT HOWE

A dissertation submitted in partial fulfillment of the
requirements for the degree of

DOCTOR OF PHILOSOPHY IN BIOLOGICAL AND BIOMEDICAL SCIENCES

2023

Oakland University
Rochester, Michigan

Thesis Advisory Committee:

Sang Hoon Rhee, Ph.D., Chair
Gerard Madlambayan, Ph.D.
Mi Hye Song, Ph.D.

To my mother, Patricia, brother, Zane, and love of my life, Chelsey

ACKNOWLEDGMENTS

I would like to express my sincerest gratitude to my mentor, Dr. Sang Rhee, who made this project possible. I appreciate his continuous encouragement, guidance, and support throughout my academic career. Dr. Rhee has pushed me to grow not only as a scientist, but also a person. I couldn't have asked for a better mentor on my journey.

I would also like to give my warmest thanks to my wonderful committee members, Dr Gerard Madlambayan and Dr. Mi Hye Song for their time, efforts, advice, and questions throughout my Ph.D. process here at Oakland University.

Additionally, I would like to give my thanks to my loving family for always being in my corner and supporting me. My mother and brother in particular have been a constant keystone of my success since I can remember. They have always been a source of inspiration, motivation, and laughter.

Furthermore, I want to thank my girlfriend Chelsey for being another source of support, motivation, and always believing in me. Thank you for being patient all of those nights in the lab experimenting or the office writing away.

Lastly, I'd like to extend a thanks to the Oakland University Biology Department and everyone in it. The students and faculty have all made an impact on my time here at Oakland University. In particular, I'd like to especially thank Dr. Aaron Scholl. Thanks for kindly taking me under your wing and showing me my own potential. Thank you all.

Cody Howe

ABSTRACT

STUDYING THE ROLE OF PTEN IN THE GUT AND THE GUT-BRAIN INFLAMMATORY INTERACTION

by

Cody Howe

Adviser: Sang Rhee, Ph.D.

Phosphatase and tensin homolog (Pten) deficiency causes tumorigenesis because Pten opposes PI3k-Akt signaling. However, correlation between Pten deficiency and colon cancer remains unclear due to contradicting studies. The first project examines this correlation by generating intestinal epithelial cell (IEC) – specific Pten knockout (KO) mice. However, IEC-Pten deficiency alone did not induce tumorigenesis in mice but maintained the tumor-driving potential. The expression of tumor-promoting and tumor-suppressing genes was decreased and increased, respectively, in the intestine of $Pten^{\Delta IEC/\Delta IEC}$ mice compared to controls. The abundance of Akkermansia muciniphila, capable of inducing chronic intestinal inflammation, was reduced in $Pten^{\Delta IEC/\Delta IEC}$ mice. These findings suggest that altered tumor-associated gene expression and changed gut microbiota shape a tumor-preventive microenvironment in $Pten^{\Delta IEC/\Delta IEC}$ mice. It was recently suggested that PTEN regulates TLR5-induced immune and inflammatory responses in IECs, suggesting an immunomodulatory function of PTEN in the gut. However, this alternative function of PTEN has not been evaluated in an in vivo context of protection against enteropathogenic bacteria. In the second project, $Pten^{\Delta IEC/\Delta IEC}$ mice

were subjected to the streptomycin-pre-treated mouse model of Salmonella infection. The bacterial infection in $Pten^{\Delta IEC/\Delta IEC}$ mice increased the mortality, induced gastrointestinal inflammation, up-regulated pro-inflammatory cytokines, and increased bacterial loads in extraintestinal tissues. This suggests that IEC-restricted Pten deficiency renders the host greatly susceptible to Salmonella infection and supports an immune-regulatory role of PTEN in the gut. Lastly, in the third project, chronic gut inflammation is associated with neurodegenerative diseases. However, the direct evidence for and the underlying mechanism of the gut-brain interaction remain obscure. An interleukin-10 (IL-10) KO mouse was fed piroxicam-mixed chow, where it found that the brain and gut had increased levels of IL-1β and IL-6 cytokines. These findings suggest an inflammatory link in the piroxicam-fed IL-10 KO mice. Pten is an important factor in maintaining gut homeostasis, which is important for neural function.

TABLE OF CONTENTS

ACKNOWLEDGMENTS iv

ABSTRACT v

LIST OF TABLES xii

LIST OF FIGURES xiii

LIST OF ABBREVIATIONS xvii

CHAPTER ONE
BACKGROUND AND SIGNFICANCE 1

1.1: INTRODUCTION 1

1.2: INFLAMMATORY BOWEL DISEASE 2

1.3: THE GUT EPITHELIAL BARRIER 3

1.4: THE IMPORTANCE OF THE CELL JUNCTIONS 7

1.5: THE GUT MICROBIOME 8

1.6: PHOSPHATASE AND TENSIN HOMOLOG (PTEN) 8

CHAPTER TWO
STUDYING THE ROLE OF PTEN IN THE INTESTINAL EPITHELIUM 10

2.1: INTRODUCTION 10

2.1.1: Pten in the Intestinal Epithelium 10

2.2: MATERIALS AND METHODS 13

2.2.1: Human Tissues 13

2.2.2: Animals 14

2.2.3: Quantitative Real-Time PCR 14

2.2.4: Transmission Electron Microscopy 15

TABLE OF CONTENTS—Continued

2.2.5: Immunohistochemistry 16

2.2.6: Immunofluorescence Staining 17

2.2.7: Cancer-pathway Focused Gene Analysis 18

2.2.8: Fecal Sample Collection for Microbiome Analysis 19

2.2.9: DNA Extraction from Mouse Fecal Samples 19

2.2.10: PCR Amplification and Amplicon Sequencing Using Next Generation Technology 19

2.2.11: Sequence Analysis 20

2.2.12: Alpha and Beta Diversity Analysis 21

2.2.13: Statistical Analysis 21

2.3: RESULTS 21

2.3.1: Pten mRNA Expression was Reduced in Colon Cancer Biopsies Compared to Normal Tissues 21

2.3.2: Generating the Intestinal Epithelial Cell Specific *Pten* Gene Knockout Mice 23

2.3.3: Intestinal Epithelial Cells of $Pten^{\Delta IEC/\Delta IEC}$ Mice Exhibited Enhanced Epithelial Cell Growth in the Gut 24

2.3.4: Intestinal Epithelial Cell of $Pten^{\Delta IEC/\Delta IEC}$ Mice Exhibited Enhanced Mitotic Activity 25

2.3.5: Intestinal Epithelial Cells of $Pten^{\Delta IEC/\Delta IEC}$ Mice Exhibited Enhanced Tumorigenesis in the $Apc^{min/+}$ Mouse Model of Colon Cancer 31

2.3.6: Tumor-Promoting Gene Expression was Reduced in the Intestine of $Pten^{\Delta IEC/\Delta IEC}$ Mice 34

2.3.7: Loss of the *Pten* Gene in Intestinal Epithelial Cells Resulted in Intestinal Dysbiosis 37

2.3.8: The Fecal Microbiota Communities of $Pten^{\Delta IEC/\Delta IEC}$ Mice Were Different from Those of $Pten^{+/+}$ Mice 40

2.3.9: Colon Cancer-Associated *Akkermansia Muciniphila* was Dramatically Decreased in the Feces of $Pten^{\Delta IEC/\Delta IEC}$ Mice Compared to $Pten^{+/+}$ Mice 43

2.4: DISCUSSION 45

2.5: CONCLUSION 49

CHAPTER THREE
STUDYING THE IMMUNE-REGULATORY ROLE OF PTEN IN THE GUT 50

3.1: INTRODUCTION 50

3.2: MATERIALS AND METHODS 52

3.2.1: Animals 52

3.2.2: Bacterial Strain and Culture Condition 52

3.2.3: Animal Experiments 53

3.2.4: Analysis of *S.* Typhimurium Loads in the Liver, Mesenteric Lymph Nodes, and Spleen 53

3.2.5: Tissue Histology Analysis 53

3.2.6: Enzyme-Linked Immunosorbent Assay 54

3.3: RESULTS 54

3.3.1: *Pten* Gene Deletion in IECs Increased Susceptibility to Infection of *Salmonella enterica* serovar Typhimurium in Streptomycin-Pretreated Mice 54

3.3.2: Low Inoculum of *Salmonella enterica* serovar Typhimurium Produced Massive Inflammation in the Small Intestine of $Pten^{\Delta IEC/\Delta IEC}$ Mice 57

3.3.3: *Salmonella enterica* serovar Typhimurium Infection Induced Pro-Inflammatory Cytokine Production in the Small Intestine of $Pten^{\Delta IEC/\Delta IEC}$ Mice 61

3.3.4: Bacterial Colonization was Increased in Streptomycin-Pretreated $Pten^{\Delta IEC/\Delta IEC}$ Mice 62

3.4: DISCUSSION 65

3.5: CONCLUSION 66

CHAPTER FOUR
STUDYING THE GUT-BRAIN INFLAMMATORY INTERACTION 67

4.1: INTRODUCTION 67

4.2: MATERIALS AND METHODS 68

4.2.1: Animals 68

4.2.2: Chronic Colitis Mouse Model 69

4.2.3: Enzyme-Linked Immunosorbent Assay Quantification of IL-1β and IL-6 69

4.2.4: Statistical Analysis 69

4.3: RESULTS 70

4.3.1: Bodyweight of Piroxicam-fed IL-10 KO Mice was Lower Compared to Piroxicam-fed IL-10 WT Control Mice 70

4.3.2: Colon Size and Length of Piroxicam-fed IL-10 KO Mice were Decreased Compared to Piroxicam-fed IL-10 WT Control Mice 71

TABLE OF CONTENTS—Continued

4.3.3: Pro-inflammatory Cytokine Levels were Elevated in Piroxicam-fed IL-10 KO Mice Tissues Compared to Piroxicam-fed IL-10 WT Control Mice Tissues 72

4.4: DISCUSSION 77

4.5: CONCLUSION 79

CHAPTER FIVE
OVERALL CONCLUSIONS AND FUTURE DIRECTION 80

5.1: CONCLUSIONS 80

5.2: FUTURE DIRECTION 81

REFERENCES 83

APPENDIX 101

LIST OF TABLES

Table 1 $Pten^{\Delta IEC/\Delta IEC}$ Fecal Microbiome Vs $Pten^{+/+}$ Fecal Microbiome 38

LIST OF FIGURES

Figure 1	The illustration above depicts a “zoomed-in view” of the intestinal microenvironment.	3
Figure 2	The illustration above portrays a view of junctional protein complexes between cells of the gut epithelial barrier.	5
Figure 3	The illustration above depicts the typical PI3K/Akt signaling pathway.	11
Figure 4	*PTEN* mRNA expression was decreased in human colon cancer tissues compared to normal tissues.	22
Figure 5	The illustration above shows the mating cross between $Vil^{cre/+}$ mice and $Pten^{loxp/loxp}$ mice using the Cre-lox recombinase system.	23
Figure 6	Intestinal epithelial cells of $Pten^{\Delta IEC/\Delta IEC}$ mice displayed enhanced mitotic activity compared to those of $Pten^{+/+}$ mice shown in the figures above (left and right).	24
Figure 7	The above image shows paraffin-embedded sections of the mid-colon.	25
Figure 8	Presented in the above images are electron micrographs of the colonic epithelium from 12-month-old $Pten^{\Delta IEC/\Delta IEC}$ and littermate $Pten^{+/+}$ mice.	26
Figure 9	Cell proliferation was evaluated in the colon of $Pten^{\Delta IEC/\Delta IEC}$ and littermate $Pten^{+/+}$ mice.	26
Figure 10	Paraffin-embedded sections of the mid-colon were subjected to immunofluorescence staining with PCNA antibody.	28
Figure 11	Paraffin-embedded sections of the mid-colon were subjected to immunofluorescence staining with phospho-Akt (P-Akt) antibody.	29
Figure 12	The illustration above depicts the mating cross between $Pten^{\Delta IEC/\Delta IEC}$ mice and $APC^{min/+}$ mice.	30

Figure 13	The image above shows gross images of the tumors observed throughout the small intestine (jejunum and ileum) and the colon of $Pten^{\Delta IEC/\Delta IEC}$; $Apc^{min/+}$ mice (scalebar, 1 mm).	31
Figure 14	The number of tumors was increased in $Pten^{\Delta IEC/\Delta IEC}$; $Apc^{min/+}$ mice.	32
Figure 15	$Pten^{\Delta IEC/\Delta IEC}$; $Apc^{min/+}$ mice have an increased kidney sized compared to littermate $Pten^{+/+}$; $Apc^{min/+}$ mice.	33
Figure 16	$Pten^{\Delta IEC/\Delta IEC}$; $Apc^{min/+}$ mice have an increased mortality compared to littermate $Pten^{+/+}$; $Apc^{min/+}$ mice.	33
Figure 17	The expression of cancer-associated genes was changed in the intestine of $Pten^{\Delta IEC/\Delta IEC}$ mice.	35
Figure 18	The fecal microbiome of $Pten^{\Delta IEC/\Delta IEC}$ mice was distinct from that of $Pten^{+/+}$ mice.	39
Figure 19	Relative abundance of taxonomic groups observed in the fecal samples were different between $Pten^{\Delta IEC/\Delta IEC}$ and $Pten^{+/+}$ mice.	41
Figure 20	A dual hierarchal dendrogram was generated based on the predominant genera using Ward's minimum variance clustering and Manhattan distances.	42
Figure 21	The abundance of the colitogenic bacteria *Akkermansia muciniphila* was dramatically reduced in $Pten^{\Delta IEC/\Delta IEC}$ mice compared to $Pten^{+/+}$ mice.	44
Figure 22	The illustration above represents the experimental timeline for the streptomycin-pretreatment and subsequent bacterial inoculation.	55
Figure 23	$Pten^{\Delta IEC/\Delta IEC}$ and $Pten^{+/+}$ mice were inoculated via an oral gavage with a low inoculum of S. Typhimurium (2×10^4 in a volume of 200 mL/mouse).	56

Figure 24	The photograph above shows representative gross anatomical images of the ceca obtained from both $Pten^{+/+}$ mice (left) and $Pten^{\Delta IEC/\Delta IEC}$ mice (right).	56
Figure 25	Cecum weight was measured and then graphed to compare the susceptibility to *S*. Typhimurium infection between the mouse groups	57
Figure 26	The image above shows a Hematoxylin and Eosin (H&E) staining of mice cecum sections.	58
Figure 27	The image above shows a Hematoxylin and Eosin (H&E) staining of mice small intestine sections.	59
Figure 28	The graphs above display quantified histological parameters were for H&E sections of the cecum (shown left) and small intestine (shown right) of the two mouse groups (n = 7/group).	60
Figure 29	The graphs above show pro-inflammatory cytokine levels of the small intestine of $Pten^{\Delta IEC/\Delta IEC}$ and $Pten^{+/+}$ mice.	61
Figure 30	The graph above compares the myeloperoxidase (MPO) levels in the small intestine of $Pten^{\Delta IEC/\Delta IEC}$ and $Pten^{+/+}$ mice	62
Figure 31	The images above show the bacterial load found in extraintestinal organs of $Pten^{\Delta IEC/\Delta IEC}$ and $Pten^{+/+}$ mice.	64
Figure 32	This graph shows the relative bodyweight change of IL-10 KO mice vs IL-10 WT mice.	70
Figure 33	The image above depicts the gross anatomy of the colon of both IL-10 wild-type controls (first 3 colons starting from left to right) and IL-10 KO mice (last 4 colons starting from left to right).	71
Figure 34	This graph shows the measurement of IL-1β pro-inflammatory cytokine expression in the colon tissue of piroxicam-fed IL-10 KO mice (red circles, n=17) and IL-10 WT mice (blue circles n=11).	72

Figure 35 This graph shows the measurement of IL-1β pro-inflammatory cytokine expression in the hippocampus tissue of piroxicam-fed IL-10 KO mice (red circles, n=14) and IL-10 WT mice (blue circles n=11). 73

Figure 36 This graph shows the measurement of IL-1β pro-inflammatory cytokine expression in the cerebrum tissue of piroxicam-fed IL-10 KO mice (red circles, n=16) and IL-10 WT mice (blue circles n=11). 74

Figure 37 This graph shows the measurement of IL-6 pro-inflammatory cytokine expression in the colon tissue of piroxicam-fed IL-10 KO mice (red circles, n=16) and IL-10 WT mice (blue circles n=16). 75

Figure 38 This graph shows the measurement of IL-6 pro-inflammatory cytokine expression in the hippocampus tissue of piroxicam-fed IL-10 KO mice (red circles, n=16) and IL-10 WT mice (blue circles n=16). 76

Figure 39 This graph shows the measurement of IL-6 pro-inflammatory cytokine expression in the cerebrum tissue of piroxicam-fed IL-10 KO mice (red circles, n=16) and IL-10 WT mice (blue circles n=11). 77

LIST OF ABBREVIATIONS

AJ	Adherens junction
CD	Crohn's disease
ELISA	Enzyme-linked immunosorbent assay
GI	Gastrointestinal
IBD	Inflammatory bowel disease
IBS	Irritable bowel syndrome
IEC	Intestinal epithelial cell
IL	Interleukin
KO	Knockout
MPO	Myeloperoxidase
NLR	Nod-like receptor
NOD	Nucleotide oligomerization domain
PCNA	Proliferating cell nuclear antigen
PHTS	PTEN hamartoma tumor syndrome
PIP_2	Phosphatidylinositol 4,5-bisphosphate
PIP_3	Phosphatidylinositol (3,4,5)-trisphosphate
PTEN	Phosphatase and tensin homolog
TJ	Tight junction
TLR	Toll-like receptor
UC	Ulcerative colitis

CHAPTER ONE

BACKGROUND AND SIGNIFICANCE

1.1: Introduction

Hippocrates, the father of medicine, once stated that "all disease begins in the gut". Although a generalized statement, this proverb has only begun to be appreciated due to recent understanding of chronic inflammatory diseases in the gut. It was originally believed that genetic predisposition and exposure to environmental triggers were both necessary to develop chronic inflammatory diseases or cancer. However, it is becoming more evident that chronic inflammatory diseases, such as IBD, come from a complex interplay between genetic and environmental factors, as well as, constituents of the gut microbiome (Fasano, 2020). Recent research has also identified a bidirectional connection between the enteric nervous system and central nervous system known as the gut-brain axis, where emotional and cognitive centers of the brain are linked with peripheral intestinal functions (Carabotti et al., 2015). The brain-gut axis affects functions such as motility of the gut, intestinal permeability, and immune activation. Recent advances also suggest that the gut microbiota exhibits a great influence over the gut-brain axis by their metabolites and by products (Rutsch et al., 2020). In clinical practice, dysbiosis of gut microbiota has been associated with central nervous system disorders like Parkinson's disease, Alzheimer's disease and dementia (Peterson, 2020; Stadlbauer et al., 2020). Although the exact mechanisms of these diseases remain unclear, these new finding echo Hippocrates's proverb, suggesting the cause of some of disease to be rooted in the gut.

1.2: Inflammatory Bowel Disease

Inflammatory bowel disease (IBD) is an umbrella term that is mostly encompassed by Crohn's disease (CD) and ulcerative colitis (UC). IBD is typically characterized by episodes of abdominal pain, bloody stools, diarrhea, weight loss, and an influx of neutrophiles and macrophages that produce cytokines, proteolytic enzymes, and free radicals which result in inflammation and ulceration (Stokkers & Hommes, 2004; Szigethy et al., 2010). Both CD and UC may occur in adolescents and adults and affect men and women equally (Baumgart & Sandborn, 2007). IBD has been considered one of the most prevalent gastrointestinal (GI) diseases with a growing incidence rate in newly industrialized countries, with the highest prevalence remaining in Europe and North America (Ng et al., 2017). The two diseases differ in their location and depth of involvement within the bowel wall. UC is typically marked by diffuse inflammation of the colonic mucosa, usually affecting the rectum, but may extend into or beyond the sigmoid colon, or include the colon up to the cecum; whereas CD results in transmural ulceration of any portion of the GI tract, but tends to affect the terminal ileum and colon more (McDowell et al., 2022). Although the etiology of IBD remains unknown, progress has been mad to uncover the pathogenesis of this disease. Studies have provided evidence that IBD could be associated with factors such as genetic susceptibility, intestinal microbiota dysbiosis, immunological abnormalities and other environmental components (Kaser et al., 2010; Monteleone et al., 2006). This indicates that the intestinal epithelial barrier dysfunction could be playing central role in IBD, given the importance of the intestinal epithelial barrier in inhibiting toxins and pathogenic microbes to underlying tissues.

1.3: The Gut Epithelial Barrier

The human body consists of many mucosal epithelia that form a direct barrier between the environment and the internal host milieu. The GI tract harbors the largest luminal barrier in the human body, and it prohibits the passage of potentially harmful antigens, microorganisms, and toxins by working together with immune and stromal cells (Helander & Fändriks, 2014).

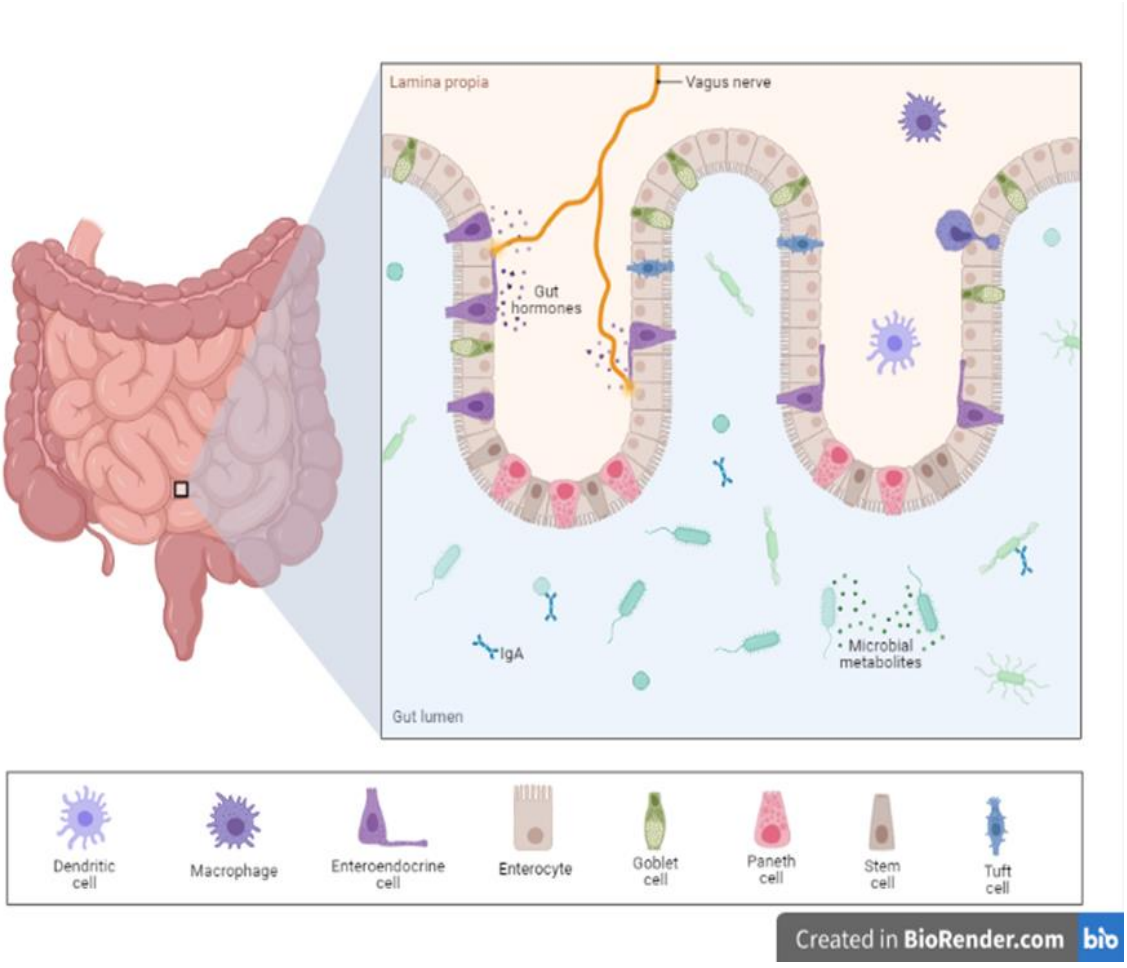

Figure 1: The illustration above depicts a "zoomed-in view" of the intestinal microenvironment. The different assortment of cells constitutes the gut epithelial barrier, which separates the gut lumen from the lamina propria. Commensal microbes, food particles, microbial metabolites, and foreign antigens reside in the gut lumen. Immune cells, like macrophages and dendritic cells, occupy the lamina propria. These immune cells will commonly reach across the barrier for antigen sampling to maintain intestinal homeostasis.

Therefore, the GI tract plays a pivotal role in the immune system (Turner, 2009). The GI barrier is comprised of a single layer of intestinal epithelium which lines the gut lumen, and it is a selectively permeable barrier to permit the flux of water, electrolytes, and essential dietary nutrients (Blikslager et al., 2007; Bröer, 2008; Ferraris & Diamond, 1997; Kunzelmann & Mall, 2002). The two major routes in which intestinal epithelium mediates selective permeability are the transcellular pathway and the paracellular pathway. The transcellular permeability pathway is typically associated with solute transport through the epithelial cells and is primarily regulated by select transporters for amino acids, electrolytes, short-chain fatty acids (SCFAs), and sugars (Bröer, 2008; Ferraris & Diamond, 1997; Kunzelmann & Mall, 2002). The paracellular permeability pathway is associated with transport in the space between epithelial cells and is regulated through intercellular junctional complexes localized at the apical-lateral membrane and along the lateral membrane (Turner, 2009; Van Itallie & Anderson, 2006). Together, these two pathways regulate the crossing of the GI barrier.

Individual intestinal epithelial cells (IECs) make a monolayer of epithelial cells to form the intestinal epithelium through cell-cell junctions. This monolayer of cells, along with many other cell types, will all come together to form the intestinal epithelial barrier. The cell-cell junction is comprised of several cell-cell structures: tight junctions (TJs), adherens junctions (AJ), gap junctions, and desmosomes (Campbell et al., 2017). These different junctions work together to modulate intestinal permeability, or barrier entry, which allows different constituents of the intestines to pass through.

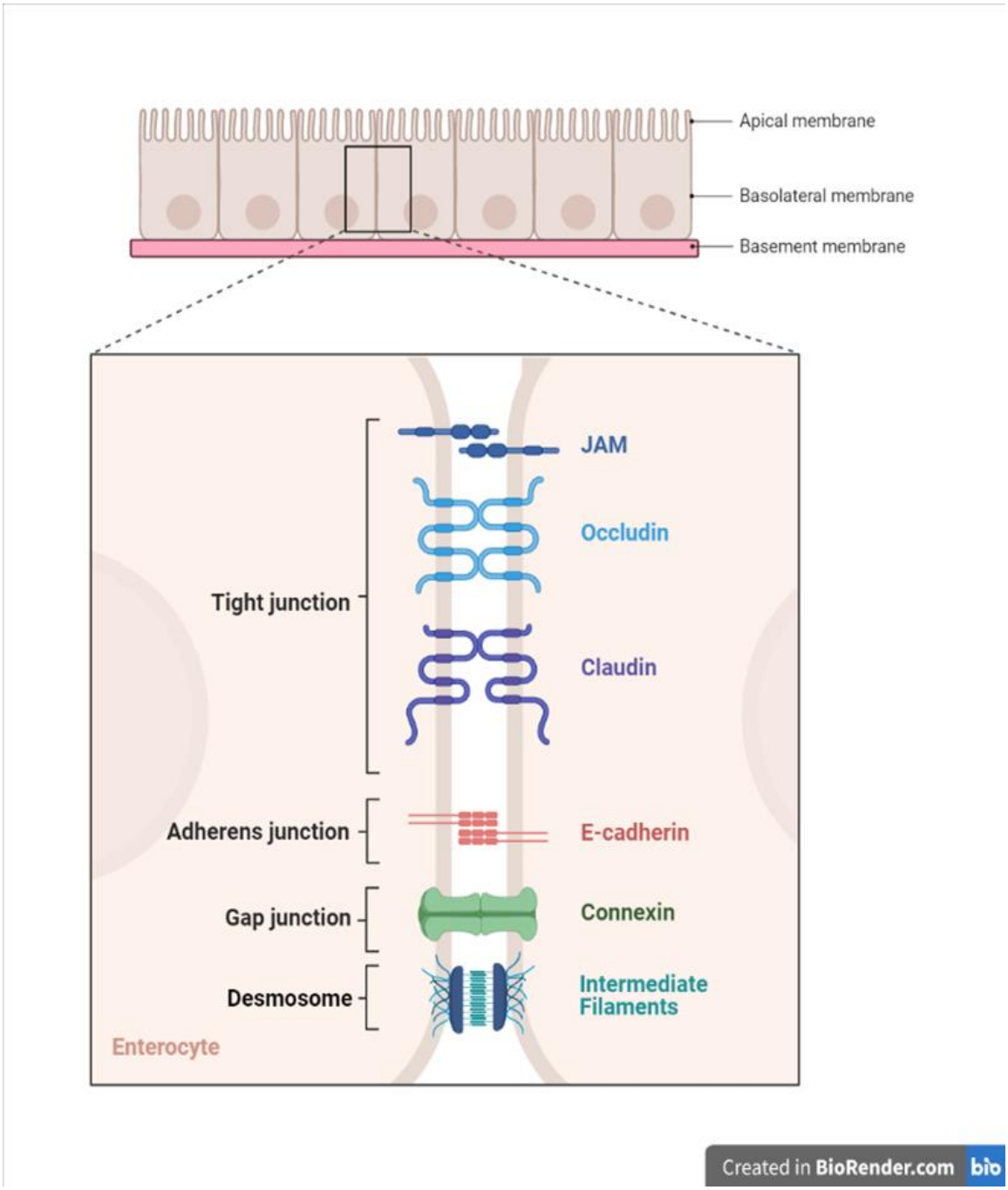

Figure 2: The illustration above portrays a view of junctional protein complexes between cells of the gut epithelial barrier. These junctional protein complexes are responsible for regulating the permeability of the gut barrier. Without proper barrier function, microbial translocation can more readily occur and promote inflammation.

These junctional complexes are comprised of transmembrane proteins that link adjacent cells to the actin cytoskeleton via cytoplasmic scaffolding proteins (Groschwitz & Hogan, 2009). TJs are the apical junctional complexes that consist of transmembrane proteins, peripheral proteins, and regulatory proteins and are mainly responsible for sealing the intercellular space (Harhaj & Antonetti, 2004; Vancamelbeke & Vermeire, 2017). The AJs and desmosomes are thought to be more important in the mechanical linkage of adjacent cell (Hartsock & Nelson, 2008). The AJ and TJ complexes are also important in the regulation of cellular proliferation, polarization, and differentiation (Cereijido et al., 2004; Tsukita & Furuse, 2000). Gap junctions provide a direct connection of cytoplasm between two neighboring cells. A gap junction channel is formed by end-to-end docking of two hemichannels or connexons, with each connexon comprised of six connexin subunits that connect across the intercellular space, and this link allows for electrical impulses, ions, and other small molecules to pass between cells (Willecke et al., 2002). Lastly, desmosomes function as cell-to-cell adhesion complexes similar to a ‘spot-weld’, where the desmosomes help meld cells together. Desmosomes are formed by desmosome-intermediate filaments complexes, which are a network of cadherin proteins, keratin intermediate filaments and linker proteins (Delva et al., 2009). Desmosomes have also been suggested to act as signaling centers which may help regulate fundamental processes such as cell proliferation, differentiation, and morphogenesis (Garrod & Chidgey, 2008). Together, these complexes, with other additional proteins, help maintain the integrity of the gut epithelial barrier and prevent the entry of antigens that could promote inflammation, and later on, inflammatory disease.

1.4: The Importance of the Cell Junctions

The intestinal epithelial barrier is a well-maintained dynamic system that is in constant contact with the gut microbiota, foreign antigens and other external environmental insults (Fasano, 2011; Nusrat et al., 2000). Failure of the gut barrier could allow these substances to invade the tissues beneath the intestinal epithelium and diffuse into the bloodstream, which could induce to secondary inflammation. The inflamed cells release pro-inflammatory cytokines and chemokines that lead to barrier impairment. One possible cause of gut barrier failure could stem from dysfunction of cell junction proteins, which would in turn cause an increase in intestinal permeability, thus allowing the passage of foreign antigens. The opening of intercellular tight junctions my act as a trigger for some disease (Farhadi et al., 2003). This increased permeability, also known as "leaky gut syndrome", may play a crucial role in the pathogenesis of many diseases (Clayburgh et al., 2004; Turner, 2009). Such diseases would include celiac disease (Bischoff et al., 2014), Crohn's disease (Gibson, 2004), multiple sclerosis (Yacyshyn et al., 1996), rheumatoid arthritis (Matei et al., 2021), type 1 diabetes (Viggiano et al., 2015), type 2 diabetes (Bischoff et al., 2014), and ulcerative colitis (Bruewer et al., 2005). The commensal gut microbiota plays a role in regulating the gut barrier by interacting through the host's pattern recognition receptors, which include toll-like receptors (TLRs) and nucleotide-binding oligomerization domain (NOD) – like receptors (NLRs) in a phenomenon known as antigen sampling. Some gut microbiota can directly interact with the gut intestinal barrier and cause dysfunction. Also, some bacterial products and metabolites can also indirectly affect the intestinal barrier function and can cause disruption of the barrier integrity.

1.5: The Gut Microbiome

The gut microbiota is comprised of all bacteria residing withing the GI tract. The gut microbiome has been an area of research interest for potential therapeutic gut microbe-host interactions. The gut microbiota plays important roles in absorption of nutrients and minerals, along with synthesis of amino acids, enzymes, SCFAs and vitamins (Moens & Veldhoen, 2012). The gut microbiota are also essential in the defense against pathogens due to competition for adhesion sites and nutrients, where some will actively destroy competition via secretion of antimicrobial peptides (Kamada et al., 2013). This is accomplished by a phenomenon known as antigen sampling. In the GI tract, lamina propria dendritic cells of the small intestine will actively sample gut bacteria by the formation of transepithelial dendrites via a mechanism dependent on the CX3CR1 chemokine receptor (Foti & Ricciardi-Castagnoli, 2005). It has been recently shown that microbiota colonization in early life is necessary for optimal development of the immune system. In experiments with germ-free animals, intestinal mucosal immunity was underdeveloped and, the animals displayed smaller mesenteric lymph nodes, Peyer's patches and reduced number of immune cells, which overall results in a weakened ability to fend off pathogenic bacteria (Sommer & Bäckhed, 2013). However, it is still not exactly clear exactly how microbial composition regulates immune homeostasis.

1.6: Phosphatase and Tensin Homolog (Pten)

Phosphatase and tensin homolog (*PTEN*), also known as *MMAC1* or *TEP1*, was independently discovered by three different labs in 1997 as a tumor suppressor gene and as a novel tyrosine phosphatase (D. M. Li & Sun, 1997; J. Li et al., 1997; Steck et al., 1997). The tumor-suppressive role of PTEN was later confirmed by a germline mutation

in *Pten* resulting in a spectrum of rare autosomal dominant disorders known as PTEN hamartoma tumor syndrome (PHTS), which was characterized by multiple hamartomas (Pilarski, 2019). Pten mutations are associated with many types of tumors such as brain, breast, prostate, kidney, ovary, and skin (Haddadi et al., 2018; Jamaspishvili et al., 2018; J. Li et al., 1997; Que et al., 2018; Steck et al., 1997; Vecchio et al., 2013). *Pten* is only second to p53 mutations to cause tumor formation (Xu et al., 2014). Pten is a 200 kb gene located on chromosome 10q23.3 and is composed of nine exons and eight introns, and encodes a 403 amino acid long proteins with a relative molecular mass of approximately 47 kDa (X. C. Zhang et al., 2012). The amino- terminal region shares sequence homology with the actin filament capping protein Tensin and the putative tyrosine-protein phosphatase Auxilin (Stiles, 2009). Tensin is an actin-binding protein located in focal adhesion sites, whereas Auxilin is involved with the uncoating of clathrin-coated vesicles (Lo et al., 1994; Zhao et al., 2001). Crystal structure of PTEN reveals a C2 domain that contain the affinity for phospholipids on membranes and a phosphatase domain that contain the CX5R signature motif for phosphatases (Lee et al., 1999). In vitro, PTEN is capable of dephosphorylating phosphopeptides as well as phospholipids, thus PTEN possess both protein and lipid phosphatase activity (C.-Y. Chen et al., 2018). The lipid phosphatase activity is closely linked with the ability of PTEN to function as a tumor suppressor, whereas protein phosphatase activity is intramolecular and regulatory in nature (X. C. Zhang et al., 2012).

CHAPTER TWO

STUDYING THE ROLE OF PTEN IN THE INTESTINAL EPITHELIUM

2.1: Introduction

2.1.1: *Pten* in the Intestinal Epithelium

The *Pten* gene encodes a phosphatase enzyme that catalyzes the dephosphorylation of the 3' carbon of the inositol ring in phosphatidylinositol 3,4,5-triphosphate [PI(3,4,5)P3] to produce phosphatidylinositol biphosphate [PI(4,5)P2]; consequently, PTEN activation antagonizes the phosphatidylinositol 3-kinase (PI3K) mediated signaling pathways (Hsu & Mao, 2015). PIP3 produced by activated PI3K induces the activation of protein kinase B (AKT) mediated signaling pathways, which leads to enhanced cell proliferation, growth, metabolism, movement, polarization, and survival (Gupta & Leslie, 2016; Song et al., 2012). Given its phosphatase activity, the activation of PTEN reduces the cellular level of PIP3, which opposes PI3K induced cell proliferative signaling pathways. Contrarily, loss of the *Pten* gene leads to unopposed activation of the PI3K-AKT pathway. This perpetuates promotion of cell proliferation and survival and ultimately results in tumor development (Haddadi et al., 2018; Jamaspishvili et al., 2018; Que et al., 2018; Vecchio et al., 2013). Because inactivation leads to tumorigenesis, Pten has been classically regarded as a tumor suppressor gene. However, several studies have shown that Pten gene deletion in IECs does not induce tumor development in mice (Choi et al., 2013; Im et al., 2014; Langlois et al., 2009; Yu et al., 2014). This suggests that PTEN may play an alternative role in the intestinal epithelium.

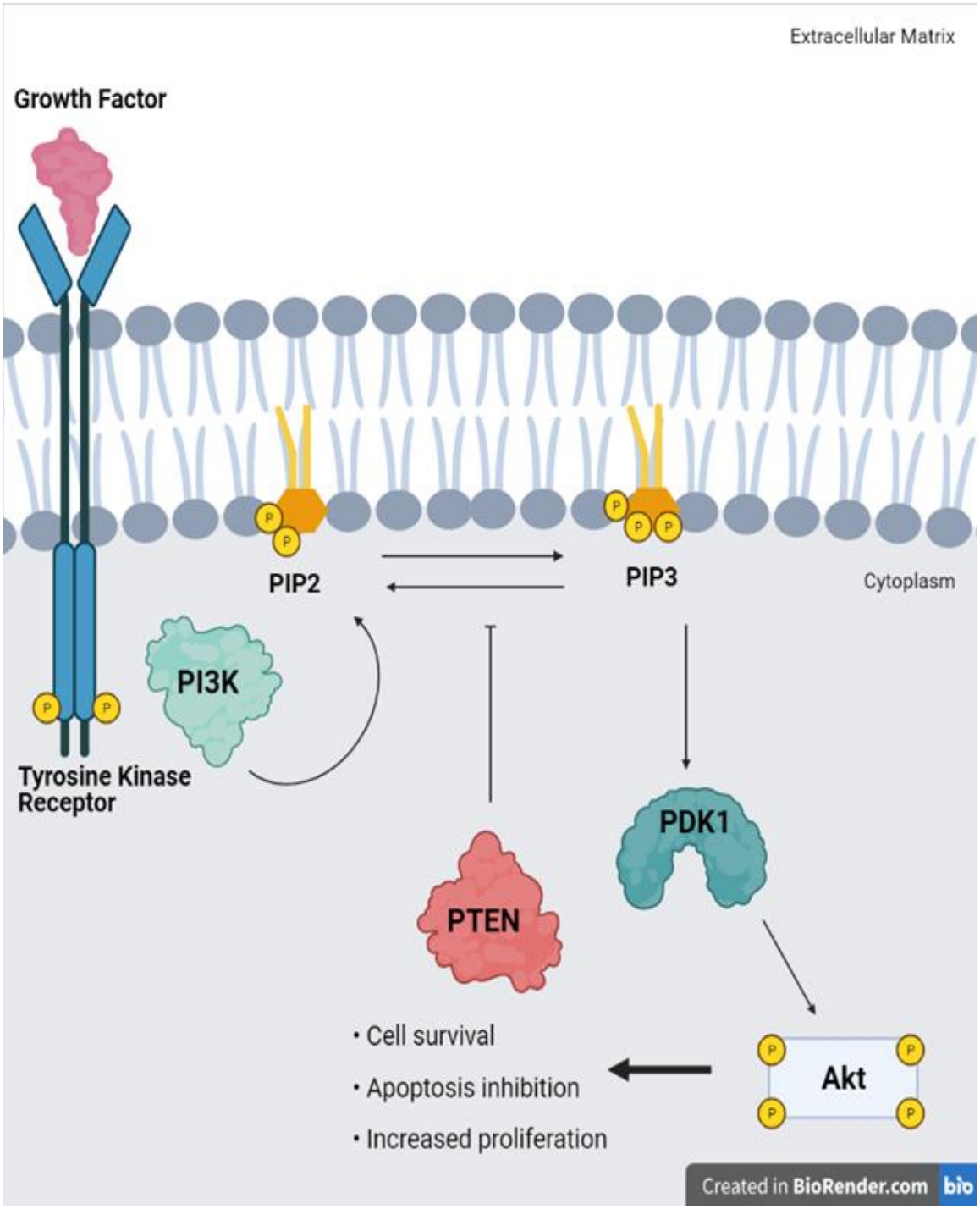

Figure 3: The illustration above depicts the typical PI3K/Akt signaling pathway. Through this pathway, cellular processes such as cell survival, apoptosis, proliferation are regulated. PTEN is a known agonist of this pathway, which results in a build-up of PIP2.

Some studies have suggested that PTEN deficiency is capable of inducing tumor development in the colon due to the tumor suppressor function of PTEN. For example, reduced PTEN expression has been observed in cancer tissues from colorectal cancer patients (Lin et al., 2015). Additionally, mutations to *Pten* may contribute to primary colon cancer development in humans (Colakoglu et al., 2008; Zhou et al., 2002). *Pten* gene alternations have also been associated with poor prognosis in patients with rectal cancer (Bohn et al., 2013). Similarly, conditional global *Pten* gene deletion, accomplished via interferon α/β-responsive gene (Mx-1) promoter-driven Cre expression, has been suggested to induce the development of small-sized tumors in the mouse intestine (Asano et al., 2003; X. C. He et al., 2007), while a global Pten knockout (KO) is embryonic lethal in mice (Cristofano et al., 1998). Together, these observations support the notion that *Pten* gene mutation may participate in the development of tumors within the colon.

In contrast, there is considerable evidence suggesting that *Pten* may not be directly associated with tumorigenesis in the colon. A study examining single nucleotide polymorphisms (SNPs) in the *PTEN* gene indicated that there may be no association between *PTEN* and colon cancer in humans (Phillips et al., 2009). Moreover, *PTEN* mRNA levels are not consistent among colorectal cancer tissues and vary depending on the tumor location (Kuramochi et al., 2016). *PTEN* mRNA expression was also seen to be preserved in human colorectal adenomas and adenocarcinomas (Taniyama et al., 2001). Together, these observations indicate that the loss of *PTEN* gene expression may not be directly associated with tumor development in the colon, thus suggesting that *PTEN* may have an alternate role in the intestinal epithelium.

2.2: Materials and Methods

2.2.1: Human Tissues

All human tissues were collected and analyzed with the approval of the UCLA Institutional Review Board (protocol: 14-000132), Wonkwang University Sanbon Hospital Institutional Review Board (protocol: 2011-07), and Seoul Paik Hospital Institutional Review Board (protocol: IIT-233). Participants (aged 32-85) that underwent colonoscopy screening provided written informed consent to the study protocol. Patients with a personal or first-degree family history of cancer were excluded. Patients with any infectious disease or intestinal inflammatory disease such as IBD were also excluded.

Two board certified gastroenterologists performed the colonoscopy and obtained the colorectal cancer tissues and adjacent normal colonic mucosa tissues (about 10 cm away from the lesion) at two independent medical centers in South Korea (Wonkwang University Sanbon Hospital and Inje University Seoul Paik Hospital). A pathologist was sent a small piece of each specimen to determine the pathological assessment. The remaining parts of the specimens were immediately immersed in RNAlater RNA stabilization reagent (Qiagen, Valencia CA) and stored at 4°C overnight and kept in liquid nitrogen until RNA isolation. Based on the pathologic determination from the pathologist, cancerous colonic tissues (adenocarcinoma) were selected for the experiment.

Similarly, unmatched normal colonic mucosa specimens were collected from tumor-free healthy subjects undergoing routine colonoscopy screening at Wonkwang University Sanbon Hospital. The patients examined in this study have never been included in any previous studies.

2.2.2: Animals

Pten floxed ($Pten^{loxP/loxP}$) (Groszer et al., 2001), Villin promoter-driven Cre expression mouse ($Vil^{Cre/+}$) (Madison et al., 2002), and $Apc^{min/+}$ mice (Kühn et al., 1993) on the C57BL/6 background were obtained from the Jackson Laboratory (Bar Harbor, ME). Intestinal epithelial cell (IEC)-specific Pten knockout (KO) mice ($Pten^{\Delta IEC/\Delta IEC}$) was generated by crossing $Pten^{loxP/loxP}$ mice with $Vil^{Cre/+}$ mice as described by previous studies (Choi et al., 2013; Im et al., 2014; Langlois et al., 2009). Mice were bred and maintained under standard SPF conditions with normal drinking water ad libitum at the animal facility of University of California Los Angeles and Oakland University under the approval of the Institutional Animal Care and Use Committees of UCLA and OU.

2.2.3: Quantitative Real-Time PCR:

Total RNA was initially isolated from human colon specimens or the full thickness of mouse intestinal tissues using RNeasy Plus Universal Midi Kit (Qiagen, Valencia, CA) as described in previous studies (Choi et al., 2010; Im et al., 2014). Then, an equal amount of RNA (4 μg in 40 μL) was transcribed into cDNA with a High-Capacity Reverse Transcription Kit obtained from Applied Biosystems (Foster City, CA). Afterwards, quantitative real-time PCR was performed with *Taq*Man Universal Master Mix to measure gene expression by following the standard conditions from Applied Biosystems in 7500 Fast Real-Time PCR system. After incubating at 50 °C (2 minutes) and activating Ampli*Taq* Gold activation at 95 °C for 10 minutes, samples were denatured at 95 °C for 15 seconds and annealed/extended at 60 °C for 1 minute for 40 cycles. The primer pair and FAM™ dye-labeled *Taq*Man® MGB (minor groove binding)

probes were purchased from Applied Biosystems. Gapdh was included as an internal control.

Using the PCR cycle (C_T) at which the probe's fluorescent intensity passes a certain threshold value (C_T) at the exponential phase, the level of expression was calculated. Through the difference in the C_T values of the target genes after normalization to RNA input level, relative gene expression was determined using the C_T value of control Gapdh. The delta/delta C_T ($2^{-\Delta\Delta C_T}$) method was used to calculate the relative gene expression. Each reaction was performed in triplicate (Livak & Schmittgen, 2001). A Mann-Whitney U-test was performed on the normalized data to check whether the relative gene expression is statistically different ($P < 0.05$).

2.2.4: Transmission Electron Microscopy

The mouse colon tissues were obtained from 3-month-old and gender-matched $Pten^{\Delta IEC/\Delta IEC}$ and $Pten^{+/+}$ mice. The dissected tissues were immersed in a solution containing 2% glutaraldehyde and 2% paraformaldehyde in 0.1 M phosphate-buffered saline (PBS) (pH 7.4) for 2 hours at room temperature and then incubated at 4 °C overnight as described in a previous publication (Im et al., 2014). On the next day, 0.5% of tannic acid was added to the tissues and incubated for 1 hour at room temperature. Then, the tissue blocks were washed five times in 0.1 M PBS buffer and post-fixed in a solution of 1% OsO_4 in PBS (pH 7.2-7.4). The combination of tannic acid/glutaraldehyde/paraformaldehyde followed by osmification increased the staining of the membranes. The samples were washed four time in sodium acetate buffer (pH 5.5), block-stained in 0.5% uranyl acetate in 0.1 M sodium acetate buffer (pH 5.5) for 12 hours at 4 °C. Next, the samples were dehydrated in graded ethanol (50%, 75%, 95%, 100%,

100%, 100%) for 10 minutes each. The samples were then passed through propylene oxide and infiltrated in mixture of Epon 812 and propylene oxide in a 1:1 ratio, and then in a 2:1 ratio for 2 hours each. The tissues were then infiltrated in pure Epon 812 overnight. Embedding was then performed in pure Epon 812 and curing was done in an oven at 60 °C for 48 hours. Sections of 60 nm thickness (gray interference color) were cut on an ultramicrotome (RMC MTX) using a diamond knife. The sections were deposited on single-hole grids coated in Formvar and carbon and double-stained in aqueous solutions of 8% uranyl acetate for 25 minutes at 60 °C and lead citrate for 3 minutes at room temperature. Thin sections were then examined with a 100CX JEOL transmission electron microscope.

2.2.5: Immunohistochemistry

Mouse colon tissues were embedded and frozen immediately. 6 μm sections were cut and fixed in acetone for 15 minutes at 4 °C. After rehydration, sections were blocked with 2% bovine serum albumin (BSA) solution for 10 minutes and incubated overnight with primary rat anti-mouse Ki-67 antibody diluted (1:100) in 2% BSA solution with 0.3% Triton X-100 at 4 °C. Negative controls were given an equivalent concentration of non-immune rat IgG. After washing with PBS, sections were incubated with biotinylated anti-rat secondary antibody (Vector Laboratories, Burlingame, CA) diluted (1:200) in 2% BSA solution with 0.3% Triton X-100 for 45 minutes at room temperature. After inactivating endogenous peroxidase, sections were processed for peroxidase immunohistochemistry. A 0.2% light green (Sigma) solution was used for counterstaining.

After using the microscope to visualized the Ki-67-stained sections, each transverse section was divided into four quadrants. Crypt cell nuclei with clear positive brown staining were counted. The ration between the number of cells labeled as Ki-67 positive and total cell count was expressed as a percentage, thus referred to as the Ki-67 proliferative cell index.

2.2.6: Immunofluorescence Staining

Tissues were fixed with 10% neutral buffered formalin solution (sigma-Aldrich, St. Louis, MO) at room temperature to visualize the expression of phosphor-AKT(Ser473) and PCNA in colon tissues. After paraffin embedment, the 5 μm thick sections were prepared. The slides with tissue sections were dewaxed with xylene for 7 minutes twice and rehydrated with 100% ethanol for 2 minutes twice. Sections were then soaked in 95% ethanol for 2 minutes and then 70% ethanol for 2 minutes. Then, slides were rinsed with distilled water and boiled in sodium citrate buffer at 95 °C for 20 minutes for antigen retrieval. Sections were then washed with TBST-T for 5 minutes twice and rinsed with distilled water. Tissues were washed with PBS (pH 7.5) (Hyclone Inc., Logan, UT) containing 0.05% Triton X-100 for 5 minutes twice to reduce surface tension. To block non-specific binding, sections were soaked in blocking buffer (Protein Block Serum-Free, Aglient, Santa Clara, CA) containing 0.1% Triton X-100 for 2 hours at room temperature. Primary antibodies (p-AKT, #9271, Cell Signaling Technology), PCNA (sc-56, Santa Cruz Biotechnology, Inc.) were diluted in blocking buffer with a 1:200 ratio. Slides containing blocked tissues were incubated in a humidified chamber at 4 °C overnight. After the incubation, slides were then soaked in PBS-T for 5 minutes and repeated 4 times. Goat anti-rabbit IgG-heavy and light chain antibody FITC conjugated

(A120-101F) and Goat anti-mouse IgG-heavy and light chain antibody FITC conjugated (A90-116F) were selected from Bethyl Laboratory, Inc (Montgomery, TX). After preparing diluted secondary antibodies with blocking buffer, the secondary antibodies were then added to the tissue sections and incubated for 2 hours at room temperature. Slides were rinsed thoroughly 5 times with PBS-T for 5 minutes each. Next, the slides were mounted with VECTASHIELD® Mounting Medium with 4',6-diamidino-2-phenylindole (DAPI) (Vector Laboratories, Burlingame, CA). Stained tissues were observed by FV10i (Olympus Inc, Center Valley, PA) with image analysis by FV10i FluoView software.

2.2.7: Cancer-Pathway Focused Gene Analysis

A cancer pathway-focused PCR gene array analysis (Cat. No. PAMM-0033Z; Qiagen, Valencia, CA) was performed in accordance with the manufacturer's instruction to analyze the cancer-associated gene expression. Immediately after harvesting the small intestinal tissues, total RNA was isolated using RNeasy Plus Universal Midi Kit (Qiagen, Valencia, CA). 1 μg of total RNA was treated with DNase. cDNA was synthesized using RT^2 First Strand kit (Qiagen, Valencia, CA). For each analysis, cDNA samples were mixed with RT^2 qPCR Master mix and distributed across the PCR array 96-well plates containing gene PCR probes and control housekeeping gene probes. The amplification cycling was performed with an ABI 7500 Fast Real Time PCR System (Applied Biosystems, Foster City, CA). Then, the data (fold-changes in C_T values for all the genes) was analyzed with SABiosciences software was provided by the manufacturer.

2.2.8: Fecal Sample Collection for Microbiome Analysis

Co-fostered Pten $^{\Delta IEC/\Delta IEC}$ mice and littermate Pten $^{+/+}$ mice were obtained from a single parental breeder cage in a SPF condition with standard breeding conditions. Pten $^{\Delta IEC/\Delta IEC}$ and Pten $^{+/+}$ mice were co-housed in a single cage after weaning. When the mice reached 3 months old, the fecal stool pellet samples were collected from the colon, and snap-frozen in liquid nitrogen before sequencing.

2.2.9: DNA Extraction from Mouse Fecal Samples

In accordance with the manufacturer's instructions, Genomic DNA was purified from fecal samples with PowerSoil® DNA Isolation Kit (MoBio, Carlsbad, CA). Approximately 2 fecal pellets were subjected to the PowerBeads tube for cell lysis. The isolated genomic DNA was eluted from the spin filter using 50 μL of elution buffer and stored at −20°C until PCR amplification.

2.2.10: PCR Amplification and Amplicon Sequencing Using Next Generation Technology

Next generation technology (bTEFAP®) can be utilized to examine a broad range of microbiomes as described in previous studies (Dowd, Callaway, et al., 2008; Dowd, Sun, et al., 2008). An updated version of bTEFAP® has adapted to non-optical sequencing technologies such as the Ion Torrent PGM as well as the Illumina MiSeq and HiSeq platforms and become one of the most widely published methods to evaluate microbiota.

V1–3 regions of Eubacterial 16S rDNA was amplified using primers the 16S universal Eubacterial primer 27F-519R set (27F AGRGTTTGATCMTGGCTCAG, and 519R GTNTTACNGCGGCKGCTG) to assess the microbial ecology of each sample on

the MiSeq with methods via the bTEFAP® DNA analysis, spans (Im et al., 2014). A single-step 30 cycle PCR using HotStarTaq Plus Master Mix Kit (Qiagen, Valencia, CA) was used under the following conditions: 94°C for 3 minutes, followed by 28 cycles of 94 °C for 30 seconds; 53 °C for 40 seconds and 72 °C for 1 minutes, final elongation 72 °C for 5 minutes. Amplicons were further purified using Agencourt Ampure beads (Agencourt Bioscience Co., Beverly, MA) and equimolar amplicons were pooled. Following PCR, all amplicon products from different samples were mixed in equal concentrations and purified using Agencourt Ampure beads (Agencourt Bioscience Co., Beverly, MA). Sequencing was performed with the Illumina MiSeq in accordance with the manufacturer's protocols.

2.2.11: Sequence Analysis

The sequence data obtained from MiSeq was elaborated through a proprietary analysis pipeline (MR DNA, Shallowater, TX). Barcodes and primers were trimmed, then short sequences < 200bp, sequences with ambiguous base calls, sequences with homopolymers exceeding 6bp, and chimeric sequences were removed. Sequences were then denoised. Operational taxonomic units (OTUs) were defined after removal of singleton sequences, clustering at 3% divergence (97% similarity) (Dowd, Callaway, et al., 2008; Edgar, 2010; Swanson et al., 2011). OTUs were then taxonomically classified using BLASTn against a curated GreenGenes/RDP/NCBI derived database and compiled into each taxonomic level (DeSantis et al., 2006).

Normalized and denoised files were then run through QIIME (Quantitative Insights Into Microbial Ecology) to generate alpha and beta diversity data, as described previously (Callaway et al., 2010; Swanson et al., 2011). Based upon weighted unifrac

analysis in the QIIME, principal coordinates analysis (PCoA) plots were generated. Additional statistical analyses were performed with NCSS2007 (NCSS, UT) and XLstat2012 (Addinsoft, NY). Significance reported for any analysis is defined as $p<0.05$.

2.2.12: Alpha and Beta Diversity Analysis

Alpha and beta diversity analysis was conducted as described in other previous studies using QIIME (Callaway et al., 2010; Swanson et al., 2011). Alpha diversity is essentially a means to evaluate how many different bacterial species are within the given sample or treatment group. Beta diversity allows comparison of the community of bacteria as a whole taking into account both how many different things are in the sample and what those things are related to phylogenetically.

2.2.13: Statistical Analysis:

Statistical analysis was conducted with GraphPad Prism (GraphPad Software, Inc., San Diego. CA) unless stated otherwise. Additional information regarding statistical analysis is presented in the corresponding figure legend. P values less than 0.05 were considered significant.

2.3: Results

2.3.1: Pten mRNA Expression was Reduced in Colon Cancer Biopsies Compared to Normal Tissues

To investigate the association of *PTEN* deficiency with colonic tumor development, we evaluated the *PTEN* mRNA expression in human colon cancer tissues. Colon cancer and adjacent normal tissues (matched) were obtained from patients with colon cancer. Normal colonic biopsies were also collected from healthy control subjects (unmatched). With quantitative real-time PCR, *PTEN* mRNA level was found to be

substantially lower in the colon cancer tissues compared to matched normal tissues. *PTEN* mRNA expression was also lower in colon cancer tissues when compared to the expression level in unmatched normal tissues. Though, the *PTEN* mRNA expression level was comparable between the normal colonic biopsies obtained from colon cancer patients and control subjects.

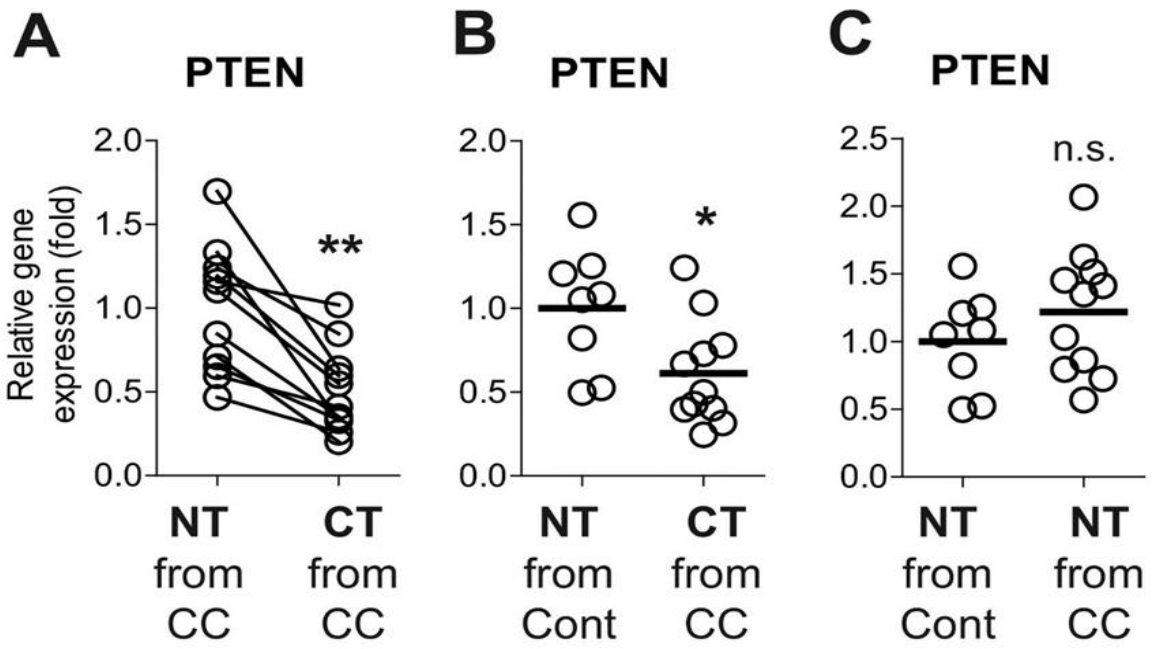

Figure 4: *PTEN* mRNA expression was decreased in human colon cancer tissues compared to normal tissues. (4A) *PTEN* mRNA levels were evaluated by qPCR with matched normal tissues (NT) and colon cancer tissues (CT) obtained from colon cancer (CC) patients (11 sets). (4B) The mRNA level was evaluated between unmatched normal tissues (n = 8) independently obtained from healthy control subjects and the colon cancer tissues (n = 11) from colon cancer patients. (4C) The mRNA expression in unmatched normal tissues (n = 8) from healthy control subjects was compared with the data in the normal tissues from colon cancer patients (n = 11). * $P < 0.05$, ** $P < 0.01$, n.s. stands for not significant (Mann-Whitney U test). Each bar indicates mean.

This data suggests that decreased *PTEN* expression is associated with colon cancer development in humans. This finding is congruent with previous studies indicating that *PTEN* deficiency may be associated with colon cancer development and metastasis in humans, along with poor patient prognosis (Wang et al., 1998; Zhou et al., 2002).

2.3.2: Generating the Intestinal Epithelial Cell Specific *Pten* Gene Knockout Mice

Villin promoter-driven Cre expression mouse ($Vil^{Cre/+}$) and *Pten* floxed ($Pten^{loxP/loxP}$) on the C57BL/6 background were purchased from the Jackson Laboratory (Bar Harbor, ME). IEC-specific *Pten* KO mice ($Pten^{\Delta IEC/\Delta IEC}$) were generated by crossing $Pten^{loxP/loxP}$ mice with $Vil^{Cre/+}$ mice. The protein villin is specific for the villi structures of IECs, and when Cre recombinase is inserted after the villin promoter, it will drive the expression of Cre solely in IECS. The loxP sequence will flank both sides of the gene sequence of *Pten* and act as a guide for Cre recombinase to cut the sequence of *Pten* specifically in IECs of the gut. This will allow the chance to study the effect of *Pten* gene deletion in mice, as an organism-wide KO of *Pten* is embryonic lethal in mice.

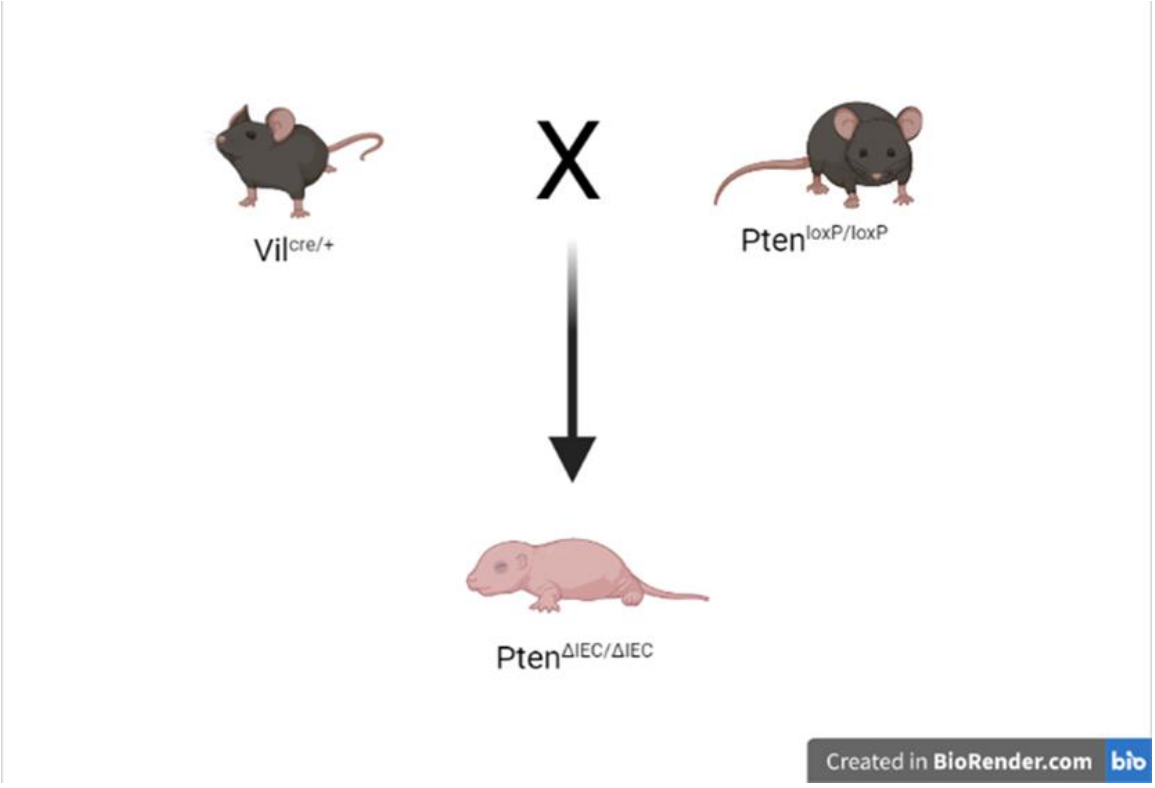

Figure 5: The illustration above shows the mating cross between $Vil^{cre/+}$ mice and $Pten^{loxp/loxp}$ mice using the Cre-lox recombinase system. Once the mice are crossed, the offspring produced will be a non-lethal, intestinal tissue-specific knockout, or $Pten^{\Delta IEC/\Delta IEC}$ mice.

2.3.3: Intestinal Epithelial Cells of Pten$^{\Delta IEC/\Delta IEC}$ Mice Exhibited Enhanced Epithelial Cell Growth in the Gut

It was observed that the small intestine and colon were considerably longer in mice with IEC specific *Pten* gene deletion (Pten$^{\Delta IEC/\Delta IEC}$) than in littermate Pten$^{+/+}$ mice. This finding suggests that Pten$^{\Delta IEC/\Delta IEC}$ mice demonstrate enhanced mitotic activity compared those of Pten$^{+/+}$ mice.

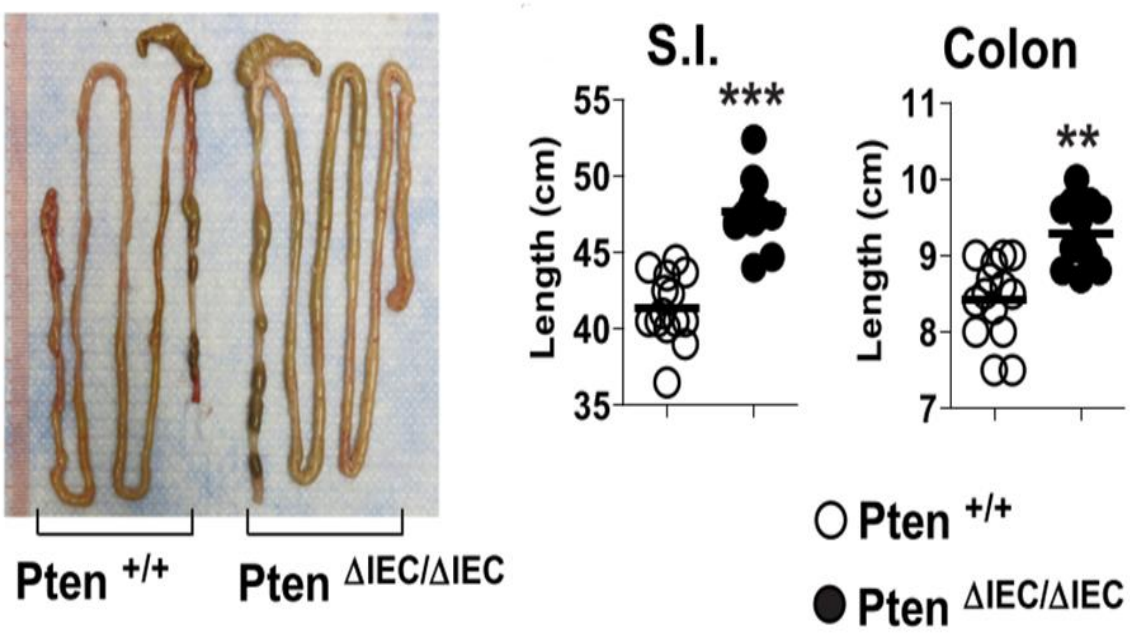

Figure 6: Intestinal epithelial cells of Pten$^{\Delta IEC/\Delta IEC}$ mice displayed enhanced mitotic activity compared to those of Pten$^{+/+}$ mice shown in the figures above (left and right). Presented to the left is the representative gross appearance of the intestine from Pten$^{\Delta IEC/\Delta IEC}$ and littermate Pten$^{+/+}$ mice. On the right, the image shows evaluated full length of the small intestine and the colon from one-year-old, sex matched mice (n=14/group).

It was also observed that the height of the villi in the colon was significantly increased, via Alcian blue staining, in Pten$^{\Delta IEC/\Delta IEC}$ mice compared to Pten$^{+/+}$ littermates. This additionally demonstrated that *Pten* gene deletion in IECs leads to an increased proliferative effect in the intestine of these mice.

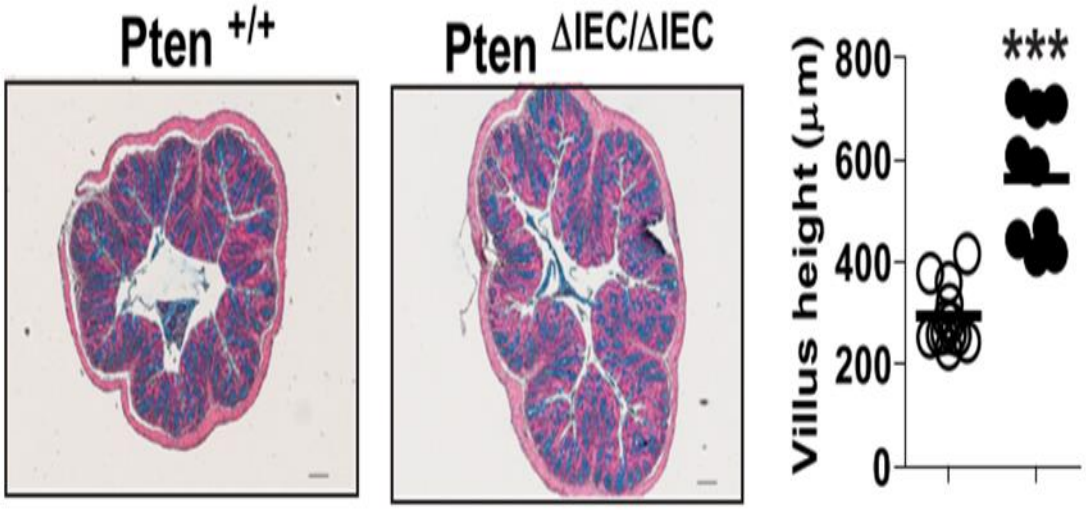

Figure 7: The above image shows paraffin-embedded sections of the mid-colon. These tissues were prepared from three-month-old, sex matched Pten$^{\Delta IEC/\Delta IEC}$ mice (n=9) and littermate Pten$^{+/+}$ (n=9) mice. The sections were then subjected to Alcian blue staining, followed by measurement of villus height under an Axio Imager Z1 microscope (Carl Zeiss, Oberkochen, Germany).

2.3.4: Intestinal Epithelial Cells of Pten$^{\Delta IEC/\Delta IEC}$ Mice Exhibited Enhanced Mitotic Activity

Despite *Pten* being typically regarded as a tumor suppressor gene, many groups have found that *Pten* gene deletion in mice does not lead to increased tumor formation (Choi et al., 2013; Im et al., 2014; Langlois et al., 2009). Thus, this study aimed to decipher why *Pten* deficiency alone in IECs is not enough to cause tumorigenesis.

First, the IECs of Pten$^{\Delta IEC/\Delta IEC}$ mice were investigated increased mitotic activity given the supposed enhanced Akt activation in these mice. Transmission electron micrographs revealed that the IECs of Pten$^{\Delta IEC/\Delta IEC}$ mice contained atypical nuclei with increased chromatids and chromosomal irregularities, while littermate control Pten$^{+/+}$ mice exhibited normal columnar epithelial cells with intact cell-to-cell interaction along the lateral surface.

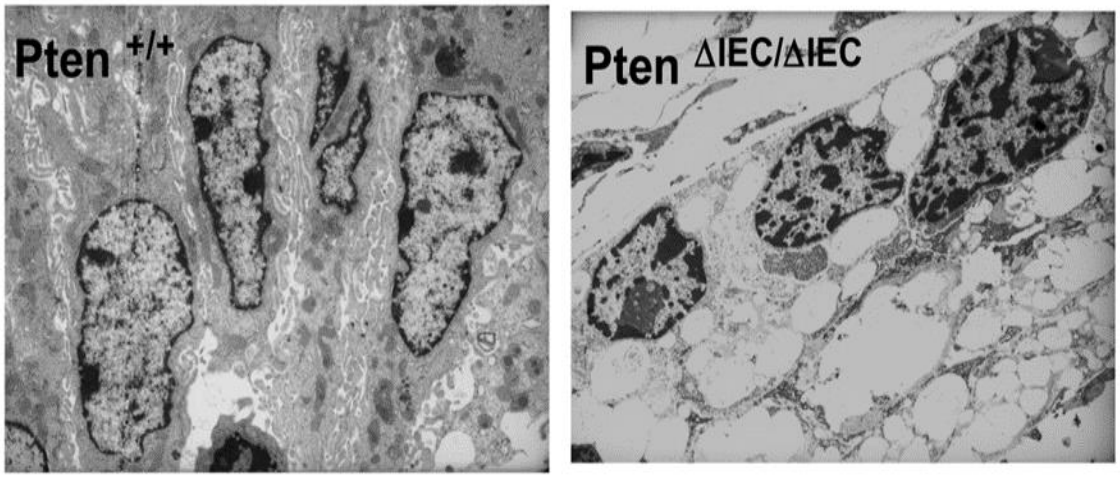

Figure 8: Presented in the above images are electron micrographs of the colonic epithelium from 12-month-old $Pten^{\Delta IEC/\Delta IEC}$ and littermate $Pten^{+/+}$ mice. The IECs of PtenΔIEC/ΔIEC mice contained atypical nuclei with increased chromatids and chromosomal irregularities.

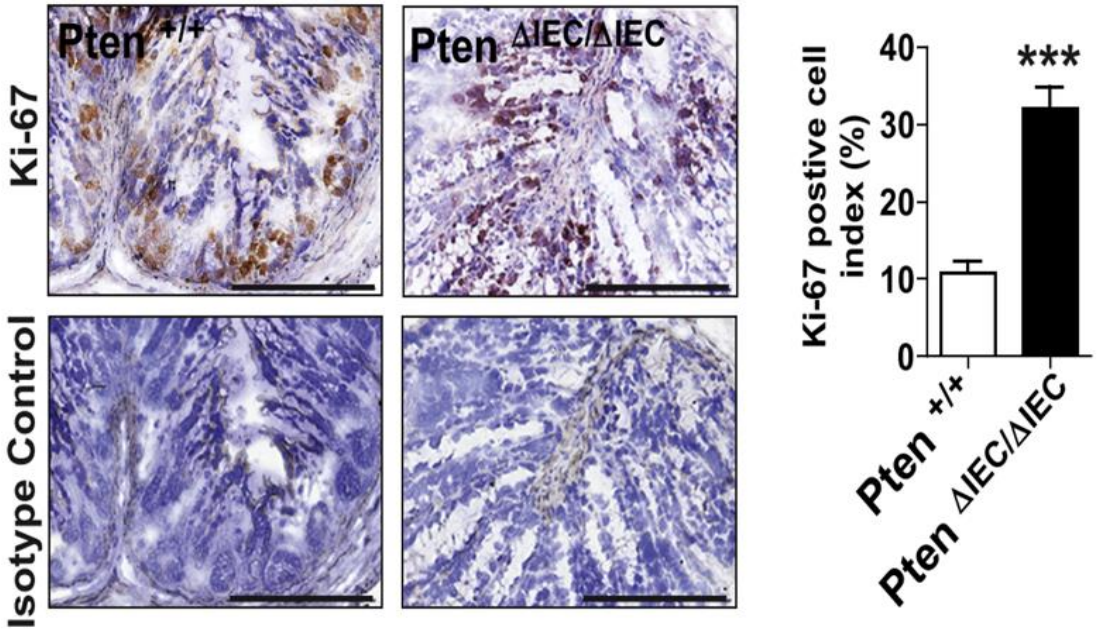

Figure 9: Cell proliferation was evaluated in the colon of $Pten^{\Delta IEC/\Delta IEC}$ and littermate $Pten^{+/+}$ mice. With frozen sections of the mouse colon, expression of the cell proliferation marker Ki-67 was evaluated by immunohistochemistry with an antibody against Ki-67 and its isotype control IgG. Ki-67 positive cell index was evaluated and presented as means ± SEM. ** $P < 0.01$, *** $P < 0.001$ (Mann-Whitney U test). Representative images from three independent experiments were presented. Each bar in the graph indicates mean. Scale bar represents 100 μm.

Similarly, by immunohistochemistry, the expression of cell proliferation marker Ki-67 was markedly increased in the colonic tissues of $Pten^{\Delta IEC/\Delta IEC}$ mice compared to $Pten^{+/+}$ control mice. Ki-67 is a well-known protein for its role in heterochromatin organization by preventing aggregation of mitotic chromosomes, thus acting as a good biomarker for cell proliferation (Sun & Kaufman, 2018). Increased cell proliferation was then further confirmed via immunofluorescence of both proliferating cell nuclear antigen (PCNA) and phosphorylated Akt (P-Akt). PCNA is known for its critical role during DNA replication. PCNA encircles DNA and functions as a processivity factor for DNA polymerase delta and DNA polymerase epsilon, allowing it to be a good biomarker for cell division, and thus, mitotic activity. Akt, or protein kinase B, is a protein in the PI3K signaling pathway which is involved in cell metabolism, cell survival, cell growth, and cell proliferation (Gupta & Leslie, 2016; Song et al., 2012). Given that PTEN would be absent from the PI3K signaling pathway, the activation of this pathway should occur unopposed, leading to increased expression of phosphorylated Akt in *Pten* deficient mice. Both PCNA and P-Akt were found to be significantly increased in the colonic tissue of $Pten^{\Delta IEC/\Delta IEC}$ mice compared to $Pten^{+/+}$ littermate control mice, which additionally supports the finding of increased proliferation of IECs. With all of these data taken together, these observations indicate that loss of the *Pten* gene in mice still increases the mitotic activity of IECs. However, even with this increased mitotic activity found in *Pten* deficient IECs, no tumor formation was discovered in any part of the small intestine or colon of these mice.

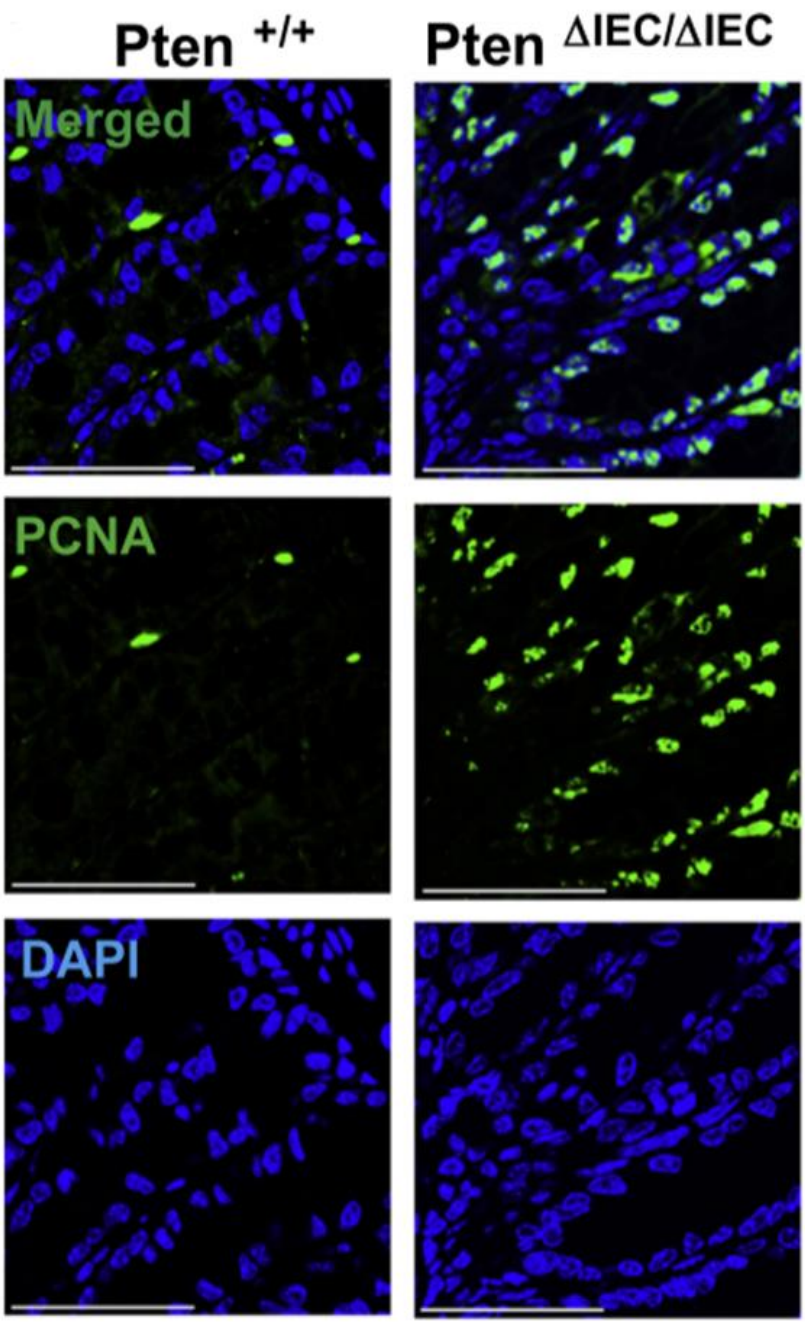

Figure 10: Paraffin-embedded sections of the mid-colon were subjected to immunofluorescence staining with PCNA antibody. An increased expression of PCNA was found in $Pten^{\Delta IEC/\Delta IEC}$ mice compared to littermate $Pten^{+/+}$ mice. Scale bar represents 50 μm.

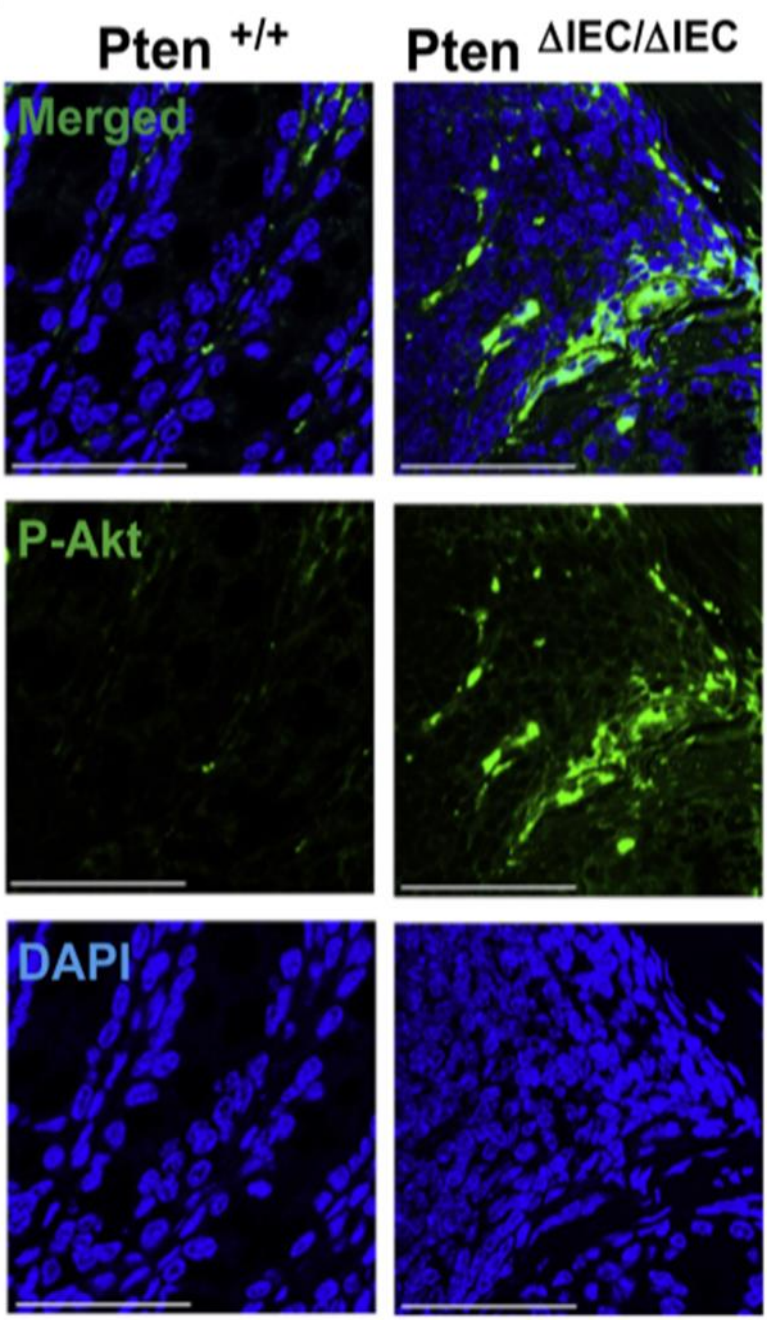

Figure 11: Paraffin-embedded sections of the mid-colon were subjected to immunofluorescence staining with phospho-Akt (P-Akt) antibody. An increased expression of P-Akt was found in $Pten^{\Delta IEC/\Delta IEC}$ compared to littermate $Pten^{+/+}$ mice. Scale bar represents 50 μm.

With no tumor formation in the *Pten* deficient mice, this brought into question if defective *Pten* in intestinal epithelial cells still retained the potential to promote tumorigenicity, or if *Pten* just participates in the regulation of immune and inflammatory responses without influencing tumor development. To answer this question, an $Apc^{min/+}$ mouse model was utilized. The $Apc^{min/+}$ model is known to exhibit multiple intestinal neoplasias, which mimic human familial adenomatous polyposis and colorectal tumors (Ren et al., 2019). $Pten^{\Delta IEC/\Delta IEC}$; $Apc^{min/+}$ mice were generated by breeding the $Pten^{\Delta IEC/\Delta IEC}$ mice with $Apc^{min/+}$ mice. Through this breeding, extensive tumor development throughout the small intestine and colon of $Pten^{\Delta IEC/\Delta IEC}$; $Apc^{min/+}$ mice was observed.

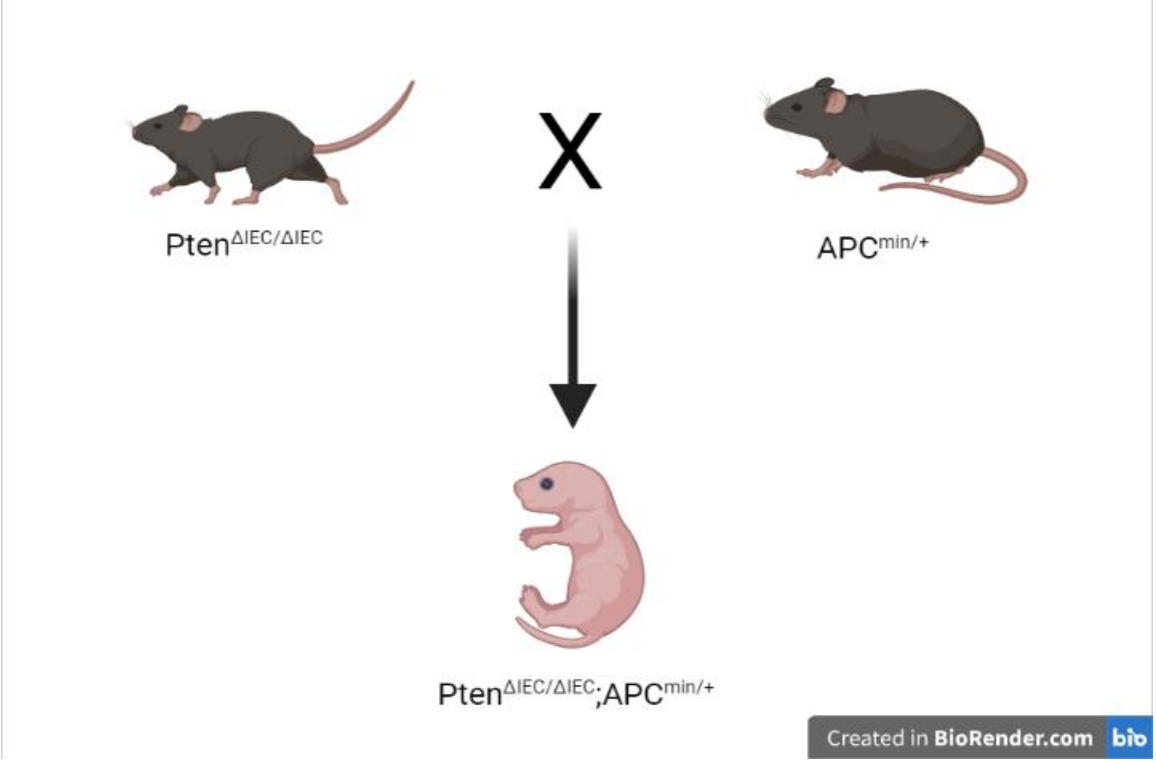

Figure 12: The illustration above depicts the mating cross between $Pten^{\Delta IEC/\Delta IEC}$ mice and $APC^{min/+}$ mice. Once crossed, the mice will produce $Pten^{\Delta IEC/\Delta IEC;}$ $APC^{min/+}$ mice. In these newly generated mice, we observed marked tumor development throughout the intestine, thus demonstrating that there remains a potential tumorigenic drive, but *Pten* deficiency alone is unable to cause tumorigenesis.

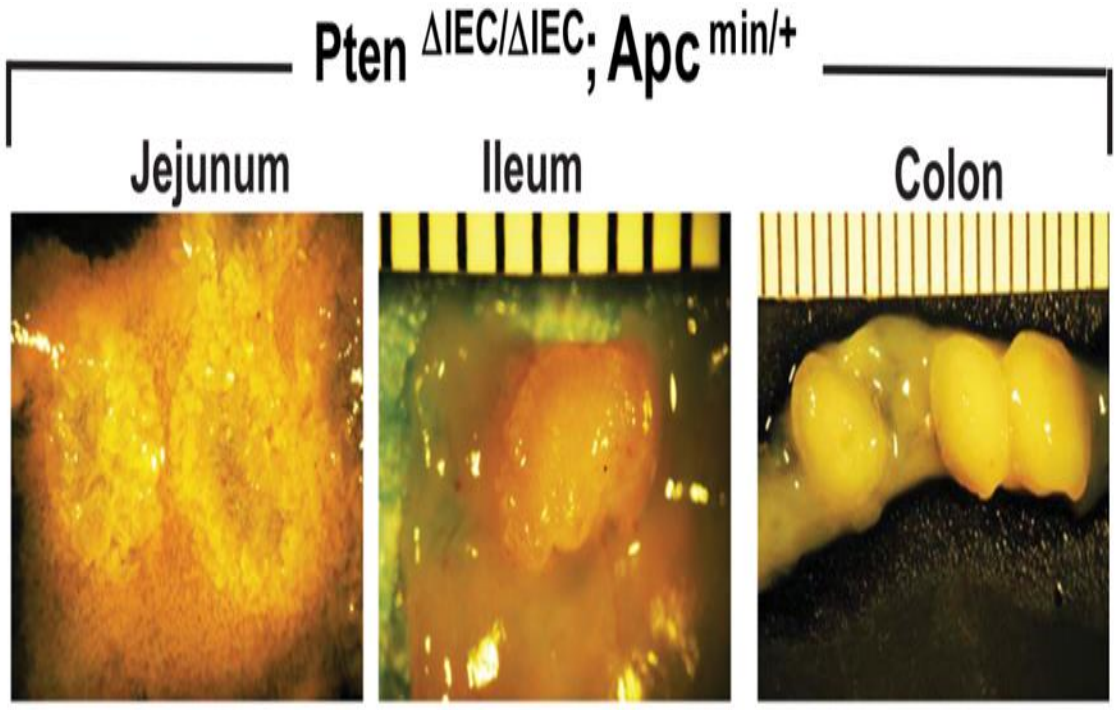

Figure 13: The image above shows gross images of the tumors observed throughout the small intestine (jejunum and ileum) and the colon of $Pten^{\Delta IEC/\Delta IEC}$; $Apc^{min/+}$ mice (scalebar, 1 mm). The mating cross resulted in explosive tumor formation, suggesting that the tumorigenic drive is still present in $Pten^{\Delta IEC/\Delta IEC}$ mice.

2.3.5: Intestinal Epithelial Cells of $Pten^{\Delta IEC/\Delta IEC}$ Mice Exhibited Enhanced Tumorigenesis in the $Apc^{min/+}$ Mouse Model of Colon Cancer

Along with enhanced tumor formation, the number of tumors in the intestine was dramatically higher in $Pten^{\Delta IEC/\Delta IEC}$; $Apc^{min/+}$ mice (lane 3) compared to $Pten^{\Delta IEC/+}$; $Apc^{min/+}$ control mice (lane 2) and $Pten^{+/+}$; $Apc^{min/+}$ control mice (lane 1). This finding suggests that the tumorigenic-drive in *Pten* deficient cells remains, however, *Pten* gene deletion alone is not enough to cause tumorigenesis in any part of the intestine or the colon.

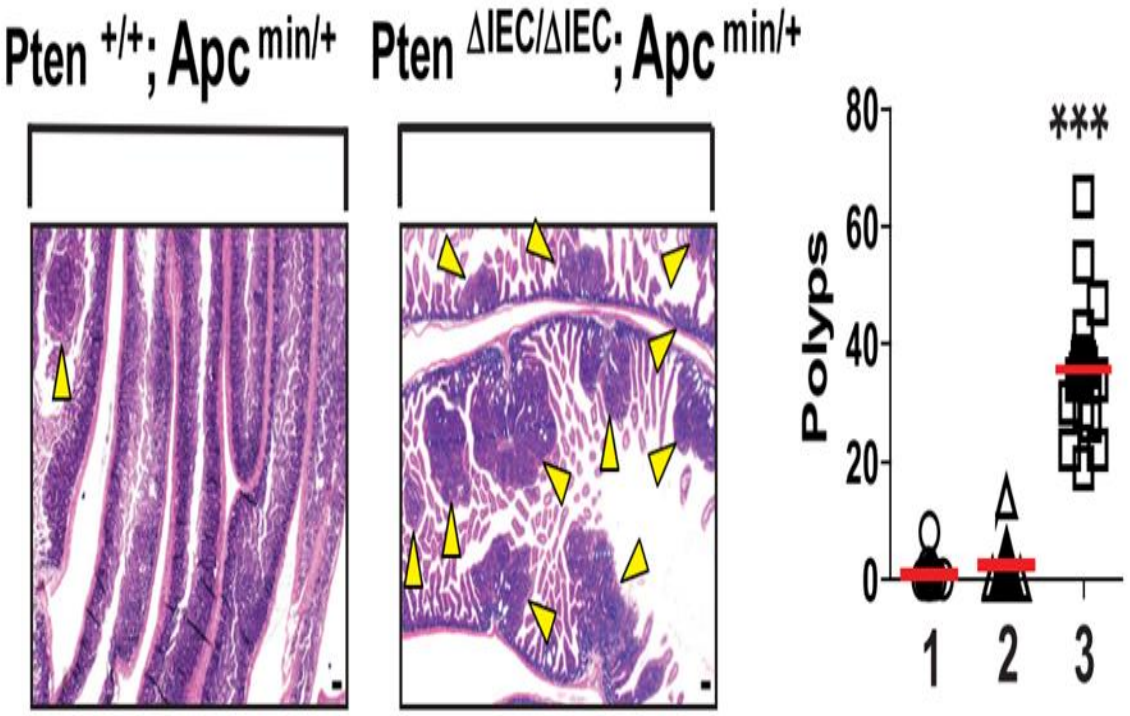

Figure 14: The number of tumors was increased in Pten$^{\Delta IEC/\Delta IEC}$; Apc$^{min/+}$ mice. The left images show full length of the small intestine was obtained from 5 to 6 weeks-old Pten$^{\Delta IEC/\Delta IEC}$; Apc$^{min/+}$ and littermate Pten$^{+/+}$; Apc$^{min/+}$ mice, and prepared in a 'swiss-roll' method for H&E staining. The arrowheads indicate an individual tumor mass observed under microscope (scale bar, 100 μm). Shown in the graph on the right, using stereoscopic microscopy, the number of visible tumors (≥1.0 mm in diameter) was evaluated throughout the small intestine of the mice: lane 1, Pten$^{+/+}$; Apc$^{min/+}$ (n=12); lane 2, Pten$^{\Delta IEC/+}$; Apcmin$^{/+}$ (n=12); lane 3, Pten$^{\Delta IEC/\Delta IEC}$; Apc$^{min/+}$ mice (n=19). ** P < 0.01, *** P < 0.001 (Mann-Whitney U test).

Pten$^{\Delta IEC/\Delta IEC}$; Apc$^{min/+}$ mice additionally had enlarged spleens compared to age-matched littermate Pten$^{+/+}$; Apc$^{min/+}$ control mice. The enlarged spleens in these mice signifies a systemic effect upon the mouse in response to the severe intestinal tumor development. Furthermore, it was also found that approximately 90% of Pten$^{\Delta IEC/\Delta IEC}$; Apc$^{min/+}$ mice failed to survive past 3 months of age due to the extensive tumorigenesis in the intesine, whereas more than 90% of littermate Pten$^{+/+}$; Apc$^{min/+}$ control mice survived until 3 months of age.

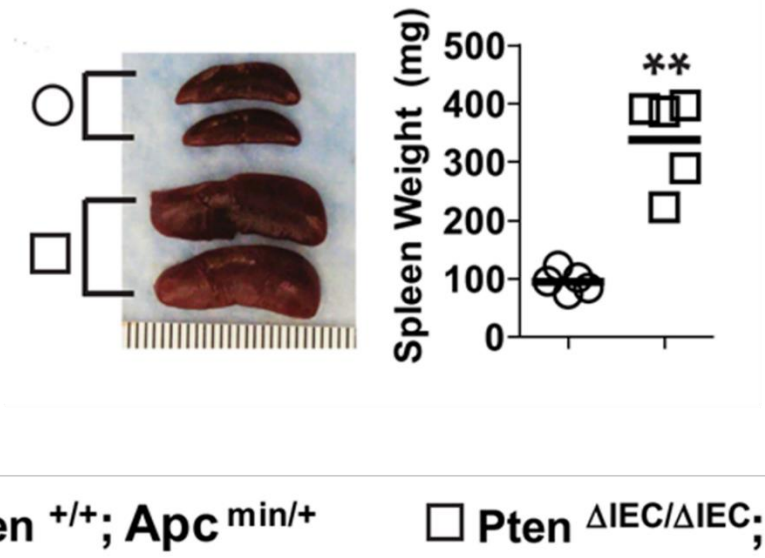

Figure 15: $Pten^{\Delta IEC/\Delta IEC}$; $Apc^{min/+}$ mice have an increased kidney sized compared to littermate $Pten^{+/+}$; $Apc^{min/+}$ mice. The data above displays gross images and weight of the spleen obtained from $Pten^{+/+}$; $Apc^{min/+}$ and $Pten^{\Delta IEC/\Delta IEC}$; $Apc^{min/+}$ mice (n=5/group). ** P < 0.01, *** P < 0.001 (Mann-Whitney U test).

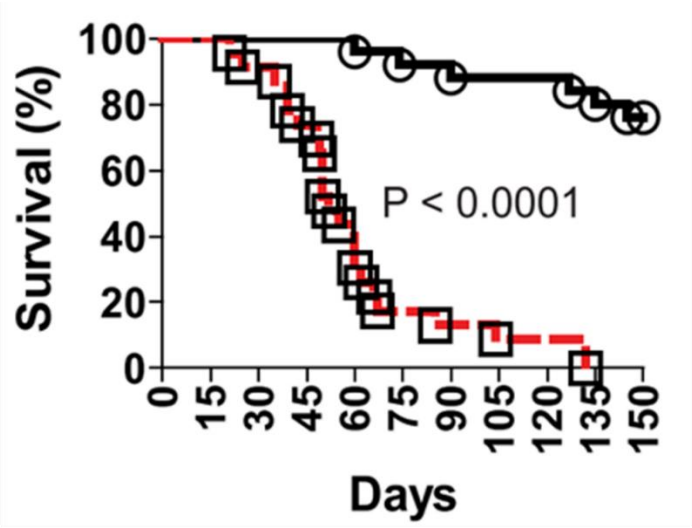

Figure 16: $Pten^{\Delta IEC/\Delta IEC}$; $Apc^{min/+}$ mice have an increased mortality compared to littermate $Pten^{+/+}$; $Apc^{min/+}$ mice. The mouse mortality was evaluated between $Pten^{+/+}$; $Apc^{min/+}$ (n=25) and $Pten^{\Delta IEC/\Delta IEC}$; $Apc^{min/+}$ mice (n=23) over 5 months after birth. Difference in survival was shown by Kaplan-Meier plot. The log rank (Mantel-Cox) test was used to compare significant survival difference (P < 0.0001).

Altogether, these data suggest that the *Pten* gene deletion in IECs significantly promotes tumor development in an $Apc^{min/+}$ background. This also further demonstrates that although tumorigenesis does not occur in mice with IEC *Pten* gene deletion alone, the IECs of these mice still possess the tumorigenic-driving potential to promote tumor development in the intestine and colon.

2.3.6: Tumor-Promoting Gene Expression was Reduced in the Intestine of $Pten^{\Delta IEC/\Delta IEC}$ Mice

Finding that Pten deficiency alone did not give rise to tumor development in $Pten^{\Delta IEC/\Delta IEC}$ mice, led to answering the question of why *Pten* gene deletion in intestinal epithelial cells did not lead to tumor development. To address this question, analysis of tumor-associated gene expression in the intestine of $Pten^{\Delta IEC/\Delta IEC}$ mice was compared to $Pten^{+/+}$ littermate mice. This was performed using a cancer pathway-focused PCR array analysis followed by individual qPCR of significant genes of interest.

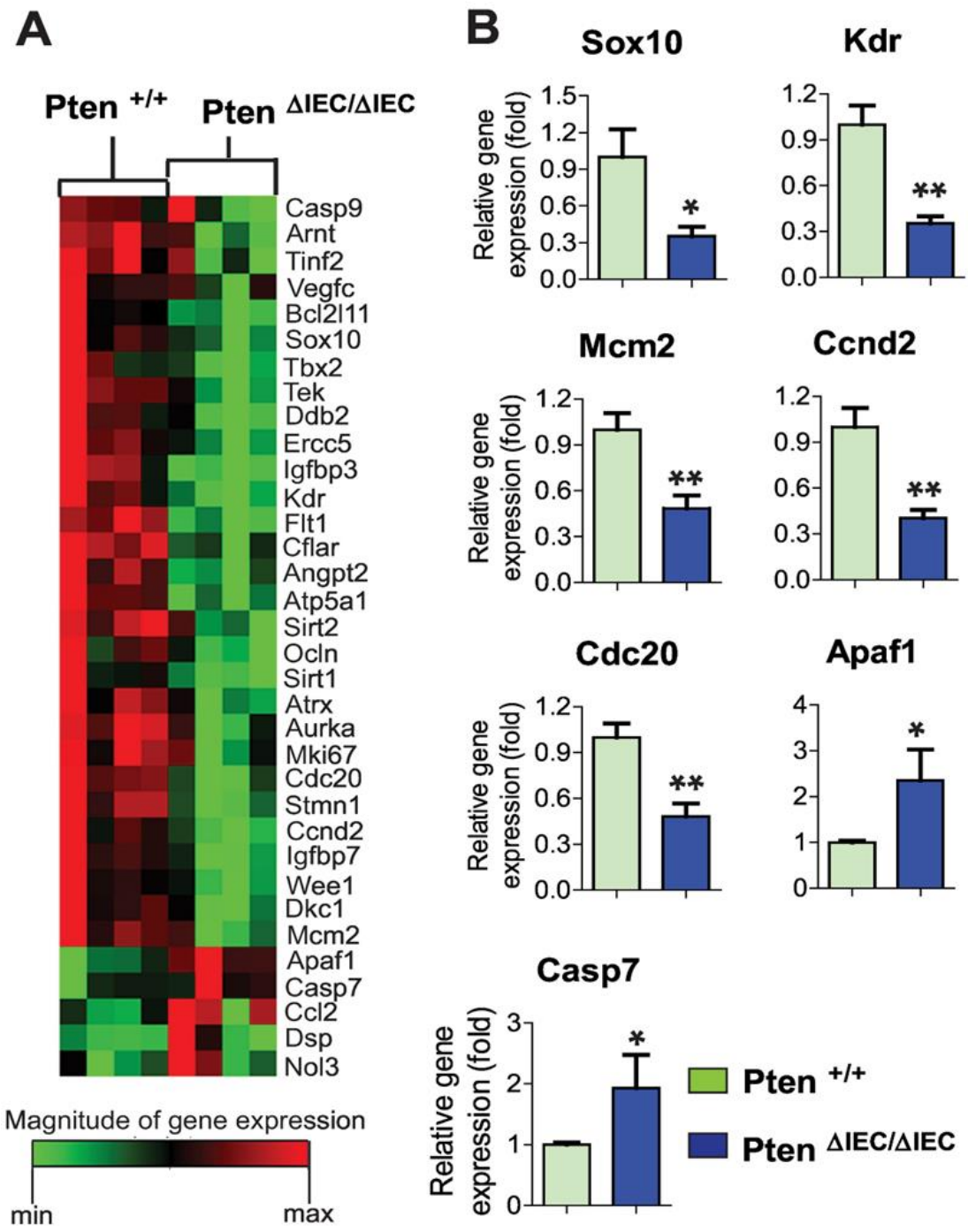

Figure 17: The expression of cancer-associated genes was changed in the intestine of Pten$^{\Delta IEC/\Delta IEC}$ mice. (17A) An array of cancer-associated gene expression was analyzed using the mouse small intestine. Gene expression profiles with significant difference were visualized in the heat map (n = 4/group) (17B). To confirm the representative gene expression exhibiting a significant difference from the array data, individual qPCR was independently performed using the mouse small intestine (n = 6/group). Data are the representative of three independent experiments. Error bars indicate ± SEM. * $P < 0.05$, ** $P < 0.01$ (Mann-Whitney U test).

It was found that the expression of tumor-promoting genes Ccnd2, Cdc20, Mcm2, Kdr, and Sox10 was downregulated in the intestine of $Pten^{\Delta IEC/\Delta IEC}$ mice compared to $Pten^{+/+}$ littermate mice, along with other various genes associated with tumorigenesis. Sox10 is a member of the SOX transcription family, which is known for regulating canonical Wnt/β-catenin signaling. Elevated SOX10 expression has been associated with promoting tumor progression (Cronin et al., 2018). A heightened Kdr (Vegfr2) expression can predict a poor prognosis in colon cancer patients due to its crucial role in colon cancer progression (S.-D. Zhang et al., 2015). Because Mcm2 regulated DNA replication, an enhanced Mcm complex that includes Mcm2 has been suggested to regulate different types of tumor development (Y. Liu et al., 2013). Enhanced Ccnd2 expression is linked to colon carcinogenesis due to Ccnd2 promoting cell proliferation by favoring the G1/S cell cycle transition (Mermelshtein et al., 2005). Cdc20 ubiquitinates the cyclin-dependent kinase (Cdk) inhibitor p21, which is a negative regulator of the cell division cycle (Pei & Xiong, 2005). Cdc20 activation results in p21 degradation, producing an enhanced cell mitosis and resulting tumorigenesis (Amador et al., 2007). Activation of Sox10, Kdr, Mcm2, Ccnd2 and Cdc20 would promote tumor development, however, the reduced expression of these genes found in the intestine of $Pten^{\Delta IEC/\Delta IEC}$ mice appears to play a significant role in preventing tumor development.

Tumor-suppressing genes Apaf1 and Casp7 were found to have increased expression in the intestine of $Pten^{\Delta IEC/\Delta IEC}$ mice compared to $Pten^{+/+}$ littermate mice. Apaf1 plays a part in the formation of apoptosomes, which leads to the activation of initiator caspases, including Casp9. Casp7, the executioner, is then activated, which induces apoptosis (Galluzzi et al., 2016). Because of their essential roles in apoptosis, it

is likely that the elevated expression of Apaf1 and Casp7 may be promoting cell apoptosis in the intestine of $Pten^{\Delta IEC/\Delta IEC}$ mice, conferring a tumor-suppressive effect.

These findings from the gene expression array data demonstrates that *Pten* deficient IECs downregulated the expression of tumor-promoting genes, while upregulating tumor-suppressing gene expression, ultimately resulting in a tumor-suppressive effect.

2.3.7: Loss of the *Pten* Gene in Intestinal Epithelial Cells Resulted in Intestinal Dysbiosis

Recently, evidence indicated that the gut microflora has a sizable impact on the promotion and suppression of colon cancer in humans because of the ability of certain commensal bacteria to stimulate inflammatory or anti-inflammatory responses (Buchta Rosean & Rutkowski, 2017; J. Chen et al., 2017). The fecal microbiome of sex and age (3 months old) matched $Pten^{\Delta IEC/\Delta IEC}$ and littermate $Pten^{+/+}$ mice that were co-housed since their birth were analyzed to account for the failure of Pten deficiency in intestinal epithelial cells to induce intestinal tumor development. Through 16S ribosomal RNA (rRNA) gene sequencing, the observed operational taxonomic unit (OTU) counts for $Pten^{\Delta IEC/\Delta IEC}$ and $Pten^{+/+}$ mice were evaluated, and found no significant difference between the groups with regard to species richness (count of different species in each sample group). However, using the Shannon diversity index and taking species richness as well as evenness (relative abundance of different species) into account revealed a significant difference between the two fecal microbial groups of the $Pten^{\Delta IEC/\Delta IEC}$ mice compared to $Pten^{+/+}$ littermate control mice.

Variable =17,821	Observed species				Shannon Diversity Index			
	Mean:	STD Dev:	Means of Ranks:	Statistics:	Mean:	STD Dev:	Means of Ranks:	Statistics:
$Pten^{\Delta IEC/\Delta IEC}$	1407.375	137.670	9.875	P=0.083	6.443	0.607	10.625	P=0.015
$Pten^{+/+}$	1020.286	372.455	5.857		4.959	1.304	5.000	

Table 1: $Pten^{\Delta IEC/\Delta IEC}$ Fecal Microbiome Vs $Pten^{+/+}$ Fecal Microbiome. Species richness and evenness were different between the fecal microbiomes of $Pten^{\Delta IEC/\Delta IEC}$ and $Pten^{+/+}$ mice. No significant differences between $Pten^{\Delta IEC/\Delta IEC}$ and $Pten^{+/+}$ mice were observed with regards to species. However, taking species richness as well as evenness into account, there is a significant difference found between the groups. The mean rarefaction predicted OTUs data for the mouse groups were measured at a depth of 17,821 sequences. Presented are the observed species and the Shannon index showing the mean value.

Next, the bacterial community structure was analyzed using weighted UniFrac distance matrices. Principle coordinate analysis (PCoA) plots were used to visualize the data in these matrices, and analysis of similarities (ANOSIM) was utilized to determine if there was a significant difference between the bacterial communities. $Pten^{\Delta IEC/\Delta IEC}$ mice and littermate $Pten^{+/+}$ mice fecal samples in the weighted PCoA plot form two separate clusters, suggesting that *Pten* deficient mice had a changed fecal microbiome. With the ANOSIM R value ($R = 0.64$, $P = 0.001$), we determined that there is a significant difference between the sample groups.

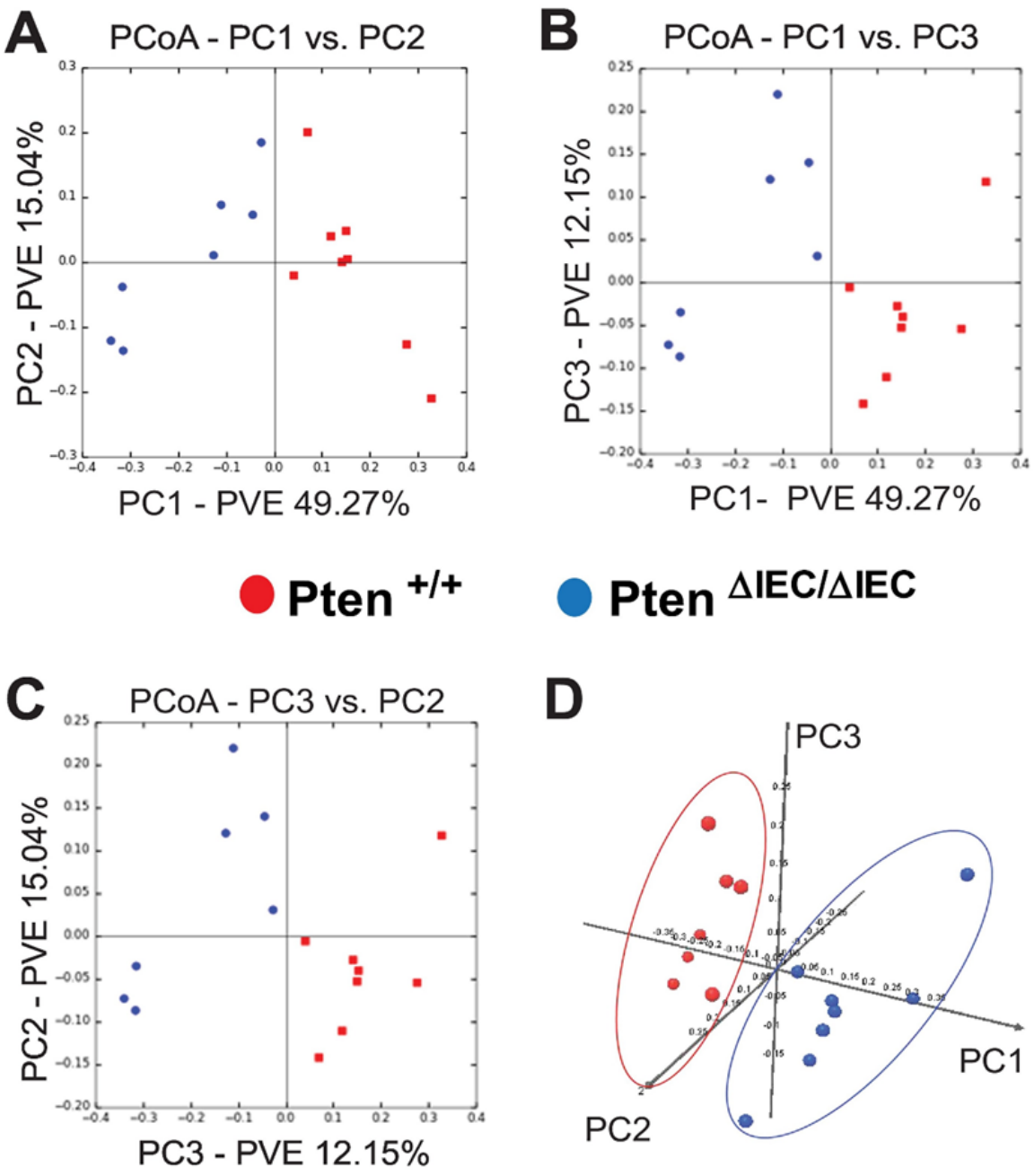

Figure 18: The fecal microbiome of Pten$^{\Delta IEC/\Delta IEC}$ mice was distinct from that of Pten$^{+/+}$ mice. The bacterial community structure of the fecal samples from Pten$^{+/+}$ and Pten$^{\Delta IEC/\Delta IEC}$ mice was analyzed using weighted UniFrac distance matrices. (A to C) Principal coordinate analysis plots represent the three highest discriminating axes. The primary vector PC1 explains 49.27% of the variation between the groups, while PC2 and PC3 represent 15.04% and 12.15%, respectively. PVE, percent variance explained (D) The first three vectors together exhibit 76.4% of the variation among the groups. Each dot represents individual microbiota samples from the mouse. (n = 8/each group).

While the species diversity itself was comparable between the fecal samples of $Pten^{\Delta IEC/\Delta IEC}$ and $Pten^{+/+}$ mice, these data taken together demonstrate that Pten gene deficiency in intestinal epithelial cells did alter the species composition of the fecal microbiome.

2.3.8: The Fecal Microbiota Communities of $Pten^{\Delta IEC/\Delta IEC}$ Mice Were Different from Those of $Pten^{+/+}$ Mice

It was determined that 100% of analyzed sequences from all $Pten^{\Delta IEC/\Delta IEC}$ and $Pten^{+/+}$ mouse samples belonged to the bacteria kingdom, with no detectable archaeal or eukaryotic contamination. The majority (>98.7%) of analyzed sequences from the mice were from 4 major phyla: Bacteroidetes ($Pten\Delta^{IEC/\Delta IEC}$ vs. $Pten^{+/+}$, 45.07% vs. 36.34%), Firmicutes (47.47% vs. 31.30%), Verrucomicrobia (2.88% vs. 28.61%), and Proteobacteria (3.46% vs. 2.55%). Among these major phyla constituting the fecal microbiota, it is worth noting that the phylum of Verrucomicrobia was substantially reduced in $Pten^{\Delta IEC/\Delta IEC}$ mice compared to $Pten^{+/+}$ mice.

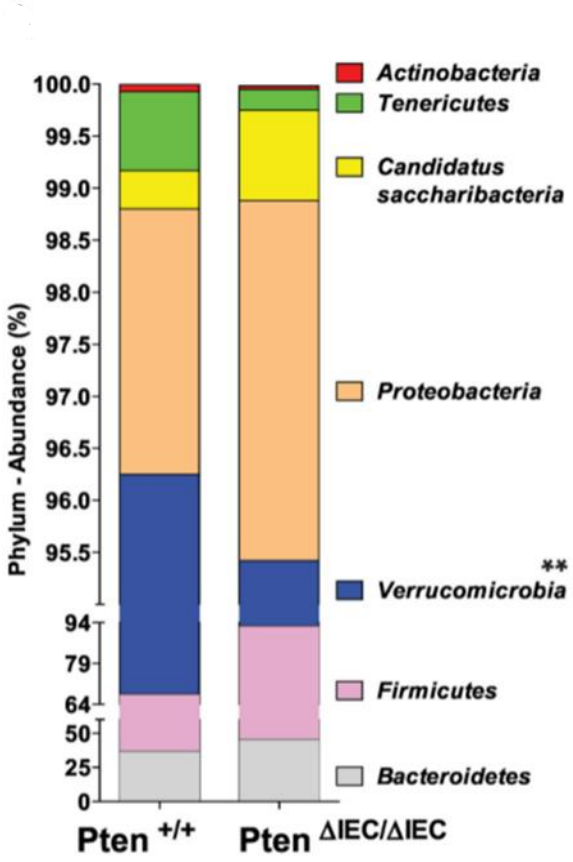

Figure 19: Relative abundance of taxonomic groups observed in the fecal samples were different between Pten$^{\Delta IEC/\Delta IEC}$ and Pten$^{+/+}$ mice. The abundance of the phyla detected in the fecal samples of Pten$^{\Delta IEC/\Delta IEC}$ and Pten$^{+/+}$ mice. Bacteroidetes, Firmicutes, Verrucomicrobia, and Proteobacteria are the 4 major phyla encompassing the majority of sequences (>98.7%). A statistically significant difference between the groups was identified in Verrucomicrobia. ** $P < 0.01$ (Mann-Whitney U test).

It was then examined whether any specific bacterial genera were significantly different between the samples, and a wide range of genera whose abundances were significantly different between the groups was identified. To provide a visual overview combined with analysis, a dual hierarchical dendrogram was generated to display the data for the predominant genera with clustering related to the different groups. Based on the distinct clustering, a significant difference in the predominant genera detected between Pten$^{\Delta IEC/\Delta IEC}$ and Pten$^{+/+}$ mice was observed.

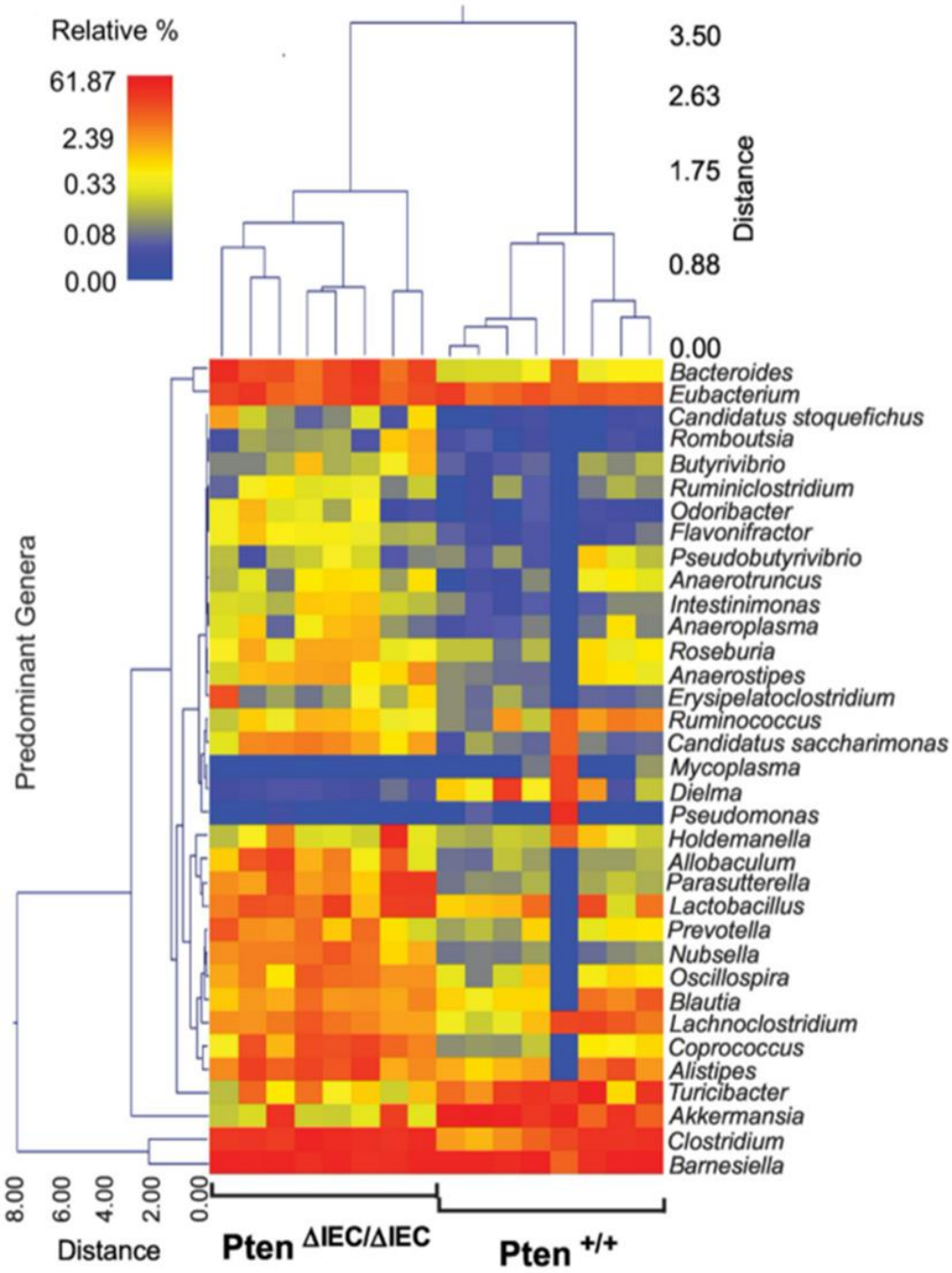

Figure 20: A dual hierarchal dendrogram was generated based on the predominant genera using Ward's minimum variance clustering and Manhattan distances. Samples with more similar microbial populations are mathematically clustered closer together. The samples with a more similar consortium of genera cluster closer together with the length of connecting lines (top of heatmap) related to the similarity; shorter lines between two samples indicate closely matched microbial consortia. The heatmap represents the relative percentages of each genus. The legend for the heatmap is provided in the upper left corner. The predominant genera are represented along the right Y-axis.

Altogether, these data suggest that the fecal microbial communities from $Pten^{\Delta IEC/\Delta IEC}$ mice are easily distinguishable and different from $Pten^{+/+}$ mice, further demonstrating that Pten gene deletion in intestinal epithelial cells changed the fecal microbiome.

2.3.9: Colon Cancer-Associated Akkermansia Muciniphila was Dramatically Decreased in the Feces of $Pten^{\Delta IEC/\Delta IEC}$ Mice Compared to $Pten^{+/+}$ Mice

Next, the bacterial genera whose abundances were significantly changed between $Pten^{\Delta IEC/\Delta IEC}$ and littermate $Pten^{+/+}$ mice was examined. Although there were a wide range of genera that were found to be significantly different between the mouse groups, the two most notable differences were found in the relative abundances of *Akkermansia* (28.61% in $Pten^{+/+}$ → 2.88% in $Pten^{\Delta IEC/\Delta IEC}$) and *Clostridium* (7.89% → 20.27%). At the level of bacterial species, we observed that the abundance of *Akkermansia muciniphila* (28.61% in $Pten^{+/+}$ → 2.88% in $Pten^{\Delta IEC/\Delta IEC}$) was greatly reduced in the fecal samples of $Pten^{\Delta IEC/\Delta IEC}$ mice compared to $Pten^{+/+}$ mice, while the abundance of *Clostridium* sp. was increased (6.97% in $Pten^{+/+}$ → 19.23% in $Pten^{\Delta IEC/\Delta IEC}$).

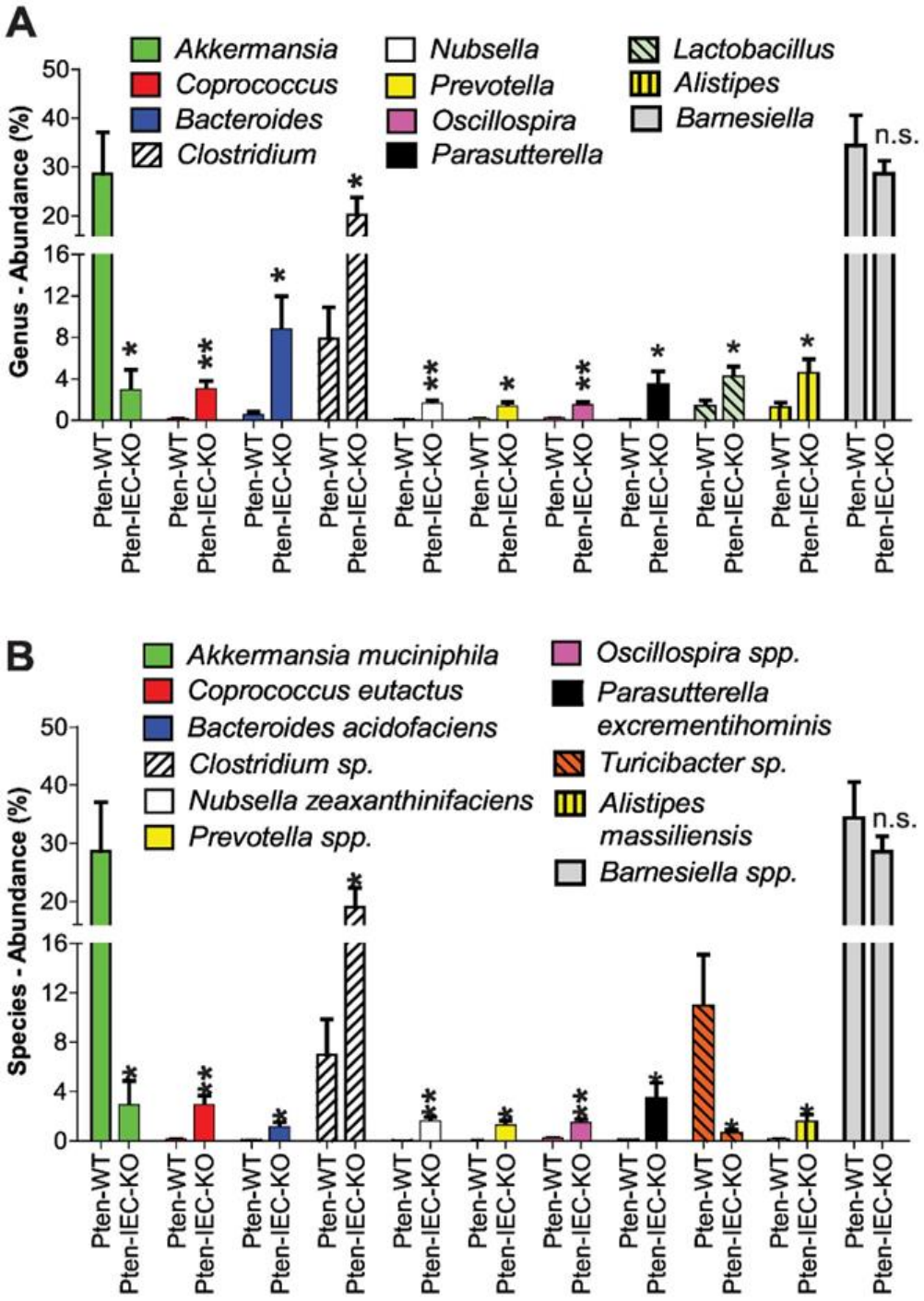

Figure 21: The abundance of the colitogenic bacteria *Akkermansia muciniphila* was dramatically reduced in $Pten^{\Delta IEC/\Delta IEC}$ mice compared to $Pten^{+/+}$ mice. Major bacteria identified in the fecal samples of $Pten^{+/+}$ and $Pten^{\Delta IEC/\Delta IEC}$ mice (n = 8/group) were analyzed to compare the abundance at the genus (21A) and species (21B) level. Results are means ± SD, * $P < 0.05$, ** $P < 0.01$ (Mann-Whitney *U* test). n.s., not significant.

Akkermansia muciniphila, member of the *Verrucomicrobia* phylum, is a mucin-degrading bacterium (Derrien et al., 2017). Because of this ability, *Akkermansia muciniphila* has great potential to induce colonic inflammation (Ganesh et al., 2013). It has been suggested that *Akkermansia muciniphila* colonization can noticeably increase tumor development in an Apc mouse model of colon cancer, and it may also promote tumorigenesis in human colon cancer (Dingemanse et al., 2015; Weir et al., 2013). Therefore, it is reasonable to believe that the greatly decreased abundance of *Akkermansia muciniphila* would participate in providing a tumor-suppressing microenvironment to prevent tumor development in $Pten^{\Delta IEC/\Delta IEC}$ mice.

2.4: Discussion

Colon tumorigenesis is influence by a range of factors such as chronic inflammatory conditions, genetic aberrations, impaired tumor-immune responses, and environmental carcinogens. Among these factors, new evidence suggests that complex interactions between the gut microbiome and host have a significant impact on tumor prevention and progression. For example, *Fusobacterium nucleatum* accumulates in the colon cancer tissue where it promotes malignant transformation (Kostic et al., 2012). *Bacteroides fragilis* has been found at a greater prevalence in stool samples of colorectal cancer patients compared to controls and is known to promote colon tumorigenesis by enhancing the T_{h17} inflammatory response (Toprak et al., 2006; Wu et al., 2009). It has been suggested that monocolonization of commensal microbe *Escherichia coli NC101* promotes chronic inflammation of the colon and increases tumorigenesis in IL-10 KO mice treated with azoxymethane (Arthur et al., 2012). *Enterococcus faecalis* can cause a chromosomal aberration (aneuploidy) in the colonic epithelial cells of IL-10 KO mice

(Balish & Warner, 2002; Kim et al., 2005). The amount of *Akkermansia muciniphila* has been measured to be 4 times higher in colorectal cancer patients compared to healthy subjects (Weir et al., 2013). In addition to this, *Akkermansia muciniphila* colonization exacerbates tumor development in the intestine of $Apc^{min/+}$ mice (Dingemanse et al., 2015). On the contrary, probiotic bacteria, including *Lactobacillus* and *Bifidobacterium* species, have been shown to exert a tumor-suppressive effect in the colon (Cipe et al., 2015).

The mechanisms by which gut bacteria modulates tumor-promoting or tumor-suppressing effects remain elusive. Given that long-term inflammation causes DNA damage and chromosomal instability, it seems logical that bacteria which can cause chronic inflammatory disease could be a major culprit of promoting tumor development (Cipe et al., 2015). Consistent with this notion, *Lactobacillus* and *Bifidobacterium,* which both possess potent anti-inflammatory effects in the intestine, have been shown to be able to suppress tumor formation (Lightfoot et al., 2013; Ringel et al., 2011).

Akkermansia muciniphila is a relatively abundant bacteria found in the colon of humans that comprises approximately 1-4% of the colonic microbiota and has strong clinical relevance to a variety of diseases, including IBD and metabolic disorders (Collado et al., 2007; Derrien et al., 2008, 2017; Dingemanse et al., 2015). *Akkermansia muciniphila* has the clinically relevant function of breaking down high-molecular-weight glycoproteins released as mucins from IECs, thus allowing bacteria to regulate the selectively permeable gut barrier system, which separates the host from intraluminal environment containing enteric bacteria, toxins and food antigens (Derrien et al., 2017). Because of its ability to break down mucus, *Akkermansia muciniphila* enriched in the

colon can act as a pathobiont to develop inflammatory conditions, which significantly increases the risk of tumor development (Ganesh et al., 2013; Long & Sands, 2018; Seregin et al., 2017). Notably, the fecal microbiome analysis data presented in this study identified a dramatically reduced abundance of *Akkermansia muciniphila* in $Pten^{\Delta IEC/\Delta IEC}$ (2.88%) mice compared to $Pten^{+/+}$ (28.61%) littermates. Given the inflammatory impact *Akkermansia muciniphila* possess, it is reasonable to believe that the decreased abundance of the bacterial species has a role in preventing intestinal tumorigenesis in $Pten^{\Delta IEC/\Delta IEC}$ mice. This idea is further supported by the differing growth rates of intestinal tumors that was observed in $Pten^{\Delta IEC/\Delta IEC}$ mice. Many studies have demonstrated that $Pten^{\Delta IEC/\Delta IEC}$ mice do not develop tumors in the duodenum and jejunum of the intestine by 12 months (Choi et al., 2013; Im et al., 2014; Langlois et al., 2009). However, other studies have suggested that approximately 19% of $Pten^{\Delta IEC/\Delta IEC}$ mice develop tumors in the duodenum and jejunum of the intestine by 12 months (Byun et al., 2011). This sizable discrepancy between these data strongly supports that gut microbial differences between housing facilities may have an important impact on tumor formation in mice with similar genetic predisposition.

A genetic predisposition may mediate the activation of tumor-promoting signaling pathways, which would lead to increased cell proliferation and consequent tumorigenesis. Conversely, tumor-suppressing signaling pathways can be activated to induce apoptotic cell death, leading to tumor prevention or suppression. Thus, the dynamic balance between tumor-promoting and tumor-suppressing pathways play an important role in inhibiting the initial cellular event of tumor growth (Ucker & Levine, 2018). Similarly, altered expression of tumor-promoting or tumor-suppressing genes have a crucial role in

signaling networks contributing to tumorigenesis. Many studies have indicated that activation of Sox10, Kdr, Mcm2, Ccnd2 and Cdc20 have important functions in singling networks that promote tumor growth (Amador et al., 2007; Cronin et al., 2018; Y. Liu et al., 2013; Mermelshtein et al., 2005; Pei & Xiong, 2005; S.-D. Zhang et al., 2015). The activation of Apaf1 and Casp7 mediates cell apoptosis, which results in a contrasting tumor-suppressing effects (Galluzzi et al., 2016). In this study, reduced expression of Sox10, Kdr, Mcm2, Ccnd2 and Cdc20 genes was identified, along with elevated expression of Apaf1 and Casp7 genes in the intestine of $Pten^{\Delta IEC/\Delta IEC}$ mice compared to $Pten^{+/+}$ mice. Therefore, in addition to the reduced abundance of pro-inflammatory bacteria *Akkermansia muciniphila* in the colon of $Pten^{\Delta IEC/\Delta IEC}$ mice, decreased expression of tumor-promoting genes and increased levels of tumor-suppressing genes may explain why intestinal tumors did not develop in $Pten^{\Delta IEC/\Delta IEC}$ mice.

Pten deficiency alone is unable to induce intestinal tumorigenesis in mice. However, *PTEN* deficiency in humans has well-characterized deleterious impacts in colorectal cancer patients. *PTEN* gene alteration can be indicative of relapse, metastasis, and poor prognosis in colorectal cancer patients (Bohn et al., 2013; Colakoglu et al., 2008; Dicuonzo et al., 2001). It has been suggested that impaired TGF-β signaling pathways, promoted PI3K-Akt signaling pathways, or altered cell migration and interaction with the extracellular matrix may contribute to the deleterious impacts of *PTEN* deficient colorectal cancer patients (Colakoglu et al., 2008; Dicuonzo et al., 2001; Tamura et al., 1998; Yu et al., 2014). However, the underlying mechanisms remain unknown.

2.5: Conclusion

In this study, human colon cancer tissues had reduced mRNA expression of the tumor suppressor gene *PTEN* compared to controls, which implies the involvement of *PTEN* impairment in the development of colon cancer. However, *Pten* deficiency in IECs did not induce tumorigenesis in mice. It was found that both the intestinal microflora and tumor-associated gene expression had been shifted toward a tumor-suppressing condition in the gut of $Pten^{\Delta IEC/\Delta IEC}$ mice. Therefore, these findings suggest that the gut microbiome, alongside a changed tumor-associated gene expression, plays a crucial part in shaping the tumor microenvironment in the colon.

CHAPTER THREE

STUDYING THE IMMUNE-REGULATORY ROLE OF PTEN IN THE GUT

3.1: Introduction

In support of an alternative function of PTEN, it has been recently discovered that PTEN is capable of regulating the immune and inflammatory response in IECs by controlling Toll-like receptor 5 (TLR5), which is a microbial sensing mechanism (Mitchell et al., 2018). PIP2 generated by active PTEN mediates localization of the adaptor protein MAL/TIRAP to the plasma membrane, which allows MAL/TIRAP to bind to the cytoplasmic region of TLR5 (Choi et al., 2013). Moreover, MAL/TIRAP functions as a bridge between TLR and MYD88, an additional adaptor protein (Kagan & Medzhitov, 2006). Thus, the loss of the *Pten* gene impedes the recruitment of MAL/TIRAP and MYD88 to TLR5 in IECs, which are cells in constant contact with luminal milieu such as the gut microbiota and other nutrients(Choi et al., 2013). Therefore, PTEN is capable of regulating the gut microbe–induced immune and inflammatory response via modulation of adaptor protein recruitment because microbial sensing through TLRs is required to elicit potent innate and adaptive immune responses in the gut (Choi et al., 2013; Im et al., 2014). This evidence indicates that PTEN may have other unidentified roles yet to discover.

Salmonella enterica is a Gram-negative enteropathogenic bacteria that can cause self-limiting gastrointestinal disorder or typhoid fever in humans (Gut et al., 2018). A particular susceptible strain of mice has a defective mutation in the natural resistance associated macrophage protein (Nramp) gene, which are sensitive to an infection of

Salmonella enterica serovar Typhimurium (*S*. Typhimurium), resulting in disease symptoms similar to *Salmonella*-induced typhoid fever (Govoni & Gros, 1998; Tsolis et al., 1999). However, most inbred mice, like C57BL/6 and BALB/c1 strains, do not exhibit disease symptoms, such as intestinal inflammation, due to gut commensal microbes that produce inhibitory molecules and outcompete *Salmonella* for nutrients when housed in a conventional or specific pathogen free condition (Erova et al., 2016; Kaiser et al., 2012).

To overcome this inherent natural resistance found in inbred mice, a 20 mg pretreatment of streptomycin can be administered, which then renders C57BL/6 mice susceptible to infection of *Salmonella* and thus eliciting colitis (Barthel et al., 2003). The antibiotic-pretreatment of streptomycin depletes the gut commensal microbiota in the intestine, thus eliminating competition and hinderances. The C57BL/6 mice develop marked inflammation in the solely in the cecum and colon when infected with an intragastric administration of high inoculum of *S*. Typhimurium. Thus, this streptomycin-pretreated mouse model is an established and highly reproducible animal model for studying the mechanism of intestinal inflammation produce from a *Salmonella* infection (Hapfelmeier & Hardt, 2005; Kaiser et al., 2012).

Due to the immune regulatory function of PTEN in IECs, it was hypothesized that loss of the *Pten* gene in IECS would compromise intestinal immune responses in the intestine, thus rending the host greatly susceptible to *S.* Typhimurium infection. IEC-restricted Pten gene knockout mice were found to be highly prone to *S.* Typhimurium infection, which was characterized by massive inflammation in the small intestine and

cecum. This data suggests an that *Pten* has an important immune regulatory function in response to pathogenic microbial infection in the gut.

3.2: Materials and Methods

3.2.1: Animals

IEC-restricted *Pten* gene knockout ($Pten^{\Delta IEC/\Delta IEC}$) mice were generated by mating Pten-floxed ($Pten^{loxP/loxP}$) mice (Groszer et al., 2001) with Villin promoter-driven Cre expression mice ($Vil^{Cre/+}$) (Madison et al., 2002) purchased from Jackson Laboratory (Bar Harbor, ME). $Pten^{\Delta IEC/\Delta IEC}$ mice were backcrossed into the C57BL/6 background for at least 6 generations prior to performing experiments as described in previous studies (Choi et al., 2013; Im et al., 2014; Langlois et al., 2009). Mice were bred and maintained under standard SPF conditions with normal drinking water *ad libitum* at the animal facility of University of California Los Angeles and Oakland University under the approval of the Institutional Animal Care and Use Committee (IACUC) of UCLA and OU.

3.2.2: Bacterial Strain and Culture Condition

Salmonella enterica serovar Typhimurium strain (14028) (Fields et al., 1986) was obtained from American Type Culture Collection (ATCC) and selected for this study. *S.* Typhimurium was cultivated in Luria-Betani (LB) broth (10g Bacto tryptone, 5g yeast extract, 10g NaCl per L) solidified by the addition of 1.5% (wt/vol) agar when needed. The bacteria was cultivated for 12 hours at 37°C in LB broth while shaking at 225 RPM for liquid culture as described in a previous study (Stecher et al., 2006). Next, the bacterial culture was diluted (1:20) in fresh LB medium, followed by cultivating for 4 hours with gentle aeration to ensure the exponential growth phase. Then, the cultivated bacteria were collected by gentle centrifugation and washed three times in ice-cold

phosphate-buffered saline (PBS). Afterwards, the pellets were resuspended in cold PBS (2×10^4 CFU/200 mL). The *Salmonella* strain was periodically assessed on Salmonella-Shigella agar plates for purity.

3.2.3: Animal Experiments

8-week-old and sex-matched $Pten^{\Delta IEC/\Delta IEC}$ and littermate $Pten^{+/+}$ control mice were pretreated with an oral gavage of streptomycin (25 mg/mouse) for 24 hours. The mice were inoculated with a low inoculum of *S.* Typhimurium (2×10^4 in a volume of 200 mL/mouse) using a blunt gastric tube. The mice health condition was then monitored for 24 hours after inoculation, where a moribund state was considered as an experimental endpoint for determining mortality.

3.2.4: Analysis of *S.* Typhimurium Loads in the Liver, Mesenteric Lymph Nodes, and Spleen

The mice were pretreated with streptomycin for 24 hours and then given an oral gavage of *S.* Typhimurium (2×10^4 per mouse). After 48 hours, the mice were then euthanized, and the liver, mesenteric lymph nodes, and spleen were aseptically harvested from the mice. To analyze bacterial colonization, the mice tissues were homogenized in 4°C PBS (0.5% Tergitol, 0.5% bovine serum albumin) as described in a previous study (Barthel et al., 2003). The bacterial loads were determined by plating appropriate dilutions on MacConkey agar plates.

3.2.5: Tissue Histology Analysis

Mice were euthanized after 24 hours of bacterial inoculation, and the small intestine and cecum were fixed in 10% buffered formalin, dehydrated, and embedded in paraffin. Tissue sections were cut (5 mm) and prepared for Hematoxylin & Eosin (H&E)

staining. Images were first visualized with an Axio Imager Z1 microscope (Carl Ziess) and captures with an AxioCam digital camera. Images were then processed with Adobe Photoshop. The histological severity of colitis was graded in a blind fashion as described in previous studies (Choi et al., 2010; Rhee et al., 2015).

3.2.6: Enzyme-Linked Immunosorbent Assay

The entirety of mouse small intestine was homogenized in RIPA lysis buffer. Total protein lysates were then subjected to an enzyme-linked immunosorbent assay (ELISA) to measure cytokines mouse KC, MIP3a, IL-6 and myeloperoxidase (MPO) using appropriate kits from R&D Systems and LSBio Inc. following manufacturer's instructions. The concentration of cytokine was normalized by total protein concentration. All assays were performed in triplicate and data was expressed as Mean ± SEM.

3.3: Results

3.3.1: *Pten* Gene Deletion in IECs Increased Susceptibility to Infection of *Salmonella enterica* serovar Typhimurium in Streptomycin-Pretreated Mice

Mice are inherently resistant to *Salmonella* infection, unlike humans, who are susceptible to infection by *Salmonella.* This natural resistance can be overcome by oral administration of streptomycin, which transiently depletes the microbiota, and renders the mouse exceptionally susceptible to *Salmonella* infection (Barthel et al., 2003). After a single pretreatment of streptomycin, oral administration of a high inoculum of *Salmonella* (10^8 CFU) causes acute intestinal inflammation within 6 to 8 hours, presented by massive growth of the pathogenic bacteria and noticeable cecum and colon inflammation (Altmeyer et al., 2010; Barthel et al., 2003). Use of this mouse model allowed the

investigation whether *Pten* gene deletion in IECs could enhance susceptibility to enteric salmonellosis in $Pten^{\Delta IEC/\Delta IEC}$ mice and littermate $Pten^{+/+}$ controls.

8-week-old and sex-matched $Pten^{\Delta IEC/\Delta IEC}$ mice and littermate $Pten^{+/+}$ mice were pretreated with an oral, intragastric administration of streptomycin (25 mg/mouse) for 24 hours. Mice were then infected with a low inoculum of *S.* Typhimurium (2×10^4 CFU) via an oral gavage.

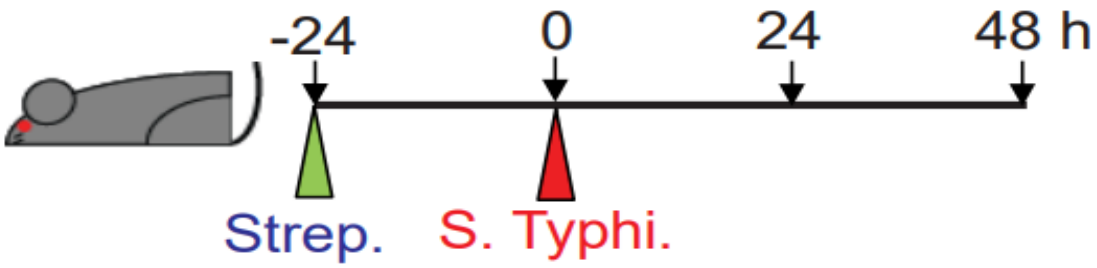

Figure 22: The illustration above represents the experimental timeline for the streptomycin-pretreatment and subsequent bacterial inoculation. Sex matched, 8-week-old $Pten^{\Delta IEC/\Delta IEC}$ and littermate $Pten^{+/+}$ mice were pretreated with an oral gavage of streptomycin (25 mg/mouse) for 24 hours. The mice were then inoculated via an oral gavage with a low inoculum of S. Typhimurium (2×10^4 in a volume of 200 mL/mouse).

$Pten^{\Delta IEC/\Delta IEC}$ mice were observed to exhibit an increased mortality 48 hours after bacterial infection compared to $Pten^{+/+}$ control mice. Next, the ceca of the mice was examined because it is the most sensitive portion of the intestinal tract of the streptomycin mouse model of salmonellosis (Altmeyer et al., 2010; Barthel et al., 2003). The ceca $Pten^{\Delta IEC/\Delta IEC}$ mice not only appeared pale with reduced cecal contents, but the ceca were also shriveled to a small size with exudate. Whereas the ceca of the $Pten^{+/+}$ control mice had a grossly normal appearance. Lastly, the weight of the ceca from $Pten^{\Delta IEC/\Delta IEC}$ mice were significantly lower compared to $Pten^{+/+}$ control mice, which suggest that $Pten^{\Delta IEC/\Delta IEC}$ mice were experiencing enhanced susceptibility to the infection

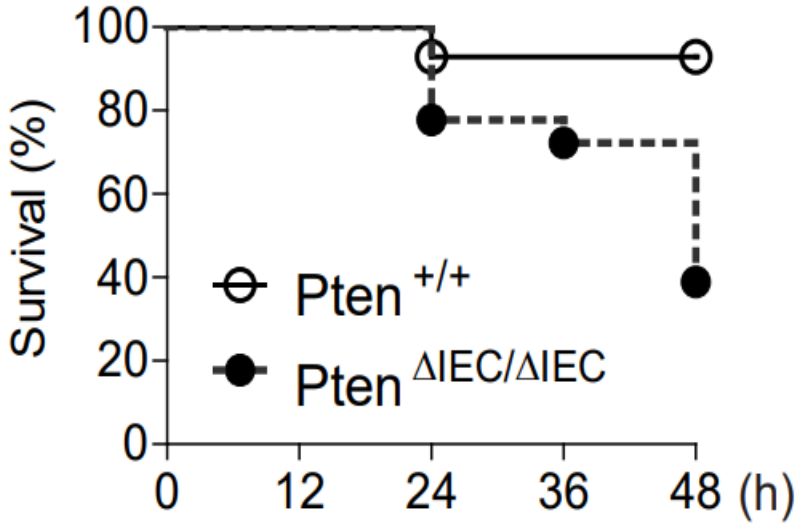

Figure 23: $Pten^{\Delta IEC/\Delta IEC}$ and $Pten^{+/+}$ mice were inoculated via an oral gavage with a low inoculum of S. Typhimurium (2×10^4 in a volume of 200 mL/mouse). The mouse health condition was monitored for 48 h after inoculation. Mouse mortality was evaluated by Kaplan-Meier plot. The log-rank (Mantel-Cox) test was used to compare significant survival difference (P = 0.0033). Data were analyzed with results accumulated by 3 independent experiments. $Pten^{\Delta IEC/\Delta IEC}$ (n = 18); $Pten^{+/+}$ (n = 15).

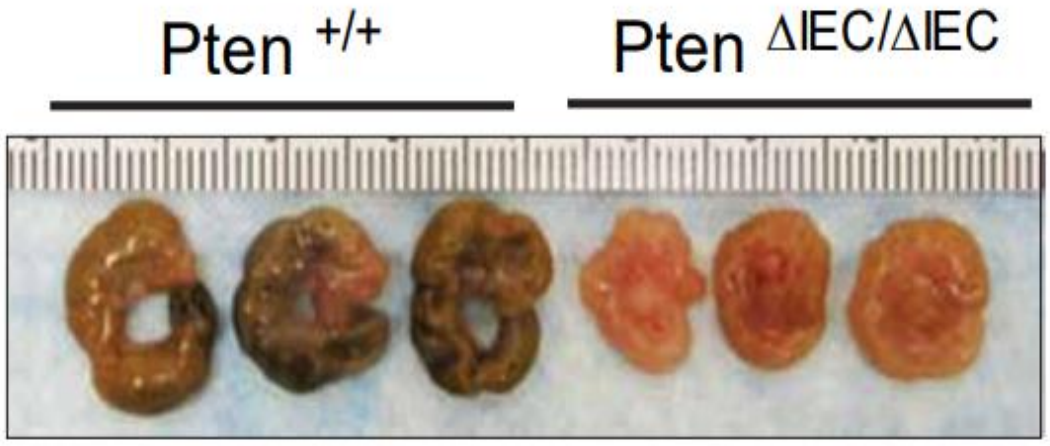

Figure 24: The photograph above shows representative gross anatomical images of the ceca obtained from both $Pten^{+/+}$ mice (left) and $Pten^{\Delta IEC/\Delta IEC}$ mice (right). The ceca of the $Pten^{\Delta IEC/\Delta IEC}$ mice were much smaller with reduced fecal contents compared to $Pten^{+/+}$ control mice.

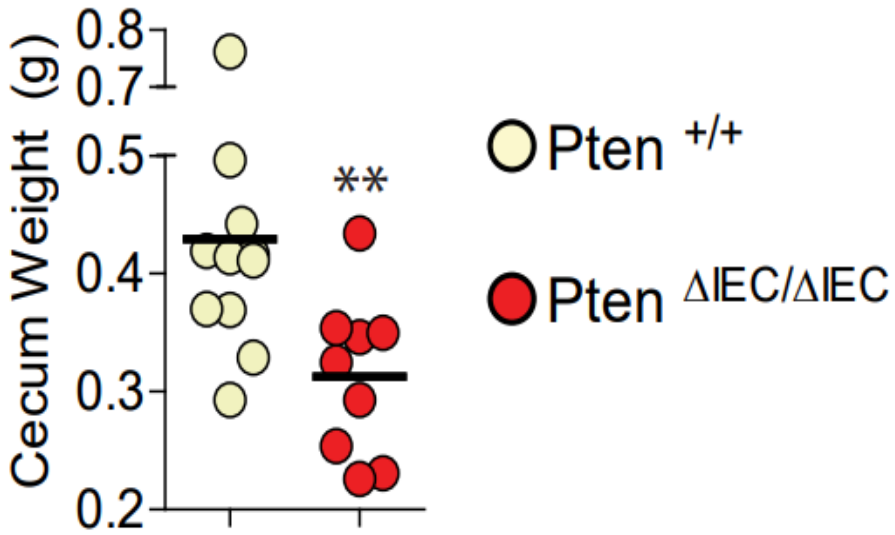

Figure 25: Cecum weight was measured and then graphed to compare the susceptibility to *S.* Typhimurium infection between the mouse groups. $Pten^{\Delta IEC/\Delta IEC}$ (n = 10); $Pten^{+/+}$ (n = 9). *** $P < 0.001$ (Mann-Whitney U test).

Together these data show that a deficiency of the *Pten* gene in the intestinal epithelium render mice unable to resist infection with a low inoculum of *S.* Typhimurium in a streptomycin-pretreated mouse model.

3.3.2: Low Inoculum of *Salmonella enterica* serovar Typhimurium Produced Massive Inflammation in the Small Intestines of $Pten^{\Delta IEC/\Delta IEC}$ Mice

High inoculum of *S.* Typhimurium (10^8 CFU) in the streptomycin-pretreated mouse model can induce substantial inflammation in the cecum and colon, however, the small intestine in not usually inflamed by bacterial infection (Altmeyer et al., 2010; Barthel et al., 2003). In this study, it was found that just a low dose (2×10^4 CFU) infection of *S.* Typhimurium not only increased mortality, but also induced inflammation in the ceca of streptomycin-pretreated $Pten^{\Delta IEC/\Delta IEC}$ mice.

Next, it was examined whether a low dose *S.* Typhimurium infection is also capable of producing deleterious inflammation in the small intestine of $Pten^{\Delta IEC/\Delta IEC}$ mice. Tissue sections of the cecum from streptomycin-pretreated $Pten^{\Delta IEC/\Delta IEC}$ mice exhibited massive inflammation in response to the low inoculum of *S.* Typhimurium, in line with the inflamed gross appearance of ceca previously mentioned. However, the ceca of the streptomycin-pretreated $Pten^{+/+}$ mice appear to have normal histology of the epithelia and mucosa.

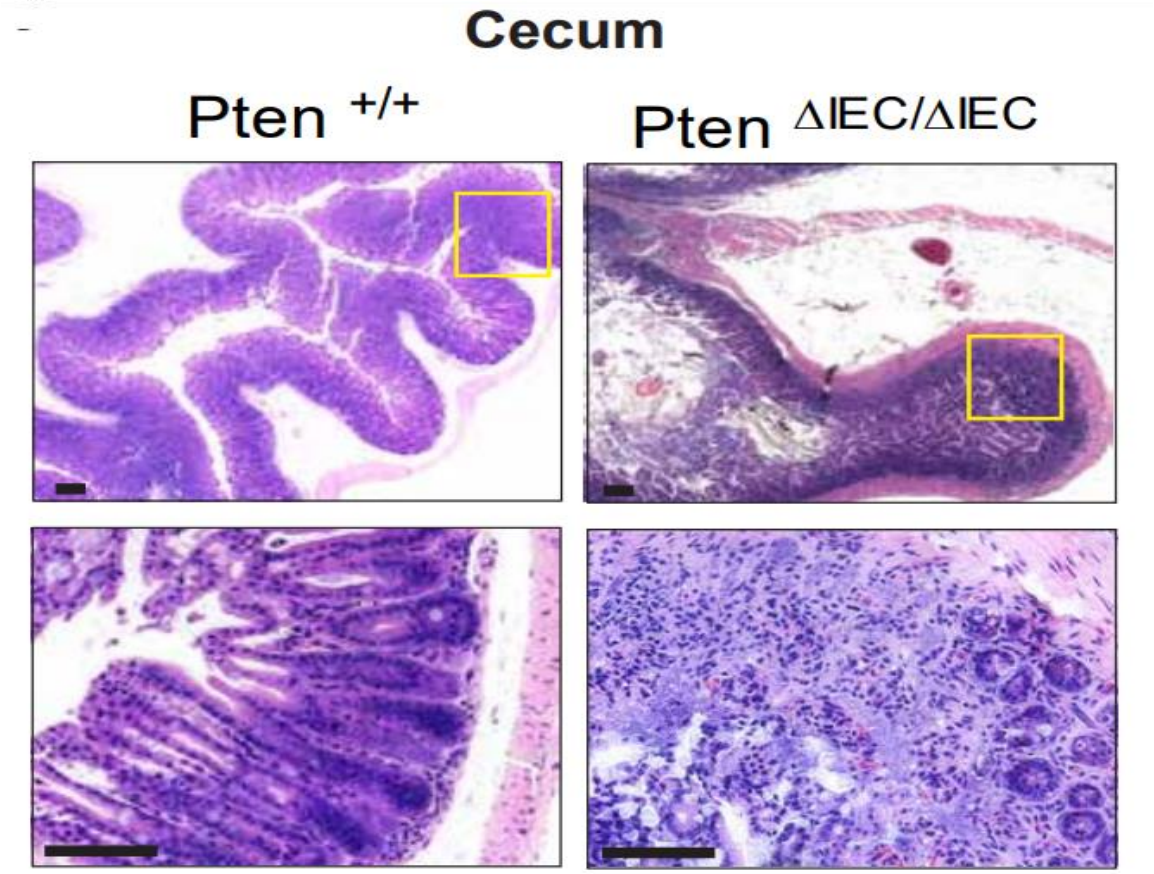

Figure 26: The above image shows a Hematoxylin and Eosin (H&E) staining of mice cecum sections. The antibiotic pre-treated $Pten^{\Delta IEC/\Delta IEC}$ and $Pten^{+/+}$ mice were infected with an oral gavage of S. Typhimurium (2×10^4/200 mL/mouse). 24 hours after the infection, the mice were euthanized to harvest the intestinal tissues. Tissues were fixed in 10% buffered formalin and subsequently embedded in paraffin and then stained. The photographs are representative images of the damage and inflammation in the cecum. Inset area (box in yellow) was enlarged.

Surprisingly, just a low inoculum of *S.* Typhimurium produced extensive inflammation in the small intestine of streptomycin-pretreated Pten$^{\Delta IEC/\Delta IEC}$ mice. Although, Pten$^{+/+}$ mice maintained fairly normal structure of the epithelia and mucosa in the small intestine.

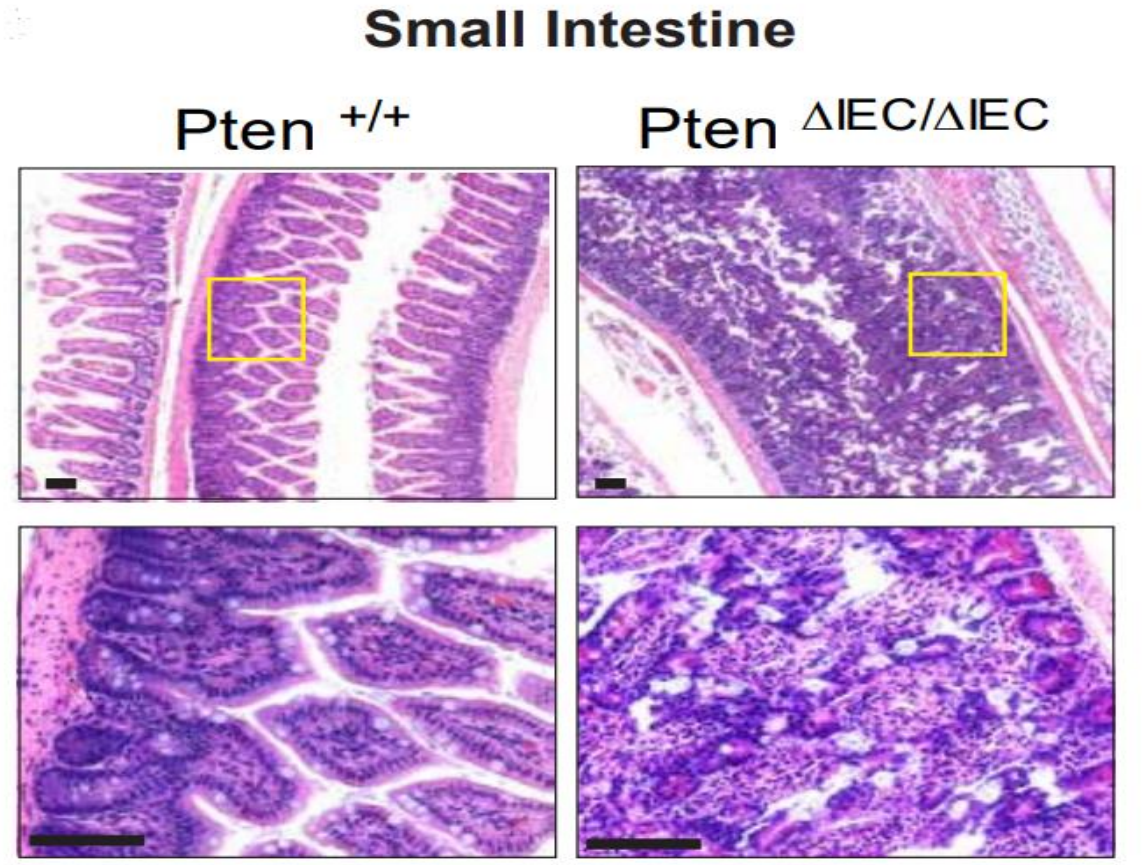

Figure 27: The image above shows a Hematoxylin and Eosin (H&E) staining of mice small intestine sections. The antibiotic pre-treated Pten$^{\Delta IEC/\Delta IEC}$ and Pten$^{+/+}$ mice were infected with an oral gavage of S. Typhimurium (2×10^4/200 mL/mouse). 24 hours after the infection, the mice were euthanized to harvest the intestinal tissues. Tissues were fixed in 10% buffered formalin and subsequently embedded in paraffin and then stained. The photographs are representative images of the damage and inflammation in the small intestine. Insert area (box in yellow) was enlarged.

Microscopic examination of the intestinal tissue histology revealed that streptomycin-pretreated Pten$^{\Delta IEC/\Delta IEC}$ mice exhibited prominent abscesses, massive neutrophil infiltration, increased epithelial erosion and enhanced necrosis in both the

small intestine and the cecum in response to the infection by *S.* Typhimurium. However, these histological parameters were almost negligible in the intestinal tissues of control mice.

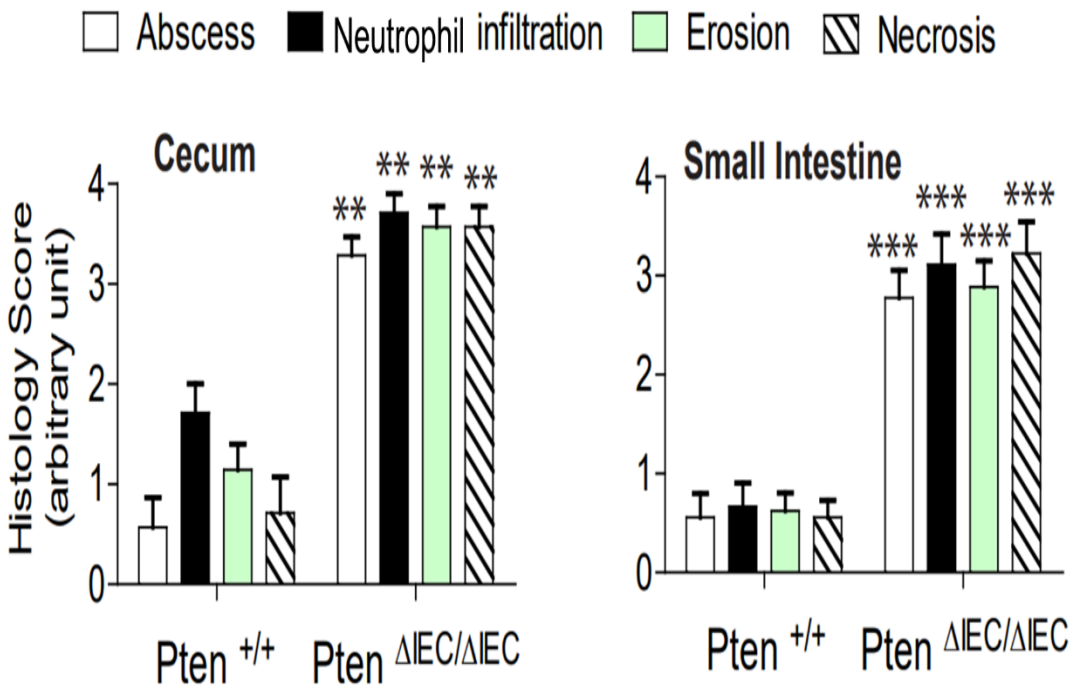

Figure 28: The graphs above display quantified histological parameters were for H&E sections of the cecum (shown left) and small intestine (shown right) of the two mouse groups (n = 7/group). $Pten^{\Delta IEC/\Delta IEC}$ mice had significantly increased inflammation in the cecum and small intestine compared to $Pten^{+/+}$ controls. ** $P < 0.01$, *** $P < 0.001$ (Mann-Whitney U test).

It was observed that a low inoculum of *S.* Typhimurium did not induce noticeable inflammation in the cecum and small intestine of the streptomycin-pretreated $Pten^{+/+}$ mice. However, this data clearly exhibits that the streptomycin-pretreated $Pten^{\Delta IEC/\Delta IEC}$ mice had considerable inflammation in the cecum and small intestine in response to low dose *S.* Typhimurium infection. Therefore, these results suggest that *Pten* deficiency in IECs significantly increases the susceptibility to enteropathogenic bacterial infection.

3.3.3: *Salmonella enterica* serovar Typhimurium Infection Induced Pro-Inflammatory Cytokine Production in the Small Intestine of $Pten^{\Delta IEC/\Delta IEC}$ Mice

The production of pro-inflammatory cytokines in the intestinal tissues was then analyzed. It was identified that infection by *S.* Typhimurium markedly up-regulated the production of various pro-inflammatory cytokines (KC, MIP3a, and IL-6) in the small intestine of streptomycin-pretreated $Pten^{\Delta IEC/\Delta IEC}$ mice compared to $Pten^{+/+}$ mice.

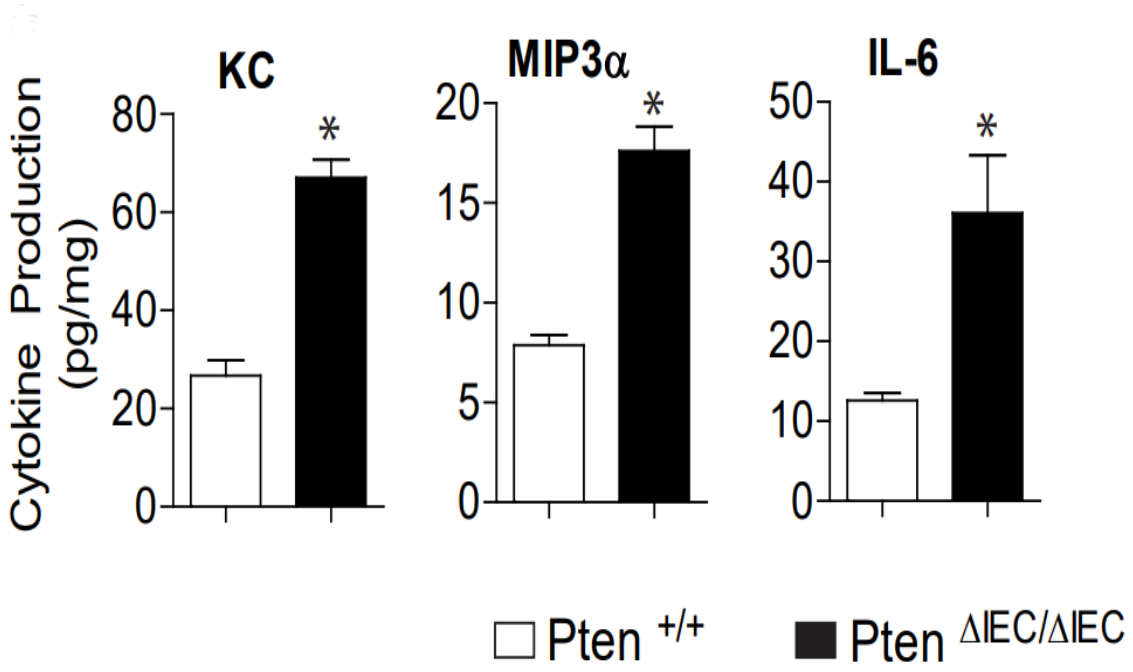

Figure 29: The graphs above show pro-inflammatory cytokine levels of the small intestine of $Pten^{\Delta IEC/\Delta IEC}$ and $Pten^{+/+}$ mice. $Pten^{\Delta IEC/\Delta IEC}$ and $Pten^{+/+}$ mice were pretreated with streptomycin, followed by an oral gavage of S. Typhimurium (2×10^4/200 ml/mouse). 24 hours after administration, the mice were euthanized to harvest the small intestine. The total protein was extracted from the mouse small intestine, followed by ELISA to measure the level of KC, MIP3a, and IL-6 production. Data were expressed as mean ± SEM (n= 4 mice per group, each with triplicate determinations). * $P < 0.05$ (Mann-Whitney U test).

Myeloperoxidase (MPO) production was also significantly increased in the small intestine of $Pten^{\Delta IEC/\Delta IEC}$ mice compared to $Pten^{+/+}$ controls. MPO has an important role in the initiation and progression of inflammatory disorders by generating hypochlorous acid.

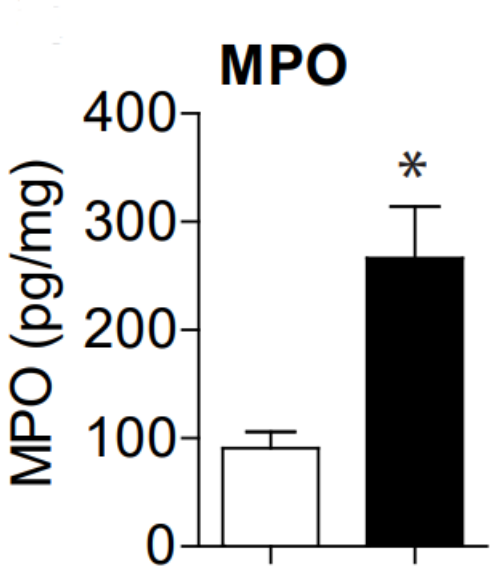

Figure 30: The graph above compares the myeloperoxidase (MPO) levels in the small intestine of $Pten^{\Delta IEC/\Delta IEC}$ and $Pten^{+/+}$ mice. $Pten^{\Delta IEC/\Delta IEC}$ and $Pten^{+/+}$ mice were pretreated with streptomycin, followed by an oral gavage of S. Typhimurium (2×10^4/200 mL/mouse). 24 hours after administration, the mice were euthanized to harvest the small intestine. The total protein was extracted from the mouse small intestine, followed by ELISA to measure the level of MPO. Data were expressed as mean ± SEM (n= 4 mice per group, each with triplicate determinations). * $P < 0.05$ (Mann-Whitney U test).

3.3.4: Bacterial Colonization was Increased in Streptomycin-pretreated $Pten^{\Delta IEC/\Delta IEC}$ Mice

S. Typhimurium can penetrate the intestinal epithelial barrier by infiltrating microfold cells (M cells) or by transportation through dendritic cells, leading to severe inflammation of the cecum and colon. Additionally, *S.* Typhimurium is capable of translocation and colonization of the mesenteric lymph node (MLN), where thereafter *S.* Typhimurium can migrate to the spleen and liver (Bravo-Blas et al., 2019). It was next examined whether the bacterial load in extraintestinal organs could be increased in $Pten^{\Delta IEC/\Delta IEC}$ mice due to the previous finding that a low inoculum of *S.* Typhimurium in streptomycin-pretreated $Pten^{\Delta IEC/\Delta IEC}$ mice elicited deleterious inflammation in the small intestine and cecum. The tissue homogenates were plated using a serial dilution on

MacConkey agar plates and then incubated to evaluate bacteria colony growth. The bacterial load determined by the number of CFUs was observed to be significantly increased in the MLN, liver, and spleen of $Pten^{\Delta IEC/\Delta IEC}$ mice, whereas bacterial colony formation from the tissues of $Pten^{+/+}$ mice was almost negligible. An enlarged spleen is indicative of bacterial infection in mice. Consistent with this notion, streptomycin-pretreated $Pten^{\Delta IEC/\Delta IEC}$ mice presented enlarged spleens in response to the *S.* Typhimurium infection compared to controls.

These data together suggest that the translocation and extraintestinal colonization of *S.* Typhimurium will be enhanced in the IEC-restricted *Pten* gene deficient condition. Additionally, these results indicate that PTEN expression in the intestinal epithelium should play a key role in the innate and adaptive immune defenses that protect the host from invasion by *S.* Typhimurium.

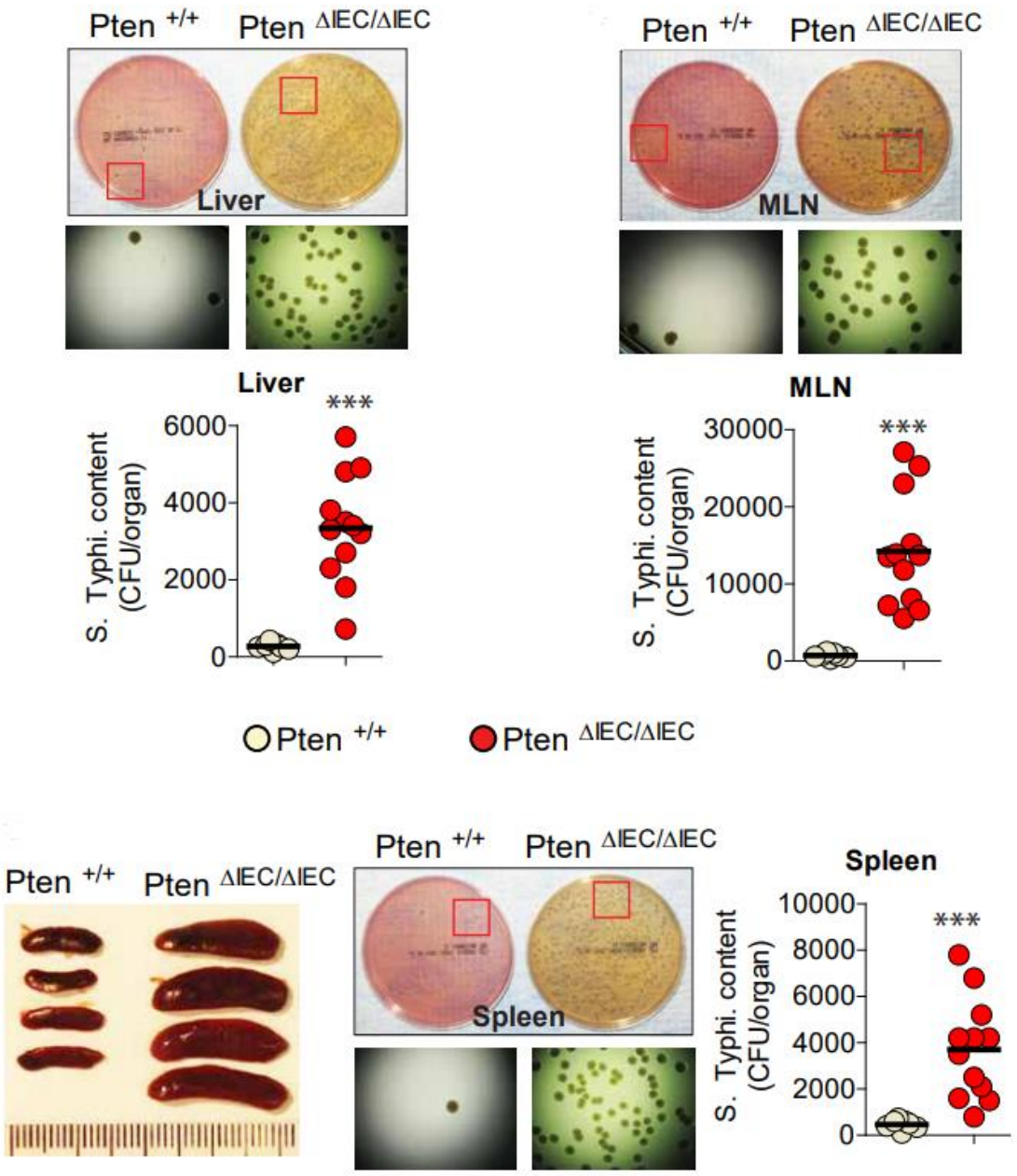

Figure 31: The images above show the bacterial load found in extraintestinal organs of $Pten^{\Delta IEC/\Delta IEC}$ and $Pten^{+/+}$ mice. The mice were pretreated with streptomycin, followed by an oral gavage of S. Typhimurium (2×10^4/200 mL/mouse). The liver (top left), mesenteric lymph node (MLN) (top right), and spleen (bottom center) were harvested in 48 hours and homogenized in PBS. The sample dilutions were plated on MacConkey agar plates and incubated in 37°C. The photograph is representative images of the culture plates, and the inset area was enlarged to visualize the bacterial colonies. Gross appearance of the spleen from the mice was compared, and ruler markings indicate mm measurement. The bacterial loads were determined by counting the number of colony forming units (CFU) per organ. $Pten^{+/+}$ (n = 7); $Pten^{\Delta IEC/\Delta IEC}$ (n = 12), *** $P < 0.001$ (Mann-Whitney U test).

3.4 Discussion

Using the streptomycin-pretreated mouse model of *S.* Typhimurium infection, it was observed that a low dose of *S.* Typhimurium did not induce intestinal inflammation in $Pten^{+/+}$ mice. However, streptomycin-pretreated $Pten^{\Delta IEC/\Delta IEC}$ mice developed deleterious inflammation throughout the small intestine and cecum in response to a low dose of *S.* Typhimurium infection. These data clearly demonstrate that *Pten* deficiency in IECs dramatically enhance the susceptibility to bacterial infection. Therefore, PTEN plays an important role in mediating defense against enteropathogenic bacteria in the gut.

PTEN is an essential mediator of microbial sensing and subsequent immune activation signaling in the intestine. PIP2, produced by PTEN, tethers MAL/TIRAP to the plasma membrane, where it thereby facilitates the interaction of MAL/TIRAP with TLR5 in the membrane of IECs (Choi et al., 2013). TLR5, which is potently expressed in IECs, plays a canonical role in the intestinal epithelium for microbial sensing and in shaping the innate and adaptive immune system of the gastrointestinal tract (Rhee et al., 2006). In this context, PTEN should at least be considered an immune regulating factor in the gut, in addition to its role as a tumor suppressor. Nevertheless, it has remained elusive whether PTEN deficiency in IECs can influence susceptibility to enteropathogenic bacterial infection. Therefore, this study provides important data to fill in the gap between an immune regulatory effect of PTEN and *in vivo* susceptibility to pathogenic bacterial infection.

Regarding the immune effector mechanism resulting from PTEN-mediated signaling, it is possible that antimicrobial peptides, intestinal lamina propria dendritic cells, macrophages, and T cell responsiveness could participate from protecting the hose

from enteropathogenic bacterial infection (Ellenbroek et al., 2017; H. Liu et al., 2016; Vijayan et al., 2018). A group of antimicrobial peptides, which constitute an efficient innate immune mechanism to eliminate invading microbes, can be upregulated by TLR5-induced signaling pathways in the gut (Vijayan et al., 2018). Likewise, TLR5 activation has been suggested to not only activate dendritic cells and macrophages in the intestinal mucosa, but also to mediate effector T cell responses, which are the key players of adaptive immunity (Ellenbroek et al., 2017; H. Liu et al., 2016). Therefore, it is reasonable to consider PTEN an essential regulatory factor of the gut mucosal immune response, because the level of PIP2, which is controlled by PTEN, is critical for an TLR5 immune activation in IECs.

3.5: Conclusion

This study provides *in vivo* data demonstrating that *Pten* gene deletion in IECs renders mice exceedingly susceptible to enteropathogenic bacterial infection, thus building upon a previously reported study accounting for how PTEN is capable of regulating TLR5-mediated immune and inflammatory responses (Choi et al., 2013). These findings presented in this study provide *in vivo* data which demonstrates strong evidence that PTEN has an immune regulatory function in the GI tract. Additionally, this project connects the gap between the PTEN-associated immune mechanism suggested in an *in vitro* setting and relevant *in vivo* significance for enteropathogenic bacterial infection.

CHAPTER FOUR

STUDYING THE GUT-BRAIN INFLAMMATORY INTERACTION

4.1: Introduction

The gut and brain are fairly separated anatomically, but emerging evidence suggests that these two organs may communicate and influence each other's physiological functioning in a bidirectional manner (Rhee et al., 2009). In the descending pathway of the gut-brain axis, psychological stress has been proposed to play an important role in the development and progression of irritable bowel syndrome (IBS) and may also increase the chances of IBD (Jones et al., 2006; Levenstein et al., 2000). Psychological stress has also been suggested to increase intestinal permeability, which would allow luminal contents into the submucosa, which could trigger the immune system and cause an inflammatory response (Zong et al., 2019). In the ascending pathway of the gut-brain axis, signals from the gut create an effect on the brain. In this case, it has been suggested that the human appendix contains α-synuclein aggregates that accumulate in Lewy bodies of Parkinson's disease (Killinger et al., 2018). Additionally, patients with IBD experience transient cognitive impairments such as "brain fog". Which is typically characterized by memory issues, disorientation, hazy thought processes, and slow cognitive reaction time (Petruo et al., 2017; Yelland, 2017). Emerging evidence suggests that the enteric microbiota has a crucial impact on the gut-brain axis, not only interacting with various intestinal cells, but also with the central nervous system through neuroendocrine and metabolic pathways (Carabotti et al., 2015). Patients with IBD tend to have higher rates psychological, such as depression and anxiety (Gracie et al., 2018).

Gut microbiota have been noted to have a role in influencing anxiety and depressive-like behaviors (Foster & McVey Neufeld, 2013; Naseribafrouei et al., 2014). Altogether, these studies suggest a communitive-link between the gut and brain, and that chronic intestinal inflammation may influence brain functionality. However, evidence for an underlying mechanism between the chronically inflamed gut and brain remains elusive.

To further study the gut-brain inflammatory interaction, an interleukin-10 knockout (IL-10 KO) mouse, which is a known mouse model of chronic enterocolitis (Kühn et al., 1993), Mice deficient in IL-10 will spontaneously develop chronic colitis, however, the incidence rate of colitis in this model is low and prolonged (Chichlowski et al., 2010). To overcome this challenge, IL-10 KO mice were fed a piroxicam-mixed chow. The mixed chow contains a non-steroidal anti-inflammatory drug that inhibits cyclooxygenase (COX) enzymes and suppresses the colonic level of prostaglandin E2 (PGE2) (Berg et al., 2002). This suppression of PGE2 leads to damage of the gut-mucosa lining and impaired mucosal integrity, which gives way to translocation of luminal bacteria to trigger inflammation (Agard et al., 2013). Thus, the IL-10 KO condition combined with piroxicam-mixed chow feeding more closely mimic IBD.

4.2: Materials and Methods

4.2.1: Animals

IL-10 KO mice and IL-10 WT mice were obtained from the Jackson Laboratory (Bar Harbor, ME). Mice were bred and maintained under standard SPF conditions with normal drinking water ad libitum at the animal facility of Oakland University under the approval of the Institutional Animal Care and Use Committees of UCLA and OU.

4.2.2: Chronic Colitis Mouse Model

IL-10 KO and IL-10 WT mice were fed three cycles of piroxicam-mixed chow for seven days. Piroxicam was purchased from Millipore Sigma (St. Louis, MO) and sent to Research Diets Inc. (New Brunswick, NJ), where the piroxicam was pressed into custom pellets and purchased for mouse consumption. The two mice groups were then fed normal mice pellet chow for seven days for recovery to mimic the chronicity of colitis.

4.2.3: Enzyme-Linked Immunosorbent Assay Quantification of IL-1β, IL-6 and High-Mobility Group Box 1

Enzyme-linked immunosorbent assay (ELISA) kits (mouse IL-1β and IL-6) compatible with tissue extract samples from RayBiotech Inc. (Norcross, GA) were utilized. The cerebrum, hippocampus, and colon tissues were homogenized in radioimmunoprecipitation assay lysis buffer supplemented with cOmplete Protease Inhibitor Cocktail and Phosphatase Inhibitor Cocktail 2 and 3 (Millipore Sigma, St. Louis, MO), followed by evaluation of the total protein concentration using the Pierce BCA Protein Assay Kit (Thermo Fisher Scientific). ELISA was performed in accordance with the manufacturer's instruction. The concentration was normalized according to the total protein concentration of the sample. All assays were performed in triplicate, and data are shown as means ± SEM.

4.2.4: Statistical Analysis

Data of body weight change were compared by using a student T-test. Results are provided as means ± SD. $P < 0.05$ was considered significant. Additional information regarding statistical analysis is described in the corresponding figure legends. Statistical analysis was conducted with Microsoft Office Excel (Microsoft, Redmond, WA).

4.3: Results

4.3.1: Bodyweight of Piroxicam-fed IL-10 KO Mice was Lower Compared to Piroxicam-fed IL-10 WT Control Mice

IL-10 KO and IL-10 WT mice were fed 3 cycles of piroxicam-mixed chow for 7 days, then both mice groups were allowed 7 days of regular chow for recovery in order to mimic chronic colitis. Bodyweights were collected from IL-10 KO mice and IL-10 WT my for 36 days. It was observed that the piroxicam-fed IL-10 KO mice exhibited decreased bodyweight compared to wild-type control mice, thus indicating that the IL-10 KO mice were experiencing colitis symptoms.

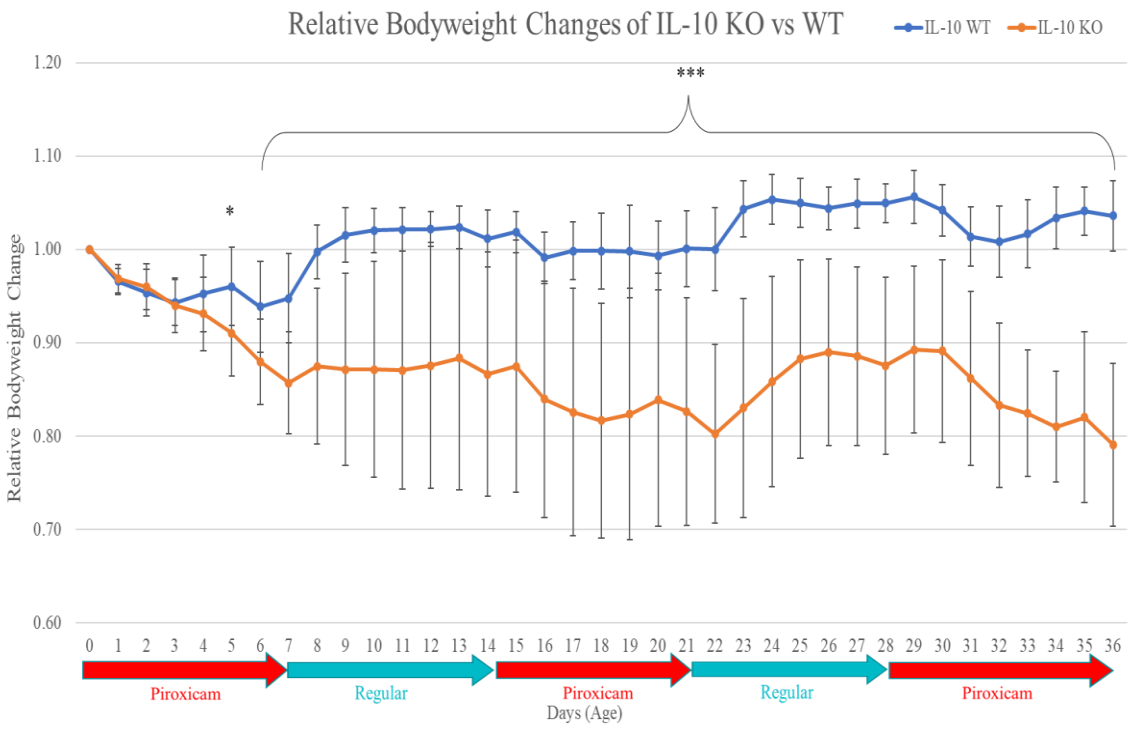

Figure 32: This graph shows the relative bodyweight change of IL-10 KO mice vs IL-10 WT mice. Piroxicam mixed chow was given to both mice groups for 7 days, then given regular chow for 7 days to allow for recovery. The graph depicts decreasing bodyweight in the IL-10 KO mice compared to control mice indicating that these mice are experiencing IBD symptoms. Data was shown as mean ± SD. Bodyweight comparison significance was calculated using independent student T-test. * $P < 0.05$, ** $P < 0.01$, *** $P < 0.001$ was considered significant.

4.3.2: Colon Size and Length of Piroxicam-fed IL-10 KO Mice were Decreased Compared to Piroxicam-fed IL-10 WT Control Mice

After harvesting tissues, the gross anatomical size and length of the piroxicam-fed IL-10 KO mice colons were found to be smaller and decreased in length compared to controls. Additionally, the piroxicam-fed IL-10 KO mice appeared to have notably smaller ceca compared to IL-10 WT control mice.

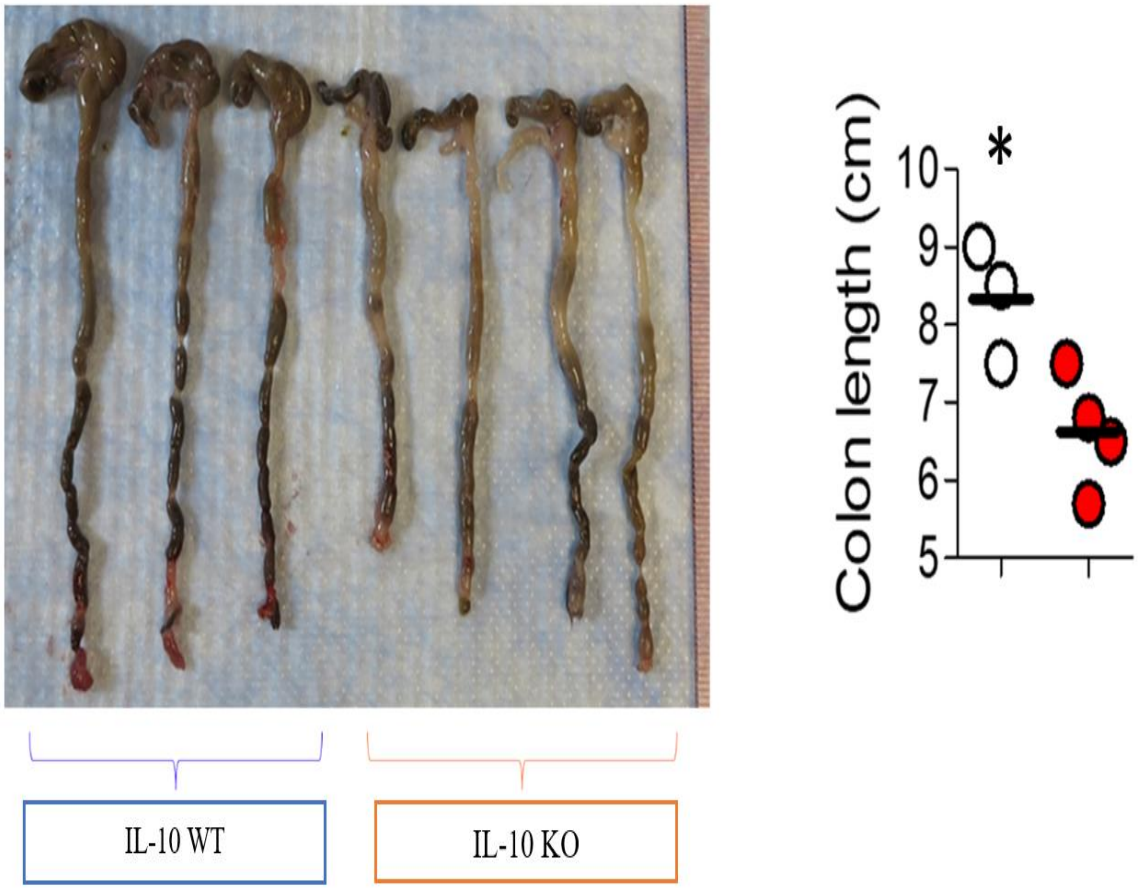

Figure 33: The image above depicts the gross anatomy of the colon of both IL-10 wild-type controls (first 3 colons starting from left to right) and IL-10 KO mice (last 4 colons starting from left to right). The colons of the IL-10 knockout mice appear inflamed with a white, pale appearance along with notably smaller cecum and length. On the right, the lengths were quantified and graphed. Control colons (white circle) were confirmed to have increased length compared to IL-10 KO mice (red circle). * $P<0.05$ was considered significant based on a one-tailed statistic test.

4.3.3: Pro-inflammatory Cytokine Levels were Elevated in Piroxicam-fed IL-10 KO Mice Tissues Compared to Piroxicam-fed IL-10 WT Control Mice Tissues

In order to observe the inflammatory connection between the gut and brain, the expression of pro-inflammatory cytokines IL-1β and IL-6 was measured in the mice cerebrum, hippocampus and colon tissues.

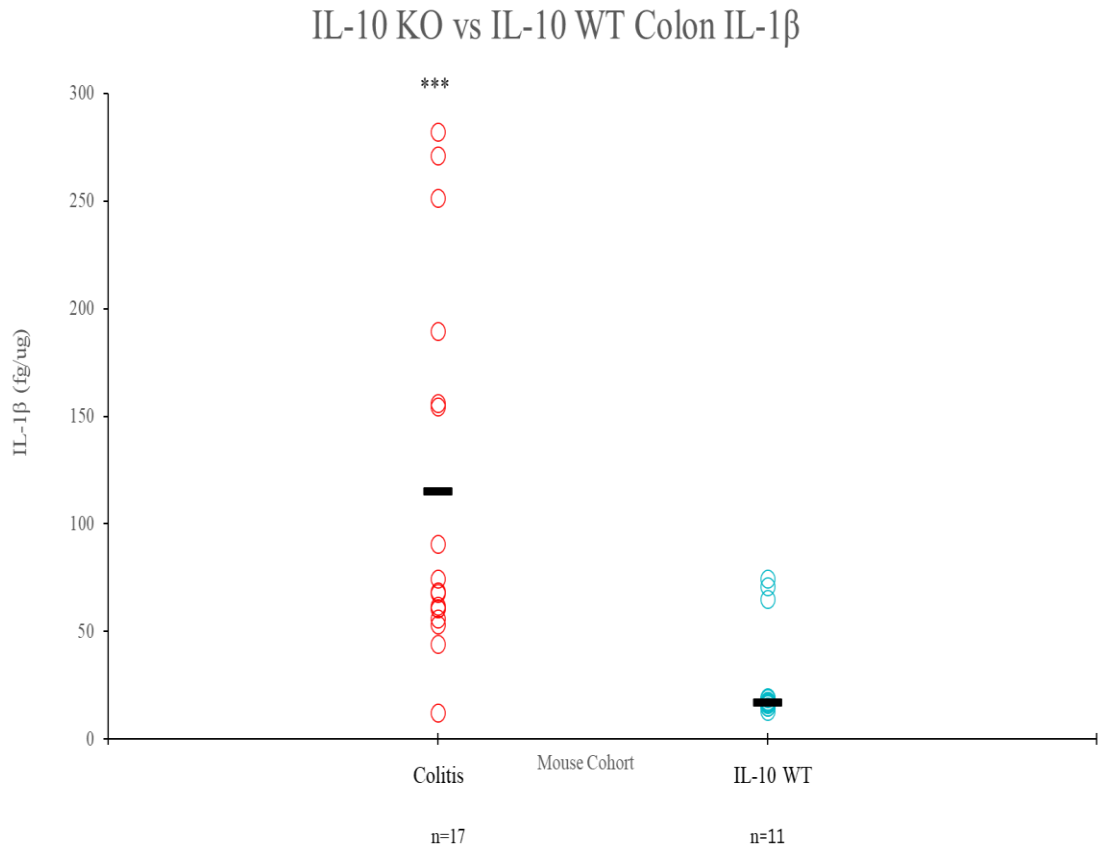

Figure 34: This graph shows the measurement of IL-1β pro-inflammatory cytokine expression in the colon tissue of piroxicam-fed IL-10 KO mice (red circles, n=17) and IL-10 WT mice (blue circles n=11). The average for each group is marked by a black bar. This data shows that IL-1β production was increased in IL-10 KO mice colon tissues compared to IL-10 controls, which demonstrates that IL-10 KO mice are experiencing colitis. * $P<0.05$, ** $P < 0.01$, *** $P <0.001$ was considered significant based on a one-tailed statistic test.

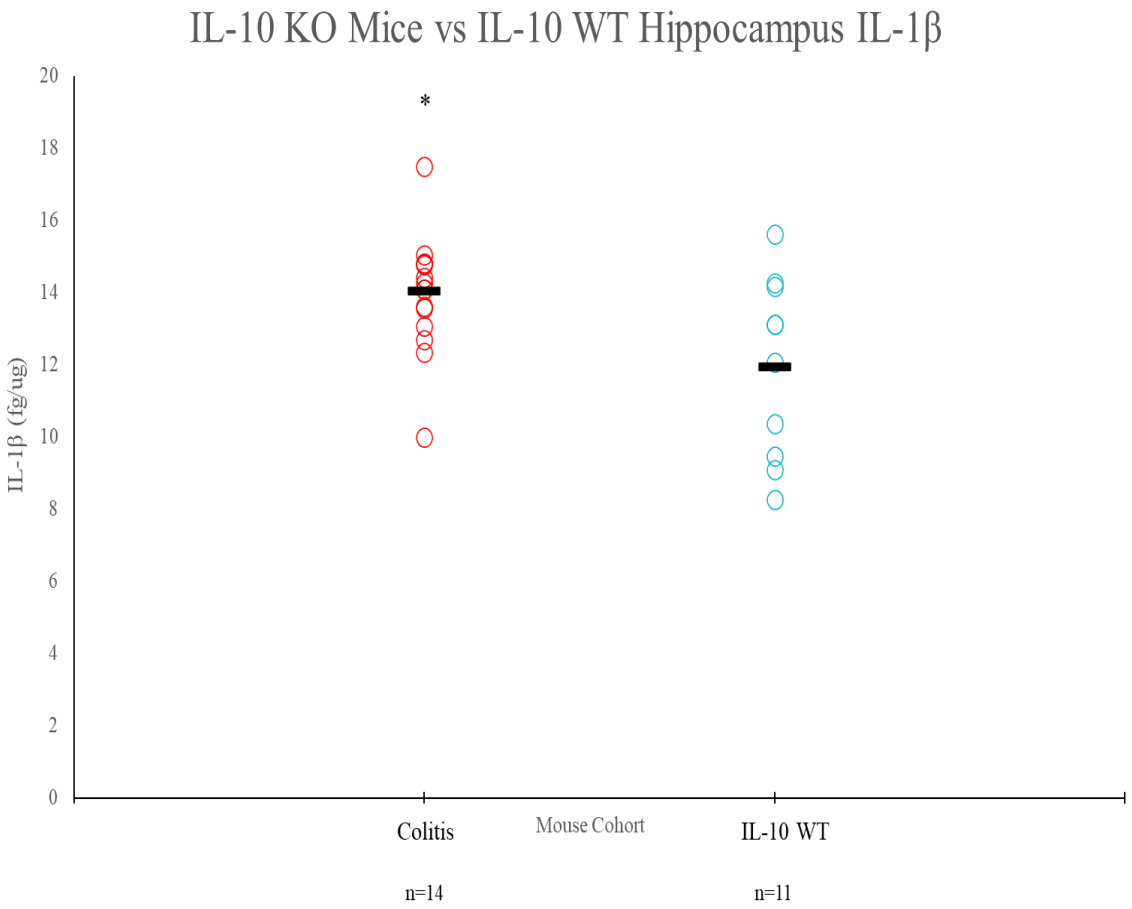

Figure 35: This graph shows the measurement of IL-1β pro-inflammatory cytokine expression in the hippocampus tissue of piroxicam-fed IL-10 KO mice (red circles, n=14) and IL-10 WT mice (blue circles n=11). The average for each group is marked by a black bar. This data shows that IL-1β production was increased in IL-10 KO mice hippocampus tissues compared to IL-10 controls, which supports that IL-10 KO mice are experiencing neuroinflammation. * $P<0.05$ was considered significant based on a one-tailed statistic test.

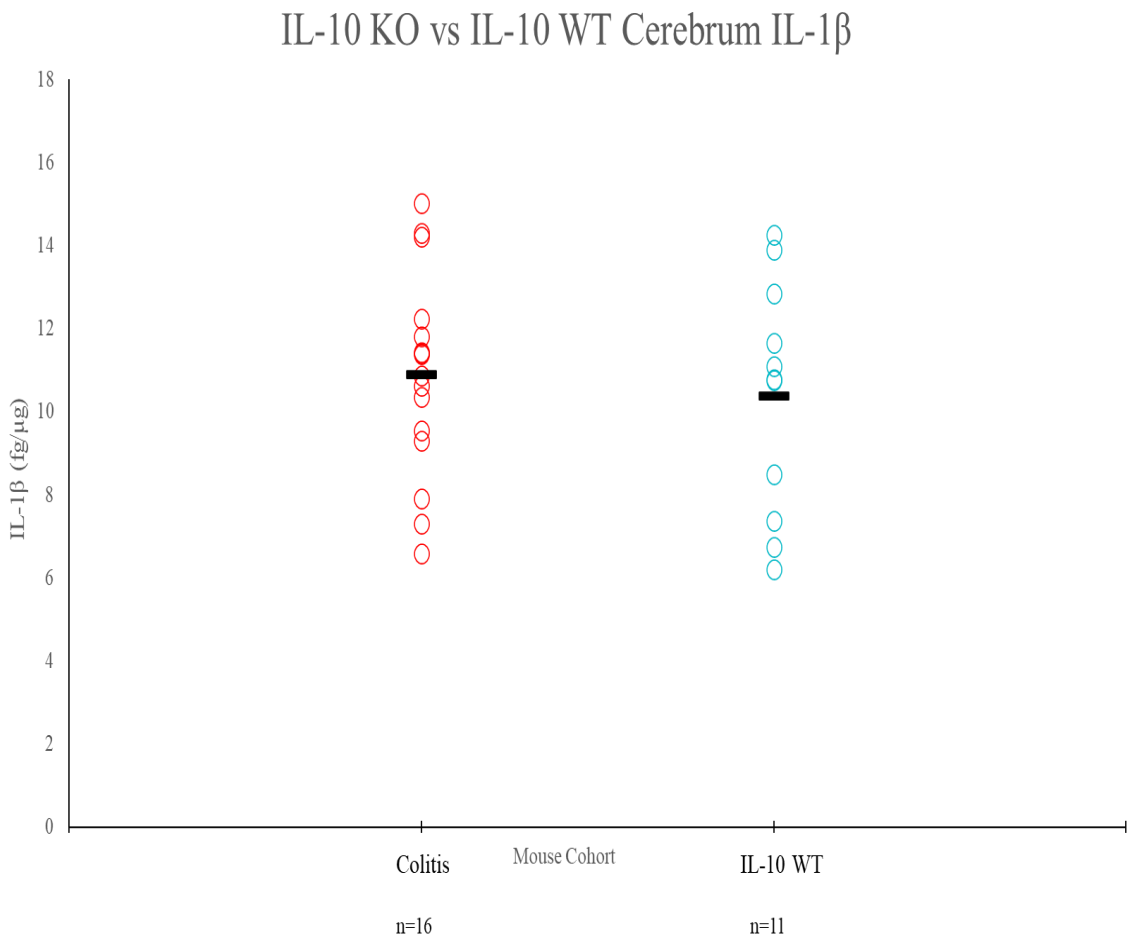

Figure 36: This graph shows the measurement of IL-1β pro-inflammatory cytokine expression in the cerebrum tissue of piroxicam-fed IL-10 KO mice (red circles, n=16) and IL-10 WT mice (blue circles n=11). The average for each group is marked by a black bar. This data shows that IL-1β production was increased in IL-10 KO mice cerebrum tissues compared to IL-10 controls, which supports that IL-10 KO mice are experiencing neuroinflammation. * $P<0.05$ was considered significant based on a one-tailed statistic test.

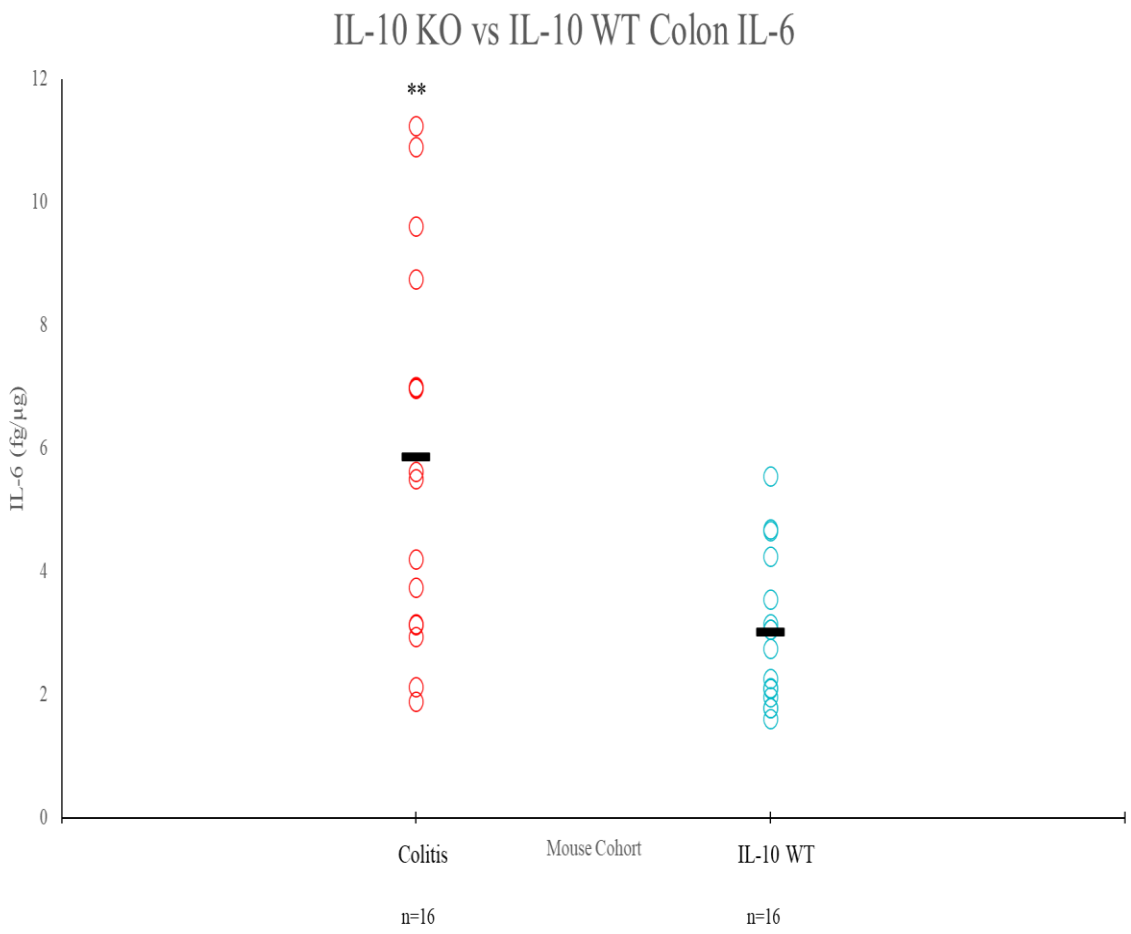

Figure 37: This graph shows the measurement of IL-6 pro-inflammatory cytokine expression in the colon tissue of piroxicam-fed IL-10 KO mice (red circles, n=16) and IL-10 WT mice (blue circles n=16). The average for each group is marked by a black bar. This data shows that IL-6 production was increased in IL-10 KO mice colon tissues compared to IL-10 controls, which demonstrates that IL-10 KO mice are experiencing colitis. * $P<0.05$, ** $P < 0.01$ was considered significant based on a one-tailed statistic test.

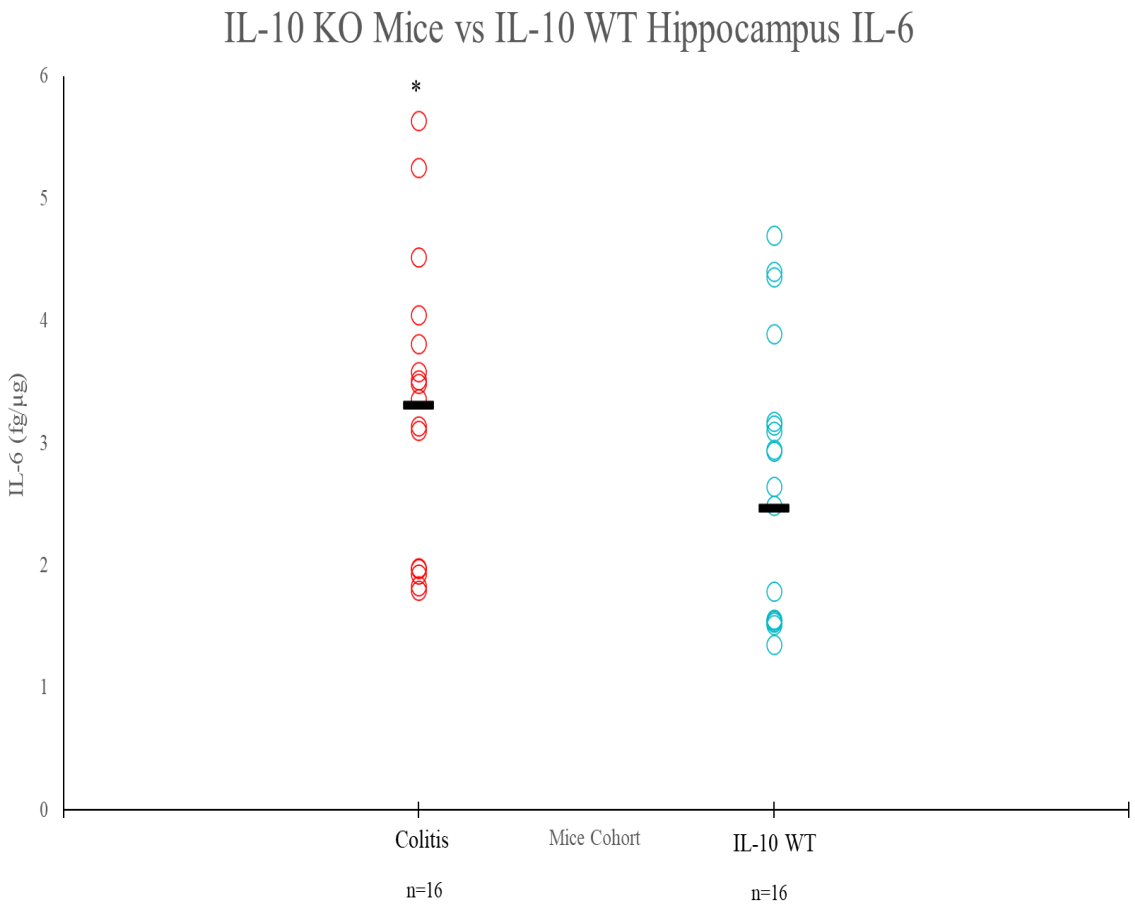

Figure 38: This graph shows the measurement of IL-6 pro-inflammatory cytokine expression in the hippocampus tissue of piroxicam-fed IL-10 KO mice (red circles, n=16) and IL-10 WT mice (blue circles n=16). The average for each group is marked by a black bar. This data shows that IL-6 production was increased in IL-10 KO mice hippocampus tissues compared to IL-10 controls, which supports that IL-10 KO mice are experiencing neuroinflammation. * $P<0.05$ was considered significant based on a one-tailed statistic test.

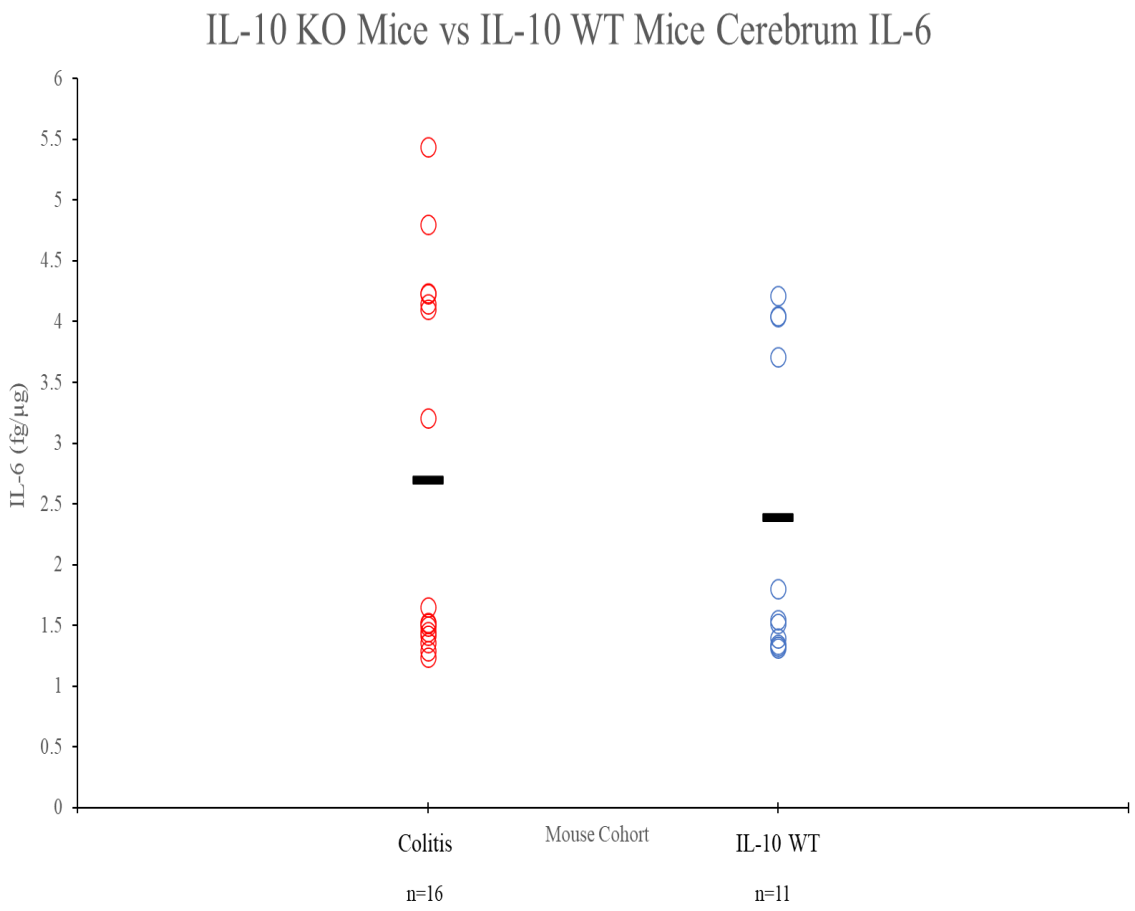

Figure 39: This graph shows the measurement of IL-6 pro-inflammatory cytokine expression in the cerebrum tissue of piroxicam-fed IL-10 KO mice (red circles, n=16) and IL-10 WT mice (blue circles n=11). The average for each group is marked by a black bar. This data shows that IL-6 production was increased in IL-10 KO mice cerebrum tissues compared to IL-10 controls, which supports that IL-10 KO mice are experiencing neuroinflammation. * $P<0.05$ was considered significant based on a one-tailed statistic test.

4.4: Discussion

IBD is a chronic inflammatory disease affecting the gastrointestinal tract, and can develop in a variety of ways. For instance, a defective mucosal barrier resulting in decreased permeability has been shown in patients with IBD (Michielan & D'Incà, 2015; Vanuytsel et al., 2021). It has also been suggested that commensal gut microbes can cause IBD by creating abnormal immune responses in genetically susceptible individuals

(Y. Chen et al., 2021; Loh & Blaut, 2012). Patients with IBD tend to develop extraintestinal manifestations in other organs such as the skin, joint, eyes, liver, pancreas and kidneys (Rogler et al., 2021). Those with IBD seem to be at a higher risk of dementia and Parkinson's disease (Killinger et al., 2018; Villumsen et al., 2019). A longitudinal cohort study recently identified that patients with IBD have a four-times increased risk for dementia, including Alzheimer disease, compared to healthy control patients (B. Zhang et al., 2021). However, the mechanism between the gut-brain axis has remained elusive.

This present study provides evidence that there may be an inflammatory link in the ascending pathway of the gut-brain axis. It was shown that piroxicam-fed IL-10 KO mice undergoing chronic colitis had an increased level of pro-inflammatory cytokines IL-1β and IL-6 in the hippocampus and cerebrum tissues compared to piroxicam-fed IL-10 control mice. This finding supports that IBD can lead to neuroinflammation in mice. Based on previous a previous study from this lab, it is hypothesized that HMGB1 could be a key molecule that can mediate neuroinflammatory responses in chronic colitis mice (Mitchell et al., 2022).

High mobility group box 1 (HMGB1) is a highly conserved chromatin-binding nuclear protein present in all cell types. HMGB1 is able to activate the transmembrane protein receptor for advanced glycation end-products (RAGE) and TLRs as a damage-associated molecular pattern when secreted into the extracellular environment (Sims et al., 2010; Wakabayashi et al., 2018). Additionally, HMGB1 has the ability to induce the production of pro-IL-1β in macrophages (Q. He et al., 2012). Elevated levels of HMGB1 protein have been found in stool samples of patients with IBD (Vitali et al., 2011).

Therefore, it is hypothesized that when IECs are necrotic or damaged, HMGB1 is released into the extracellular environment, where it can travel in the bloodstream cause a second wave of inflammation in peripheral tissues, such as neuroinflammation in the brain.

4.5: Conclusion

In conclusion, this study provides support for the ascending connection between the gut-brain axis via an inflammatory link. It was found that piroxicam-fed IL-10 KO mice undergoing chronic colitis had an increased level of pro-inflammatory cytokines IL-1β and IL-6 in the cerebrum, hippocampus and colon tissues compared to piroxicam-fed IL-10 control mice. It is hypothesized that this inflammatory link is derived from an HMGB1-associated pyroptosis mechanism based on previous published findings from this lab.

CHAPTER FIVE

OVERALL CONCLUSIONS AND FUTURE DIRECTION

5.1: Conclusion

These findings presented in this thesis reinforce Hippocrates famous proverb that "all disease begins in the gut" and furthers understanding of chronic inflammatory diseases. A complex interplay of genetic factors, environmental factors, as well as the gut microbiome, all contribute to the pathology of chronic inflammatory diseases like IBD. It has also been suggested that there is a bidirectional link between gut and brain where the cognitive and emotional centers of the brain are linked with peripheral intestinal functions, known as the gut-brain axis. All of which is also supported by these findings presented in this thesis.

Projects one and two examined the role of *PTEN* in IECs. In project one, human colon cancer tissues had reduced mRNA expression of *PTEN* compared to controls, suggesting that *PTEN* deficiency is involved in the formation of colon cancer. However, this project found that *Pten* deficiency in IECs of mice did not induce tumorigenesis. It was found that both the intestinal microflora and tumor-associated gene expression had been shifted toward a tumor-suppressing condition in the gut of $Pten^{\Delta IEC/\Delta IEC}$ mice. Therefore, these finding demonstrate that the shifted gut microbiome, along with a changed tumor-associated gene expression, plays a crucial part in the shaping of the tumor microenvironment in the colon. Project two further explores the role of *Pten* gene deletion in IECs by providing *in vivo* data demonstrating $Pten^{\Delta IEC/\Delta IEC}$ mice are susceptible to enteropathogenic bacterial infection, and that PTEN has an immune

regulatory function within the GI tract. Lastly, project three provides support for the ascending connection between the gut-brain axis via an inflammatory link.

5.2: Future Direction

Although the discoveries in this dissertation have expanded the understanding of both the function of *Pten* in the intestine and the ascending inflammatory link of the gut-brain axis. However, there are a few questions that have now come from the findings presented, which will require further experimentation to answer. Projects one and two deepens the understanding of the role of *Pten* in IECs, however, the specific role and exact mechanism of how *Pten* functions in IECs remains unclear. From the findings presented in the two projects, it is hypothesized that *Pten* may have an immune regulatory function by modulating intestinal permeability. The next part of the PTEN project should involve investigating the change in permeability of *Pten* deficient mice. Some experiments to further delve into the mechanism could include performing a luciferase bead assay on $Pten^{\Delta IEC/\Delta IEC}$ mice. Cell junction proteins regulate intestinal permeability in IECs. Thus, the expression of cell junction proteins such as claudins, occludin, E-cadherin, and JAMs could be explored with immunofluorescence staining and western blotting to demonstrate a decrease in permeability in both $Pten^{\Delta IEC/\Delta IEC}$ mice intestinal tissues and Pten-KO cells.

Lastly, project three explored the gut-brain axis. An inflammatory link in the ascending pathway was discovered in this project, however, the exact mechanism remains to be confirmed. Based on previous published findings from the lab (Mitchell et al., 2022), it is hypothesized to be an inflammatory HMGB-1 dependent mechanism. To confirm this HMGB-1 mediated mechanism, ELISA should be performed on $Pten^{\Delta IEC/\Delta IEC}$

mice brain, blood, and intestinal tissues. These results from the ELISA could then be confirmed with both immunofluorescence staining and western blotting to investigate the expression of HMGB1.

REFERENCES

Agard, M., Asakrah, S., & Morici, L. A. (2013). PGE2 suppression of innate immunity during mucosal bacterial infection. *Frontiers in Cellular and Infection Microbiology*, *3*, 45. https://doi.org/10.3389/fcimb.2013.00045

Altmeyer, M., Barthel, M., Eberhard, M., Rehrauer, H., Hardt, W.-D., & Hottiger, M. O. (2010). Absence of poly(ADP-ribose) polymerase 1 delays the onset of Salmonella enterica serovar Typhimurium-induced gut inflammation. *Infection and Immunity*, *78*(8), 3420–3431. https://doi.org/10.1128/IAI.00211-10

Amador, V., Ge, S., Santamaría, P. G., Guardavaccaro, D., & Pagano, M. (2007). APC/CCdc20 Controls the Ubiquitin-Mediated Degradation of p21 in Prometaphase. *Molecular Cell*, *27*(3), 462–473. https://doi.org/10.1016/j.molcel.2007.06.013

Arthur, J. C., Perez-Chanona, E., Mühlbauer, M., Tomkovich, S., Uronis, J. M., Fan, T.-J., Campbell, B. J., Abujamel, T., Dogan, B., Rogers, A. B., Rhodes, J. M., Stintzi, A., Simpson, K. W., Hansen, J. J., Keku, T. O., Fodor, A. A., & Jobin, C. (2012). Intestinal inflammation targets cancer-inducing activity of the microbiota. *Science (New York, N.Y.)*, *338*(6103), 120–123. https://doi.org/10.1126/science.1224820

Asano, A., Jin, H. K., & Watanabe, T. (2003). Mouse Mx2 gene: Organization, mRNA expression and the role of the interferon-response promoter in its regulation. *Gene*, *306*, 105–113. https://doi.org/10.1016/S0378-1119(03)00428-1

Balish, E., & Warner, T. (2002). Enterococcus faecalis Induces Inflammatory Bowel Disease in Interleukin-10 Knockout Mice. *The American Journal of Pathology*, *160*(6), 2253–2257.

Barthel, M., Hapfelmeier, S., Quintanilla-Martínez, L., Kremer, M., Rohde, M., Hogardt, M., Pfeffer, K., Rüssmann, H., & Hardt, W.-D. (2003). Pretreatment of mice with streptomycin provides a Salmonella enterica serovar Typhimurium colitis model that allows analysis of both pathogen and host. *Infection and Immunity*, *71*(5), 2839–2858. https://doi.org/10.1128/IAI.71.5.2839-2858.2003

Baumgart, D. C., & Sandborn, W. J. (2007). Inflammatory bowel disease: Clinical aspects and established and evolving therapies. *The Lancet*, *369*(9573), 1641–1657. https://doi.org/10.1016/S0140-6736(07)60751-X

Berg, D. J., Zhang, J., Weinstock, J. V., Ismail, H. F., Earle, K. A., Alila, H., Pamukcu, R., Moore, S., & Lynch, R. G. (2002). Rapid development of colitis in NSAID-treated IL-10-deficient mice. *Gastroenterology*, *123*(5), 1527–1542. https://doi.org/10.1053/gast.2002.1231527

Bischoff, S. C., Barbara, G., Buurman, W., Ockhuizen, T., Schulzke, J.-D., Serino, M., Tilg, H., Watson, A., & Wells, J. M. (2014). Intestinal permeability – a new target for disease prevention and therapy. *BMC Gastroenterology*, *14*(1), 189. https://doi.org/10.1186/s12876-014-0189-7

Blikslager, A. T., Moeser, A. J., Gookin, J. L., Jones, S. L., & Odle, J. (2007). Restoration of Barrier Function in Injured Intestinal Mucosa. *Physiological Reviews*, *87*(2), 545–564. https://doi.org/10.1152/physrev.00012.2006

Bohn, B. A., Mina, S., Krohn, A., Simon, R., Kluth, M., Harasimowicz, S., Quaas, A., Bockhorn, M., Izbicki, J. R., Sauter, G., Marx, A., & Stahl, P. R. (2013). Altered PTEN function caused by deletion or gene disruption is associated with poor prognosis in rectal but not in colon cancer. *Human Pathology*, *44*(8), 1524–1533. https://doi.org/10.1016/j.humpath.2012.12.006

Bravo-Blas, A., Utriainen, L., Clay, S. L., Kästele, V., Cerovic, V., Cunningham, A. F., Henderson, I. R., Wall, D. M., & Milling, S. W. F. (2019). Salmonella enterica Serovar Typhimurium Travels to Mesenteric Lymph Nodes Both with Host Cells and Autonomously. *Journal of Immunology (Baltimore, Md.: 1950)*, *202*(1), 260–267. https://doi.org/10.4049/jimmunol.1701254

Bröer, S. (2008). Amino Acid Transport Across Mammalian Intestinal and Renal Epithelia. *Physiological Reviews*, *88*(1), 249–286. https://doi.org/10.1152/physrev.00018.2006

Bruewer, M., Utech, M., Ivanov, A. I., Hopkins, A. M., Parkos, C. A., & Nusrat, A. (2005). Interferon-gamma induces internalization of epithelial tight junction proteins via a macropinocytosis-like process. *FASEB Journal: Official Publication of the Federation of American Societies for Experimental Biology*, *19*(8), 923–933. https://doi.org/10.1096/fj.04-3260com

Buchta Rosean, C. M., & Rutkowski, M. R. (2017). The influence of the commensal microbiota on distal tumor-promoting inflammation. *Seminars in Immunology*, *32*, 62–73. https://doi.org/10.1016/j.smim.2017.06.002

Byun, D.-S., Ahmed, N., Nasser, S., Shin, J., Al-Obaidi, S., Goel, S., Corner, G. A., Wilson, A. J., Flanagan, D. J., Williams, D. S., Augenlicht, L. H., Vincan, E., & Mariadason, J. M. (2011). Intestinal epithelial-specific PTEN inactivation results in tumor formation. *American Journal of Physiology - Gastrointestinal and Liver Physiology*, *301*(5), G856–G864. https://doi.org/10.1152/ajpgi.00178.2011

Callaway, T. R., Dowd, S. E., Edrington, T. S., Anderson, R. C., Krueger, N., Bauer, N., Kononoff, P. J., & Nisbet, D. J. (2010). Evaluation of bacterial diversity in the rumen and feces of cattle fed different levels of dried distillers grains plus solubles using bacterial tag-encoded FLX amplicon pyrosequencing. *Journal of Animal Science*, *88*(12), 3977–3983. https://doi.org/10.2527/jas.2010-2900

Campbell, H. K., Maiers, J. L., & DeMali, K. A. (2017). Interplay between tight junctions & adherens junctions. *Experimental Cell Research*, *358*(1), 39–44. https://doi.org/10.1016/j.yexcr.2017.03.061

Carabotti, M., Scirocco, A., Maselli, M. A., & Severi, C. (2015). The gut-brain axis: Interactions between enteric microbiota, central and enteric nervous systems. *Annals of Gastroenterology: Quarterly Publication of the Hellenic Society of Gastroenterology*, *28*(2), 203–209.

Cereijido, M., Contreras, R. G., & Shoshani, L. (2004). Cell Adhesion, Polarity, and Epithelia in the Dawn of Metazoans. *Physiological Reviews*, *84*(4), 1229–1262. https://doi.org/10.1152/physrev.00001.2004

Chen, C.-Y., Chen, J., He, L., & Stiles, B. L. (2018). PTEN: Tumor Suppressor and Metabolic Regulator. *Frontiers in Endocrinology*, *9*. https://www.frontiersin.org/articles/10.3389/fendo.2018.00338

Chen, J., Pitmon, E., & Wang, K. (2017). Microbiome, inflammation and colorectal cancer. *Seminars in Immunology*, *32*, 43–53. https://doi.org/10.1016/j.smim.2017.09.006

Chen, Y., Cui, W., Li, X., & Yang, H. (2021). Interaction Between Commensal Bacteria, Immune Response and the Intestinal Barrier in Inflammatory Bowel Disease. *Frontiers in Immunology*, *12*, 761981. https://doi.org/10.3389/fimmu.2021.761981

Chichlowski, M., Westwood, G. S., Abraham, S. N., & Hale, L. P. (2010). Role of mast cells in inflammatory bowel disease and inflammation-associated colorectal neoplasia in IL-10-deficient mice. *PloS One*, *5*(8), e12220. https://doi.org/10.1371/journal.pone.0012220

Choi, Y. J., Im, E., Pothoulakis, C., & Rhee, S. H. (2010). TRIF modulates TLR5-dependent responses by inducing proteolytic degradation of TLR5. *The Journal of Biological Chemistry*, *285*(28), 21382–21390. https://doi.org/10.1074/jbc.M110.115022

Choi, Y. J., Jung, J., Chung, H. K., Im, E., & Rhee, S. H. (2013). PTEN regulates TLR5-induced intestinal inflammation by controlling Mal/TIRAP recruitment. *The FASEB Journal*, *27*(1), 243–254. https://doi.org/10.1096/fj.12-217596

Cipe, G., Idiz, U. O., Firat, D., & Bektasoglu, H. (2015). Relationship between intestinal microbiota and colorectal cancer. *World Journal of Gastrointestinal Oncology*, *7*(10), 233–240. https://doi.org/10.4251/wjgo.v7.i10.233

Clayburgh, D. R., Shen, L., & Turner, J. R. (2004). A porous defense: The leaky epithelial barrier in intestinal disease. *Laboratory Investigation*, *84*(3), Article 3. https://doi.org/10.1038/labinvest.3700050

Colakoglu, T., Yildirim, S., Kayaselcuk, F., Nursal, T. Z., Ezer, A., Noyan, T., Karakayali, H., & Haberal, M. (2008). Clinicopathological significance of PTEN loss and the phosphoinositide 3-kinase/Akt pathway in sporadic colorectal neoplasms: Is PTEN loss predictor of local recurrence? *The American Journal of Surgery*, *195*(6), 719–725. https://doi.org/10.1016/j.amjsurg.2007.05.061

Collado, M. C., Derrien, M., Isolauri, E., de Vos, W. M., & Salminen, S. (2007). Intestinal Integrity and Akkermansia muciniphila, a Mucin-Degrading Member of the Intestinal Microbiota Present in Infants, Adults, and the Elderly. *Applied and Environmental Microbiology*, *73*(23), 7767–7770. https://doi.org/10.1128/AEM.01477-07

Cristofano, A. D., Pesce, B., Cordon-Cardo, C., & Pandolfi, P. P. (1998). Pten is essential for embryonic development and tumour suppression. *Nature Genetics*, *19*(4), Article 4. https://doi.org/10.1038/1235

Cronin, J. C., Loftus, S. K., Baxter, L. L., Swatkoski, S., Gucek, M., & Pavan, W. J. (2018). Identification and functional analysis of SOX10 phosphorylation sites in melanoma. *PLoS ONE*, *13*(1). https://doi.org/10.1371/journal.pone.0190834

Delva, E., Tucker, D. K., & Kowalczyk, A. P. (2009). The Desmosome. *Cold Spring Harbor Perspectives in Biology*, *1*(2), a002543. https://doi.org/10.1101/cshperspect.a002543

Derrien, M., Belzer, C., & de Vos, W. M. (2017). Akkermansia muciniphila and its role in regulating host functions. *Microbial Pathogenesis*, *106*, 171–181. https://doi.org/10.1016/j.micpath.2016.02.005

Derrien, M., Collado, M. C., Ben-Amor, K., Salminen, S., & de Vos, W. M. (2008). The Mucin Degrader Akkermansia muciniphila Is an Abundant Resident of the Human Intestinal Tract. *Applied and Environmental Microbiology*, *74*(5), 1646–1648. https://doi.org/10.1128/AEM.01226-07

DeSantis, T. Z., Hugenholtz, P., Larsen, N., Rojas, M., Brodie, E. L., Keller, K., Huber, T., Dalevi, D., Hu, P., & Andersen, G. L. (2006). Greengenes, a chimera-checked 16S rRNA gene database and workbench compatible with ARB. *Applied and Environmental Microbiology*, *72*(7), 5069–5072. https://doi.org/10.1128/AEM.03006-05

Dicuonzo, G., Angeletti, S., Garcia-Foncillas, J., Brugarolas, A., Okrouzhnov, Y., Santini, D., Tonini, G., Lorino, G., De Cesaris, M., & Baldi, A. (2001). Colorectal carcinomas and PTEN/MMAC1 gene mutations. *Clinical Cancer Research: An Official Journal of the American Association for Cancer Research*, *7*(12), 4049–4053.

Dingemanse, C., Belzer, C., van Hijum, S. A. F. T., Günthel, M., Salvatori, D., Dunnen, J. T. den, Kuijper, E. J., Devilee, P., de Vos, W. M., van Ommen, G. B., & Robanus-Maandag, E. C. (2015). Akkermansia muciniphila and Helicobacter typhlonius modulate intestinal tumor development in mice. *Carcinogenesis*, *36*(11), 1388–1396. https://doi.org/10.1093/carcin/bgv120

Dowd, S. E., Callaway, T. R., Wolcott, R. D., Sun, Y., McKeehan, T., Hagevoort, R. G., & Edrington, T. S. (2008). Evaluation of the bacterial diversity in the feces of cattle using 16S rDNA bacterial tag-encoded FLX amplicon pyrosequencing (bTEFAP). *BMC Microbiology*, *8*, 125. https://doi.org/10.1186/1471-2180-8-125

Dowd, S. E., Sun, Y., Wolcott, R. D., Domingo, A., & Carroll, J. A. (2008). Bacterial tag-encoded FLX amplicon pyrosequencing (bTEFAP) for microbiome studies: Bacterial diversity in the ileum of newly weaned Salmonella-infected pigs. *Foodborne Pathogens and Disease*, *5*(4), 459–472. https://doi.org/10.1089/fpd.2008.0107

Edgar, R. C. (2010). Search and clustering orders of magnitude faster than BLAST. *Bioinformatics (Oxford, England)*, *26*(19), 2460–2461. https://doi.org/10.1093/bioinformatics/btq461

Ellenbroek, G. H. J. M., van Puijvelde, G. H. M., Anas, A. A., Bot, M., Asbach, M., Schoneveld, A., van Santbrink, P. J., Foks, A. C., Timmers, L., Doevendans, P. A., Pasterkamp, G., Hoefer, I. E., van der Poll, T., Kuiper, J., & de Jager, S. C. A. (2017). Leukocyte TLR5 deficiency inhibits atherosclerosis by reduced macrophage recruitment and defective T-cell responsiveness. *Scientific Reports*, *7*(1), Article 1. https://doi.org/10.1038/srep42688

Erova, T. E., Kirtley, M. L., Fitts, E. C., Ponnusamy, D., Baze, W. B., Andersson, J. A., Cong, Y., Tiner, B. L., Sha, J., & Chopra, A. K. (2016). Protective Immunity Elicited by Oral Immunization of Mice with Salmonella enterica Serovar Typhimurium Braun Lipoprotein (Lpp) and Acetyltransferase (MsbB) Mutants. *Frontiers in Cellular and Infection Microbiology*, *6*, 148. https://doi.org/10.3389/fcimb.2016.00148

Farhadi, A., Banan, A., Fields, J., & Keshavarzian, A. (2003). Intestinal barrier: An interface between health and disease. *Journal of Gastroenterology and Hepatology*, *18*(5), 479–497. https://doi.org/10.1046/j.1440-1746.2003.03032.x

Fasano, A. (2011). Zonulin and Its Regulation of Intestinal Barrier Function: The Biological Door to Inflammation, Autoimmunity, and Cancer. *Physiological Reviews*, *91*(1), 151–175. https://doi.org/10.1152/physrev.00003.2008

Fasano, A. (2020). All disease begins in the (leaky) gut: Role of zonulin-mediated gut permeability in the pathogenesis of some chronic inflammatory diseases. *F1000Research*, *9*, F1000 Faculty Rev-69. https://doi.org/10.12688/f1000research.20510.1

Ferraris, R. P., & Diamond, J. (1997). Regulation of intestinal sugar transport. *Physiological Reviews*, *77*(1), 257–302. https://doi.org/10.1152/physrev.1997.77.1.257

Fields, P. I., Swanson, R. V., Haidaris, C. G., & Heffron, F. (1986). Mutants of Salmonella typhimurium that cannot survive within the macrophage are avirulent. *Proceedings of the National Academy of Sciences of the United States of America*, *83*(14), 5189–5193.

Foster, J. A., & McVey Neufeld, K.-A. (2013). Gut-brain axis: How the microbiome influences anxiety and depression. *Trends in Neurosciences*, *36*(5), 305–312. https://doi.org/10.1016/j.tins.2013.01.005

Foti, M., & Ricciardi-Castagnoli, P. (2005). Antigen sampling by mucosal dendritic cells. *Trends in Molecular Medicine*, *11*(9), 394–396. https://doi.org/10.1016/j.molmed.2005.07.001

Galluzzi, L., López-Soto, A., Kumar, S., & Kroemer, G. (2016). Caspases Connect Cell-Death Signaling to Organismal Homeostasis. *Immunity*, *44*(2), 221–231. https://doi.org/10.1016/j.immuni.2016.01.020

Ganesh, B. P., Klopfleisch, R., Loh, G., & Blaut, M. (2013). Commensal Akkermansia muciniphila Exacerbates Gut Inflammation in Salmonella Typhimurium-Infected Gnotobiotic Mice. *PLOS ONE*, *8*(9), e74963. https://doi.org/10.1371/journal.pone.0074963

Garrod, D., & Chidgey, M. (2008). Desmosome structure, composition and function. *Biochimica et Biophysica Acta (BBA) - Biomembranes*, *1778*(3), 572–587. https://doi.org/10.1016/j.bbamem.2007.07.014

Gibson, P. R. (2004). Increased gut permeability in Crohn's disease: Is TNF the link? *Gut*, *53*(12), 1724–1725. https://doi.org/10.1136/gut.2004.047092

Govoni, G., & Gros, P. (1998). Macrophage NRAMP1 and its role in resistance to microbial infections. *Inflammation Research: Official Journal of the European Histamine Research Society ... [et Al.]*, *47*(7), 277–284. https://doi.org/10.1007/s000110050330

Gracie, D. J., Guthrie, E. A., Hamlin, P. J., & Ford, A. C. (2018). Bi-directionality of Brain–Gut Interactions in Patients with Inflammatory Bowel Disease. *Gastroenterology*, *154*(6), 1635-1646.e3. https://doi.org/10.1053/j.gastro.2018.01.027

Groschwitz, K. R., & Hogan, S. P. (2009). Intestinal barrier function: Molecular regulation and disease pathogenesis. *Journal of Allergy and Clinical Immunology*, *124*(1), 3–20. https://doi.org/10.1016/j.jaci.2009.05.038

Groszer, M., Erickson, R., Scripture-Adams, D. D., Lesche, R., Trumpp, A., Zack, J. A., Kornblum, H. I., Liu, X., & Wu, H. (2001). Negative regulation of neural stem/progenitor cell proliferation by the Pten tumor suppressor gene in vivo. *Science (New York, N.Y.)*, *294*(5549), 2186–2189. https://doi.org/10.1126/science.1065518

Gupta, A., & Leslie, N. R. (2016). Controlling PTEN (Phosphatase and Tensin Homolog) Stability: A DOMINANT ROLE FOR LYSINE 66 *. *Journal of Biological Chemistry*, *291*(35), 18465–18473. https://doi.org/10.1074/jbc.M116.727750

Gut, A. M., Vasiljevic, T., Yeager, T., & Donkor, O. N. (2018). Salmonella infection - prevention and treatment by antibiotics and probiotic yeasts: A review. *Microbiology (Reading, England)*, *164*(11), 1327–1344. https://doi.org/10.1099/mic.0.000709

Haddadi, N., Lin, Y., Travis, G., Simpson, A. M., Nassif, N. T., & McGowan, E. M. (2018). PTEN/PTENP1: 'Regulating the regulator of RTK-dependent PI3K/Akt signalling', new targets for cancer therapy. *Molecular Cancer*, *17*(1), 37. https://doi.org/10.1186/s12943-018-0803-3

Hapfelmeier, S., & Hardt, W.-D. (2005). A mouse model for S. typhimurium-induced enterocolitis. *Trends in Microbiology*, *13*(10), 497–503. https://doi.org/10.1016/j.tim.2005.08.008

Harhaj, N. S., & Antonetti, D. A. (2004). Regulation of tight junctions and loss of barrier function in pathophysiology. *The International Journal of Biochemistry & Cell Biology*, *36*(7), 1206–1237. https://doi.org/10.1016/j.biocel.2003.08.007

Hartsock, A., & Nelson, W. J. (2008). Adherens and tight junctions: Structure, function and connections to the actin cytoskeleton. *Biochimica et Biophysica Acta (BBA) - Biomembranes*, *1778*(3), 660–669. https://doi.org/10.1016/j.bbamem.2007.07.012

He, Q., You, H., Li, X., Liu, T., Wang, P., & Wang, B. (2012). HMGB1 promotes the synthesis of pro-il-1β and pro-il-18 by activation of p38 MAPK and NF-kB through receptors for advanced glycation end-products in macrophages. *Asian Pacific Journal of Cancer Prevention*, *13*(4), 1365–1370. Scopus. https://doi.org/10.7314/APJCP.2012.13.4.1365

He, X. C., Yin, T., Grindley, J. C., Tian, Q., Sato, T., Tao, W. A., Dirisina, R., Porter-Westpfahl, K. S., Hembree, M., Johnson, T., Wiedemann, L. M., Barrett, T. A., Hood, L., Wu, H., & Li, L. (2007). PTEN-deficient intestinal stem cells initiate intestinal polyposis. *Nature Genetics*, *39*(2), Article 2. https://doi.org/10.1038/ng1928

Helander, H. F., & Fändriks, L. (2014). Surface area of the digestive tract – revisited. *Scandinavian Journal of Gastroenterology*, *49*(6), 681–689. https://doi.org/10.3109/00365521.2014.898326

Hsu, F., & Mao, Y. (2015). The structure of phosphoinositide phosphatases: Insights into substrate specificity and catalysis. *Biochimica et Biophysica Acta*, *1851*(6), 698–710. https://doi.org/10.1016/j.bbalip.2014.09.015

Im, E., Jung, J., Pothoulakis, C., & Rhee, S. H. (2014). Disruption of Pten Speeds Onset and Increases Severity of Spontaneous Colitis in Il10−/− Mice. *Gastroenterology*, *147*(3), 667-679.e10. https://doi.org/10.1053/j.gastro.2014.05.034

Jamaspishvili, T., Berman, D. M., Ross, A. E., Scher, H. I., De Marzo, A. M., Squire, J. A., & Lotan, T. L. (2018). Clinical implications of PTEN loss in prostate cancer. *Nature Reviews Urology*, *15*(4), Article 4. https://doi.org/10.1038/nrurol.2018.9

Jones, M. P., Dilley, J. B., Drossman, D., & Crowell, M. D. (2006). Brain–gut connections in functional GI disorders: Anatomic and physiologic relationships. *Neurogastroenterology & Motility*, *18*(2), 91–103. https://doi.org/10.1111/j.1365-2982.2005.00730.x

Kagan, J. C., & Medzhitov, R. (2006). Phosphoinositide-Mediated Adaptor Recruitment Controls Toll-like Receptor Signaling. *Cell*, *125*(5), 943–955. https://doi.org/10.1016/j.cell.2006.03.047

Kaiser, P., Diard, M., Stecher, B., & Hardt, W.-D. (2012). The streptomycin mouse model for Salmonella diarrhea: Functional analysis of the microbiota, the pathogen's virulence factors, and the host's mucosal immune response. *Immunological Reviews*, *245*(1), 56–83. https://doi.org/10.1111/j.1600-065X.2011.01070.x

Kamada, N., Seo, S.-U., Chen, G. Y., & Núñez, G. (2013). Role of the gut microbiota in immunity and inflammatory disease. *Nature Reviews Immunology*, *13*(5), Article 5. https://doi.org/10.1038/nri3430

Kaser, A., Zeissig, S., & Blumberg, R. S. (2010). Inflammatory Bowel Disease. *Annual Review of Immunology*, *28*(1), 573–621. https://doi.org/10.1146/annurev-immunol-030409-101225

Killinger, B. A., Madaj, Z., Sikora, J. W., Rey, N., Haas, A. J., Vepa, Y., Lindqvist, D., Chen, H., Thomas, P. M., Brundin, P., Brundin, L., & Labrie, V. (2018). The vermiform appendix impacts the risk of developing Parkinson's disease. *Science Translational Medicine*, *10*(465), eaar5280. https://doi.org/10.1126/scitranslmed.aar5280

Kim, S. C., Tonkonogy, S. L., Albright, C. A., Tsang, J., Balish, E. J., Braun, J., Huycke, M. M., & Sartor, R. B. (2005). Variable phenotypes of enterocolitis in interleukin 10-deficient mice monoassociated with two different commensal bacteria. *Gastroenterology*, *128*(4), 891–906. https://doi.org/10.1053/j.gastro.2005.02.009

Kostic, A. D., Gevers, D., Pedamallu, C. S., Michaud, M., Duke, F., Earl, A. M., Ojesina, A. I., Jung, J., Bass, A. J., Tabernero, J., Baselga, J., Liu, C., Shivdasani, R. A., Ogino, S., Birren, B. W., Huttenhower, C., Garrett, W. S., & Meyerson, M. (2012). Genomic analysis identifies association of Fusobacterium with colorectal carcinoma. *Genome Research*, *22*(2), 292–298. https://doi.org/10.1101/gr.126573.111

Kühn, R., Löhler, J., Rennick, D., Rajewsky, K., & Müller, W. (1993). Interleukin-10-deficient mice develop chronic enterocolitis. *Cell*, *75*(2), 263–274. https://doi.org/10.1016/0092-8674(93)80068-p

Kunzelmann, K., & Mall, M. (2002). Electrolyte Transport in the Mammalian Colon: Mechanisms and Implications for Disease. *Physiological Reviews*, *82*(1), 245–289. https://doi.org/10.1152/physrev.00026.2001

Kuramochi, H., Nakamura, A., Nakajima, G., Kaneko, Y., Araida, T., Yamamoto, M., & Hayashi, K. (2016). PTEN mRNA expression is less pronounced in left- than right-sided colon cancer: A retrospective observational study. *BMC Cancer*, *16*(1), 366. https://doi.org/10.1186/s12885-016-2400-4

Langlois, M.-J., Roy, S. A. B., Auclair, B. A., Jones, C., Boudreau, F., Carrier, J. C., Rivard, N., & Perreault, N. (2009). Epithelial phosphatase and tensin homolog regulates intestinal architecture and secretory cell commitment and acts as a modifier gene in neoplasia. *FASEB Journal: Official Publication of the Federation of American Societies for Experimental Biology*, *23*(6), 1835–1844. https://doi.org/10.1096/fj.08-123125

Lee, J.-O., Yang, H., Georgescu, M.-M., Cristofano, A. D., Maehama, T., Shi, Y., Dixon, J. E., Pandolfi, P., & Pavletich, N. P. (1999). Crystal Structure of the PTEN Tumor Suppressor: Implications for Its Phosphoinositide Phosphatase Activity and Membrane Association. *Cell*, *99*(3), 323–334. https://doi.org/10.1016/S0092-8674(00)81663-3

Levenstein, S., Prantera, C., Varvo, V., Scribano, M. L., Andreoli, A., Luzi, C., Arcà, M., Berto, E., Milite, G., & Marcheggiano, A. (2000). Stress and exacerbation in ulcerative colitis: A prospective study of patients enrolled in remission. *The American Journal of Gastroenterology*, *95*(5), 1213–1220. https://doi.org/10.1016/S0002-9270(00)00804-2

Li, D. M., & Sun, H. (1997). TEP1, encoded by a candidate tumor suppressor locus, is a novel protein tyrosine phosphatase regulated by transforming growth factor beta. *Cancer Research*, *57*(11), 2124–2129.

Li, J., Yen, C., Liaw, D., Podsypanina, K., Bose, S., Wang, S. I., Puc, J., Miliaresis, C., Rodgers, L., McCombie, R., Bigner, S. H., Giovanella, B. C., Ittmann, M., Tycko, B., Hibshoosh, H., Wigler, M. H., & Parsons, R. (1997). PTEN, a putative protein tyrosine phosphatase gene mutated in human brain, breast, and prostate cancer. *Science (New York, N.Y.)*, *275*(5308), 1943–1947. https://doi.org/10.1126/science.275.5308.1943

Lightfoot, Y. L., Yang, T., Sahay, B., & Mohamadzadeh, M. (2013). Targeting aberrant colon cancer-specific DNA methylation with lipoteichoic acid-deficient Lactobacillus acidophilus. *Gut Microbes*, *4*(1), 84–88. https://doi.org/10.4161/gmic.22822

Lin, P.-C., Lin, J.-K., Lin, H.-H., Lan, Y.-T., Lin, C.-C., Yang, S.-H., Chen, W.-S., Liang, W.-Y., Jiang, J.-K., & Chang, S.-C. (2015). A comprehensive analysis of phosphatase and tensin homolog deleted on chromosome 10 (PTEN) loss in colorectal cancer. *World Journal of Surgical Oncology*, *13*(1), 186. https://doi.org/10.1186/s12957-015-0601-y

Liu, H., Chen, F., Wu, W., Cao, A. T., Xue, X., Yao, S., Evans-Marin, H. L., Li, Y.-Q., & Cong, Y. (2016). TLR5 mediates CD172α+ intestinal lamina propria dendritic cell induction of Th17 cells. *Scientific Reports*, *6*(1), Article 1. https://doi.org/10.1038/srep22040

Liu, Y., He, G., Wang, Y., Guan, X., Pang, X., & Zhang, B. (2013). MCM-2 is a therapeutic target of Trichostatin A in colon cancer cells. *Toxicology Letters*, *221*(1), 23–30. https://doi.org/10.1016/j.toxlet.2013.05.643

Livak, K. J., & Schmittgen, T. D. (2001). Analysis of relative gene expression data using real-time quantitative PCR and the 2(-Delta Delta C(T)) Method. *Methods (San Diego, Calif.)*, *25*(4), 402–408. https://doi.org/10.1006/meth.2001.1262

Lo, S. H., Weisberg, E., & Chen, L. B. (1994). Tensin: A potential link between the cytoskeleton and signal transduction. *BioEssays*, *16*(11), 817–823. https://doi.org/10.1002/bies.950161108

Loh, G., & Blaut, M. (2012). Role of commensal gut bacteria in inflammatory bowel diseases. *Gut Microbes*, *3*(6), 544–555. https://doi.org/10.4161/gmic.22156

Long, M. D., & Sands, B. E. (2018). When Do You Start and When Do You Stop Screening for Colon Cancer in Inflammatory Bowel Disease? *Clinical Gastroenterology and Hepatology: The Official Clinical Practice Journal of the American Gastroenterological Association*, *16*(5), 621–623. https://doi.org/10.1016/j.cgh.2018.02.011

Madison, B. B., Dunbar, L., Qiao, X. T., Braunstein, K., Braunstein, E., & Gumucio, D. L. (2002). Cis elements of the villin gene control expression in restricted domains of the vertical (crypt) and horizontal (duodenum, cecum) axes of the intestine. *The Journal of Biological Chemistry*, *277*(36), 33275–33283. https://doi.org/10.1074/jbc.M204935200

Matei, D. E., Menon, M., Alber, D. G., Smith, A. M., Nedjat-Shokouhi, B., Fasano, A., Magill, L., Duhlin, A., Bitoun, S., Gleizes, A., Hacein-Bey-Abina, S., Manson, J. J., Rosser, E. C., ABIRISK Consortium, Klein, N., Blair, P. A., & Mauri, C. (2021). Intestinal barrier dysfunction plays an integral role in arthritis pathology and can be targeted to ameliorate disease. *Med (New York, N.Y.)*, *2*(7), 864-883.e9. https://doi.org/10.1016/j.medj.2021.04.013

McDowell, C., Farooq, U., & Haseeb, M. (2022). Inflammatory Bowel Disease. In *StatPearls*. StatPearls Publishing. http://www.ncbi.nlm.nih.gov/books/NBK470312/

Mermelshtein, A., Gerson, A., Walfisch, S., Delgado, B., Shechter-Maor, G., Delgado, J., Fich, A., & Gheber, L. (2005). Expression of D-type cyclins in colon cancer and in cell lines from colon carcinomas. *British Journal of Cancer*, *93*(3), Article 3. https://doi.org/10.1038/sj.bjc.6602709

Michielan, A., & D'Incà, R. (2015). Intestinal Permeability in Inflammatory Bowel Disease: Pathogenesis, Clinical Evaluation, and Therapy of Leaky Gut. *Mediators of Inflammation*, *2015*, 628157. https://doi.org/10.1155/2015/628157

Mitchell, J., Kim, S. J., Howe, C., Lee, S., Her, J. Y., Patel, M., Kim, G., Lee, J., Im, E., & Rhee, S. H. (2022). Chronic Intestinal Inflammation Suppresses Brain Activity by Inducing Neuroinflammation in Mice. *The American Journal of Pathology*, *192*(1), 72–86. https://doi.org/10.1016/j.ajpath.2021.09.006

Mitchell, J., Kim, S. J., Koukos, G., Seelmann, A., Veit, B., Shepard, B., Blumer-Schuette, S., Winter, H. S., Iliopoulos, D., Pothoulakis, C., Im, E., & Rhee, S. H. (2018). Colonic Inhibition of Phosphatase and Tensin Homolog Increases Colitogenic Bacteria, Causing Development of Colitis in Il10-/- Mice. *Inflammatory Bowel Diseases*, *24*(8), 1718–1732. https://doi.org/10.1093/ibd/izy124

Moens, E., & Veldhoen, M. (2012). Epithelial barrier biology: Good fences make good neighbours. *Immunology*, *135*(1), 1–8. https://doi.org/10.1111/j.1365-2567.2011.03506.x

Monteleone, G., Fina, D., Caruso, R., & Pallone, F. (2006). New mediators of immunity and inflammation in inflammatory bowel disease. *Current Opinion in Gastroenterology*, *22*(4), 361–364. https://doi.org/10.1097/01.mog.0000231808.10773.8e

Naseribafrouei, A., Hestad, K., Avershina, E., Sekelja, M., Linløkken, A., Wilson, R., & Rudi, K. (2014). Correlation between the human fecal microbiota and depression. *Neurogastroenterology and Motility: The Official Journal of the European Gastrointestinal Motility Society*, *26*(8), 1155–1162. https://doi.org/10.1111/nmo.12378

Ng, S. C., Shi, H. Y., Hamidi, N., Underwood, F. E., Tang, W., Benchimol, E. I., Panaccione, R., Ghosh, S., Wu, J. C. Y., Chan, F. K. L., Sung, J. J. Y., & Kaplan, G. G. (2017). Worldwide incidence and prevalence of inflammatory bowel disease in the 21st century: A systematic review of population-based studies. *The Lancet*, *390*(10114), 2769–2778. https://doi.org/10.1016/S0140-6736(17)32448-0

Nusrat, A., Turner, J. R., & Madara, J. L. (2000). IV. Regulation of tight junctions by extracellular stimuli: Nutrients, cytokines, and immune cells. *American Journal of Physiology-Gastrointestinal and Liver Physiology*, *279*(5), G851–G857. https://doi.org/10.1152/ajpgi.2000.279.5.G851

Pei, X.-H., & Xiong, Y. (2005). Biochemical and cellular mechanisms of mammalian CDK inhibitors: A few unresolved issues. *Oncogene*, *24*(17), Article 17. https://doi.org/10.1038/sj.onc.1208611

Peterson, C. T. (2020). Dysfunction of the Microbiota-Gut-Brain Axis in Neurodegenerative Disease: The Promise of Therapeutic Modulation with Prebiotics, Medicinal Herbs, Probiotics, and Synbiotics. *Journal of Evidence-Based Integrative Medicine*, *25*, 2515690X20957225. https://doi.org/10.1177/2515690X20957225

Petruo, V. A., Zeißig, S., Schmelz, R., Hampe, J., & Beste, C. (2017). Specific neurophysiological mechanisms underlie cognitive inflexibility in inflammatory bowel disease. *Scientific Reports*, *7*(1), 13943. https://doi.org/10.1038/s41598-017-14345-5

Phillips, L. S., Thompson, C. L., Merkulova, A., Plummer, S. J., Tucker, T. C., Casey, G., & Li, L. (2009). No association between phosphatase and tensin homolog genetic polymorphisms and colon cancer. *World Journal of Gastroenterology*, *15*(30), 3771–3775. https://doi.org/10.3748/wjg.15.3771

Pilarski, R. (2019). PTEN Hamartoma Tumor Syndrome: A Clinical Overview. *Cancers*, *11*(6), Article 6. https://doi.org/10.3390/cancers11060844

Que, W., Qiu, H., Cheng, Y., Liu, M., & Wu, C. (2018). PTEN in kidney cancer: A review and meta-analysis. *Clinica Chimica Acta*, *480*, 92–98. https://doi.org/10.1016/j.cca.2018.01.031

Ren, J., Sui, H., Fang, F., Li, Q., & Li, B. (2019). The application of ApcMin/+ mouse model in colorectal tumor researches. *Journal of Cancer Research and Clinical Oncology*, *145*(5), 1111–1122. https://doi.org/10.1007/s00432-019-02883-6

Rhee, S. H., Kim, H., Moyer, M. P., & Pothoulakis, C. (2006). Role of MyD88 in phosphatidylinositol 3-kinase activation by flagellin/toll-like receptor 5 engagement in colonic epithelial cells. *The Journal of Biological Chemistry*, *281*(27), 18560–18568. https://doi.org/10.1074/jbc.M513861200

Rhee, S. H., Ma, E. L., Lee, Y., Taché, Y., Pothoulakis, C., & Im, E. (2015). Corticotropin Releasing Hormone and Urocortin 3 Stimulate Vascular Endothelial Growth Factor Expression through the cAMP/CREB Pathway. *The Journal of Biological Chemistry*, *290*(43), 26194–26203. https://doi.org/10.1074/jbc.M115.678979

Rhee, S. H., Pothoulakis, C., & Mayer, E. A. (2009). Principles and clinical implications of the brain-gut-enteric microbiota axis. *Nature Reviews. Gastroenterology & Hepatology*, *6*(5), 306–314. https://doi.org/10.1038/nrgastro.2009.35

Ringel, Y., Ringel-Kulka, T., Maier, D., Carroll, I., Galanko, J. A., Leyer, G., & Palsson, O. S. (2011). Clinical trial: Probiotic Bacteria Lactobacillus acidophilus NCFM and Bifidobacterium lactis Bi-07 Versus Placebo for the Symptoms of Bloating in Patients with Functional Bowel Disorders - a Double-Blind Study. *Journal of Clinical Gastroenterology*, *45*(6), 518–525. https://doi.org/10.1097/MCG.0b013e31820ca4d6

Rogler, G., Singh, A., Kavanaugh, A., & Rubin, D. T. (2021). Extraintestinal Manifestations of Inflammatory Bowel Disease: Current Concepts, Treatment, and Implications for Disease Management. *Gastroenterology*, *161*(4), 1118–1132. https://doi.org/10.1053/j.gastro.2021.07.042

Rutsch, A., Kantsjö, J. B., & Ronchi, F. (2020). The Gut-Brain Axis: How Microbiota and Host Inflammasome Influence Brain Physiology and Pathology. *Frontiers in Immunology*, *11*. https://www.frontiersin.org/articles/10.3389/fimmu.2020.604179

Seregin, S. S., Golovchenko, N., Schaf, B., Chen, J., Pudlo, N. A., Mitchell, J., Baxter, N. T., Zhao, L., Schloss, P. D., Martens, E. C., Eaton, K. A., & Chen, G. Y. (2017). NLRP6 protects IL10−/− mice from colitis by limiting colonization of Akkermansia muciniphila. *Cell Reports*, *19*(4), 733–745. https://doi.org/10.1016/j.celrep.2017.03.080

Sims, G. P., Rowe, D. C., Rietdijk, S. T., Herbst, R., & Coyle, A. J. (2010). HMGB1 and RAGE in inflammation and cancer. *Annual Review of Immunology*, *28*, 367–388. https://doi.org/10.1146/annurev.immunol.021908.132603

Sommer, F., & Bäckhed, F. (2013). The gut microbiota—Masters of host development and physiology. *Nature Reviews Microbiology*, *11*(4), Article 4. https://doi.org/10.1038/nrmicro2974

Song, M. S., Salmena, L., & Pandolfi, P. P. (2012). The functions and regulation of the PTEN tumour suppressor. *Nature Reviews Molecular Cell Biology*, *13*(5), Article 5. https://doi.org/10.1038/nrm3330

Stadlbauer, V., Engertsberger, L., Komarova, I., Feldbacher, N., Leber, B., Pichler, G., Fink, N., Scarpatetti, M., Schippinger, W., Schmidt, R., & Horvath, A. (2020). Dysbiosis, gut barrier dysfunction and inflammation in dementia: A pilot study. *BMC Geriatrics*, *20*(1), 248. https://doi.org/10.1186/s12877-020-01644-2

Stecher, B., Paesold, G., Barthel, M., Kremer, M., Jantsch, J., Stallmach, T., Heikenwalder, M., & Hardt, W.-D. (2006). Chronic Salmonella enterica serovar Typhimurium-induced colitis and cholangitis in streptomycin-pretreated Nramp1+/+ mice. *Infection and Immunity*, *74*(9), 5047–5057. https://doi.org/10.1128/IAI.00072-06

Steck, P. A., Pershouse, M. A., Jasser, S. A., Yung, W. K. A., Lin, H., Ligon, A. H., Langford, L. A., Baumgard, M. L., Hattier, T., Davis, T., Frye, C., Hu, R., Swedlund, B., Teng, D. H. R., & Tavtigian, S. V. (1997). Identification of a candidate tumour suppressor gene, MMAC1, at chromosome 10q23.3 that is mutated in multiple advanced cancers. *Nature Genetics*, *15*(4), Article 4. https://doi.org/10.1038/ng0497-356

Stiles, B. L. (2009). Phosphatase and tensin homologue deleted on chromosome 10: Extending its PTENtacles. *The International Journal of Biochemistry & Cell Biology*, *41*(4), 757–761. https://doi.org/10.1016/j.biocel.2008.09.022

Stokkers, P. C. F., & Hommes, D. W. (2004). New cytokine therapeutics for inflammatory bowel disease. *Cytokine*, *28*(4), 167–173. https://doi.org/10.1016/j.cyto.2004.07.012

Swanson, K. S., Dowd, S. E., Suchodolski, J. S., Middelbos, I. S., Vester, B. M., Barry, K. A., Nelson, K. E., Torralba, M., Henrissat, B., Coutinho, P. M., Cann, I. K. O., White, B. A., & Fahey, G. C. (2011). Phylogenetic and gene-centric metagenomics of the canine intestinal microbiome reveals similarities with humans and mice. *The ISME Journal*, *5*(4), 639–649. https://doi.org/10.1038/ismej.2010.162

Szigethy, E., McLafferty, L., & Goyal, A. (2010). Inflammatory Bowel Disease. *Child and Adolescent Psychiatric Clinics of North America*, *19*(2), 301–318. https://doi.org/10.1016/j.chc.2010.01.007

Tamura, M., Gu, J., Matsumoto, K., Aota, S., Parsons, R., & Yamada, K. M. (1998). Inhibition of cell migration, spreading, and focal adhesions by tumor suppressor PTEN. *Science (New York, N.Y.)*, *280*(5369), 1614–1617. https://doi.org/10.1126/science.280.5369.1614

Taniyama, K., Goodison, S., Ito, R., Bookstein, R., Miyoshi, N., Tahara, E., Tarin, D., & Urquidi, V. (2001). PTEN expression is maintained in sporadic colorectal tumours. *The Journal of Pathology*, *194*(3), 341–348. https://doi.org/10.1002/path.908

Toprak, N. U., Yagci, A., Gulluoglu, B. M., Akin, M. L., Demirkalem, P., Celenk, T., & Soyletir, G. (2006). A possible role of Bacteroides fragilis enterotoxin in the etiology of colorectal cancer. *Clinical Microbiology and Infection: The Official Publication of the European Society of Clinical Microbiology and Infectious Diseases*, *12*(8), 782–786. https://doi.org/10.1111/j.1469-0691.2006.01494.x

Tsolis, R. M., Kingsley, R. A., Townsend, S. M., Ficht, T. A., Adams, L. G., & Bäumler, A. J. (1999). Of mice, calves, and men. Comparison of the mouse typhoid model with other Salmonella infections. *Advances in Experimental Medicine and Biology*, *473*, 261–274.

Tsukita, S., & Furuse, M. (2000). The Structure and Function of Claudins, Cell Adhesion Molecules at Tight Junctions. *Annals of the New York Academy of Sciences*, *915*(1), 129–135. https://doi.org/10.1111/j.1749-6632.2000.tb05235.x

Turner, J. R. (2009). Intestinal mucosal barrier function in health and disease. *Nature Reviews Immunology*, *9*(11), Article 11. https://doi.org/10.1038/nri2653

Ucker, D. S., & Levine, J. S. (2018). Exploitation of Apoptotic Regulation in Cancer. *Frontiers in Immunology*, *9*, 241. https://doi.org/10.3389/fimmu.2018.00241

Van Itallie, C. M., & Anderson, J. M. (2006). Claudins and Epithelial Paracellular Transport. *Annual Review of Physiology*, *68*(1), 403–429. https://doi.org/10.1146/annurev.physiol.68.040104.131404

Vancamelbeke, M., & Vermeire, S. (2017). The intestinal barrier: A fundamental role in health and disease. *Expert Review of Gastroenterology & Hepatology*, *11*(9), 821–834. https://doi.org/10.1080/17474124.2017.1343143

Vanuytsel, T., Tack, J., & Farre, R. (2021). The Role of Intestinal Permeability in Gastrointestinal Disorders and Current Methods of Evaluation. *Frontiers in Nutrition*, *8*. https://www.frontiersin.org/articles/10.3389/fnut.2021.717925

Vecchio, L., Seke Etet, P. F., Kipanyula, M. J., Krampera, M., & Nwabo Kamdje, A. H. (2013). Importance of epigenetic changes in cancer etiology, pathogenesis, clinical profiling, and treatment: What can be learned from hematologic malignancies? *Biochimica et Biophysica Acta (BBA) - Reviews on Cancer*, *1836*(1), 90–104. https://doi.org/10.1016/j.bbcan.2013.04.001

Viggiano, D., Ianiro, G., Vanella, G., Bibbò, S., Bruno, G., Simeone, G., & Mele, G. (2015). Gut barrier in health and disease: Focus on childhood. *European Review for Medical and Pharmacological Sciences*, *19*(6), 1077–1085.

Vijayan, A., Rumbo, M., Carnoy, C., & Sirard, J.-C. (2018). Compartmentalized Antimicrobial Defenses in Response to Flagellin. *Trends in Microbiology*, *26*(5), 423–435. https://doi.org/10.1016/j.tim.2017.10.008

Villumsen, M., Aznar, S., Pakkenberg, B., Jess, T., & Brudek, T. (2019). Inflammatory bowel disease increases the risk of Parkinson's disease: A Danish nationwide cohort study 1977-2014. *Gut*, *68*(1), 18–24. https://doi.org/10.1136/gutjnl-2017-315666

Vitali, R., Stronati, L., Negroni, A., Di Nardo, G., Pierdomenico, M., del Giudice, E., Rossi, P., & Cucchiara, S. (2011). Fecal HMGB1 is a novel marker of intestinal mucosal inflammation in pediatric inflammatory bowel disease. *The American Journal of Gastroenterology*, *106*(11), 2029–2040. https://doi.org/10.1038/ajg.2011.231

Wakabayashi, A., Shimizu, M., Shinya, E., & Takahashi, H. (2018). HMGB1 released from intestinal epithelia damaged by cholera toxin adjuvant contributes to activation of mucosal dendritic cells and induction of intestinal cytotoxic T lymphocytes and IgA. *Cell Death & Disease*, *9*(6), Article 6. https://doi.org/10.1038/s41419-018-0665-z

Wang, Z. J., Taylor, F., Churchman, M., Norbury, G., & Tomlinson, I. (1998). Genetic pathways of colorectal carcinogenesis rarely involve the PTEN and LKB1 genes outside the inherited hamartoma syndromes. *The American Journal of Pathology*, *153*(2), 363–366. https://doi.org/10.1016/S0002-9440(10)65579-4

Weir, T. L., Manter, D. K., Sheflin, A. M., Barnett, B. A., Heuberger, A. L., & Ryan, E. P. (2013). Stool Microbiome and Metabolome Differences between Colorectal Cancer Patients and Healthy Adults. *PLoS ONE*, *8*(8), e70803. https://doi.org/10.1371/journal.pone.0070803

Willecke, K., Eiberger, J., Degen, J., Eckardt, D., Romualdi, A., Güldenagel, M., Deutsch, U., & Söhl, G. (2002). *Structural and Functional Diversity of Connexin Genes in the Mouse and Human Genome*. *383*(5), 725–737. https://doi.org/10.1515/BC.2002.076

Wu, S., Rhee, K.-J., Albesiano, E., Rabizadeh, S., Wu, X., Yen, H.-R., Huso, D. L., Brancati, F. L., Wick, E., McAllister, F., Housseau, F., Pardoll, D. M., & Sears, C. L. (2009). A human colonic commensal promotes colon tumorigenesis via activation of T helper type 17 T cell responses. *Nature Medicine*, *15*(9), 1016–1022. https://doi.org/10.1038/nm.2015

Xu, W.-T., Yang, Z., & Lu, N.-H. (2014). Roles of PTEN (Phosphatase and Tensin Homolog) in Gastric Cancer Development and Progression. *Asian Pacific Journal of Cancer Prevention*, *15*(1), 17–24. https://doi.org/10.7314/APJCP.2014.15.1.17

Yacyshyn, B., Meddings, J., Sadowski, D., & Bowen-Yacyshyn, M. B. (1996). Multiple sclerosis patients have peripheral blood CD45RO+ B cells and increased intestinal permeability. *Digestive Diseases and Sciences*, *41*(12), 2493–2498. https://doi.org/10.1007/BF02100148

Yelland, G. W. (2017). Gluten-induced cognitive impairment (“brain fog”) in coeliac disease. *Journal of Gastroenterology and Hepatology*, *32*(S1), 90–93. https://doi.org/10.1111/jgh.13706

Yu, M., Trobridge, P., Wang, Y., Kanngurn, S., Morris, S. M., Knoblaugh, S., & Grady, W. M. (2014). Inactivation of TGF-β signaling and loss of PTEN cooperate to induce colon cancer in vivo. *Oncogene*, *33*(12), Article 12. https://doi.org/10.1038/onc.2013.102

Zhang, B., Wang, H. E., Bai, Y.-M., Tsai, S.-J., Su, T.-P., Chen, T.-J., Wang, Y.-P., & Chen, M.-H. (2021). Inflammatory bowel disease is associated with higher dementia risk: A nationwide longitudinal study. *Gut*, *70*(1), 85–91. https://doi.org/10.1136/gutjnl-2020-320789

Zhang, S.-D., McCrudden, C. M., Meng, C., Lin, Y., & Kwok, H. F. (2015). The significance of combining VEGFA, FLT1, and KDR expressions in colon cancer patient prognosis and predicting response to bevacizumab. *OncoTargets and Therapy*, *8*, 835–843. https://doi.org/10.2147/OTT.S80518

Zhang, X. C., Piccini, A., Myers, M. P., Van Aelst, L., & Tonks, N. K. (2012). Functional analysis of the protein phosphatase activity of PTEN. *Biochemical Journal*, *444*(3), 457–464. https://doi.org/10.1042/BJ20120098

Zhao, X., Greener, T., Al-Hasani, H., Cushman, S. W., Eisenberg, E., & Greene, L. E. (2001). Expression of auxilin or AP180 inhibits endocytosis by mislocalizing clathrin: Evidence for formation of nascent pits containing AP1 or AP2 but not clathrin. *Journal of Cell Science*, *114*(Pt 2), 353–365. https://doi.org/10.1242/jcs.114.2.353

Zhou, X.-P., Loukola, A., Salovaara, R., Nystrom-Lahti, M., Peltomäki, P., Chapelle, A. de la, Aaltonen, L. A., & Eng, C. (2002). PTEN Mutational Spectra, Expression Levels, and Subcellular Localization in Microsatellite Stable and Unstable Colorectal Cancers. *The American Journal of Pathology*, *161*(2), 439–447. https://doi.org/10.1016/S0002-9440(10)64200-9

Zong, Y., Zhu, S., Zhang, S., Zheng, G., Wiley, J. W., & Hong, S. (2019). Chronic stress and intestinal permeability: Lubiprostone regulate glucocorticoid receptor-mediated changes in colon epithelial tight junction proteins, barrier function, and visceral pain in the rodent and human. *Neurogastroenterology and Motility: The Official Journal of the European Gastrointestinal Motility Society*, *31*(2), e13477. https://doi.org/10.1111/nmo.13477

APPENDIX

IACUC Approval Letter

Oakland University
Institutional Animal Care and Use Committee
Committee Action Record

July 16, 2020	4565
Committee Review Date	**RAM Number**

PROJECT TITLE

The Study of Gastrointestinal Pathobiology

Approved [X] Disapproved [ ]

NEW PROJECT

[X] **20064** — **Sang Rhee, Ph.D.**

IACUC Project Approval Number — **Principal Investigator**

REVISED PROJECT

Your Request for Revision of your Application for Use of Vertebrate Animals has been reviewed by IACUC and given full approval.

[ ] _____ — _____

New IACUC Project Approval Number* — **Principal Investigator**

*** Please use this new approval number, with the revision number indicated, in all future activities.**

A Cover Letter, similar to that used when addressing manuscript publications, needs to be attached to the application in RAM when submitting revisions to a previously approved IACUC application, or when submitting required modifications (in order to secure approval). Address required modifications in the same chronological order as they are listed in the Committee Action Record. Strike through the parts of the application that are being revised. (Do not use the Track Changes option to do the strike through or to make required modifications or revisions. Use the Strike Through option [~~abc~~] under the font tool bar.) The revisions need to be made in a readable typeface and of a different color of type so that anyone reviewing the modifications can easily identify where they are within the application.

Authorization for Project Commencement

Keith Williams — 7/17/2020

IACUC Chairperson: Keith Williams, PhD — **Date**

Approval Period:	**July 15, 2020 through July 14, 2023**
Annual Review Dates:	**July 15, 2021 and July 15, 2022**
Project Completion Summary Due Date:	**July 14, 2023**